

**SUBSURFACE STUDY OF THE HUNTON GROUP
IN THE CHEYENNE VALLEY FIELD;
MAJOR COUNTY, OKLAHOMA**

By

KATHLEEN PATRICIA MENKE

Bachelor of Science in Arts and Science

Oklahoma State University

Stillwater, Oklahoma

1984

**Submitted to the Faculty of the Graduate College
of the Oklahoma State University
in partial fulfillment of the requirements
for the Degree of
MASTER OF SCIENCE
May, 1986**

Thesis
1986
M545s
Cop.2



SUBSURFACE STUDY OF THE HUNTON GROUP
IN THE CHEYENNE VALLEY FIELD;
MAJOR COUNTY, OKLAHOMA

Thesis Approved:

Zuhair al-shaich

Thesis Adviser

Robert E. Williams

Cary J. Stewart

Norman N. Durham

Deen of the Graduate College

PREFACE

The Hunton Group of the Cheyenne Valley Field, Major County Oklahoma is the major focus of the study. Hunton production is controlled by a variety of factors; successful wells are not drilled on structure alone. A productive reservoir rock is a bioturbated dolomitized limestone with secondary porosity created by dissolution.

The study concentrates on using subsurface data such as well control, well samples and core data. The research begins in areas of the most dense control to help develop similarities and a depositional model to use in less concentrated areas.

I wish to express my sincere thanks to Dr. Al-Shaieb, my major adviser, whose help and suggestions were sincerely appreciated. I am also thankful to my other committee members, Dr. Gary Stewart for his advisement through out the study and Mr. Robert Williams for the primary suggestion of the thesis topic and excellent ideas. I appreciate Sandy Nowakowski for a wonderful job drafting all the maps for the project.

Special thanks are due to Southwestern Energy Production Company for the financial support I received during the course of this work, and the constant approval I received from Mr. Ben Short and Mr. Charles Scharlau towards the nature of the study.

I would like to extend my deepest appreciation to my fiance, John, for his constant moral encouragement and understanding. Lastly, I wish to dedicate this thesis to my parents because of their unending support, their love, and their continual motto "Education is something that you will always have."

TABLE OF CONTENTS

Chapter	Page
I. INTRODUCTION	1
Purpose of Investigation	1
Method of Investigation	1
II. PREVIOUS WORKS	7
Stratigraphy	7
Geologic History	10
Depositional History	14
Formation of Dolomite and Diagenesis	14
Exploratory Efforts	17
III. HISTORY OF THE CHEYENNE VALLEY FIELD	20
IV. PETROGRAPHY AND PETROLOGY	25
Introduction	25
Petrologic Descriptions	25
Petrographic Descriptions	26
Introduction	26
Constituents	29
Paragenesis	29
Porosity	38
Dolomite	44
Dedolomitization	50
V. MAPPING TECHNIQUES	55
Introduction	55
Woodford Structure Map	55
Sylvan Structure Map	55
Woodford Isopach Map	56
Subcrop Map	56
Total Hunton Isopach Map	57
Production Map	57

Chapter	Page
Individual Zone Maps	58
Facies Maps	58
Isopach Maps	60
Porosity Maps	62
Fault Map	63
 VI. CROSS SECTIONS	 65
Introduction	65
Northwest-Southeast	67
Northeast-Southwest	67
 VII. DEPOSITIONAL AND DIAGENETIC HISTORY	 69
 VIII. CONCLUSIONS	 74
 SELECTED BIBLIOGRAPHY	 76
 APPENDIX-CORE DESCRIPTIONS AND PHOTOGRAPHS	 80

LIST OF TABLES

Table	Page
I. Reports on Individual Hunton Wells	23

LIST OF FIGURES

Figure	Page
1. Location of Study Area	2
2. Structural Geology of Study Area	3
3. Type Log and Correlations	4
4. Locations of Cores and Cuttings	6
5. Stratigraphic Section	8
6. Distribution of Silurian Seas (Moore, 1949)	11
7. Latitudes of North America, Eurasia, and Australia in Silurian (Mintz, 1972)	12
8. Exaggerated Example of Differential deposition by the Woodford Shale	13
9. Depositional Model of the Henryhouse Formation During Sedimentation of the Oolite-Shoal Complex (Morgan, 1985)	15
10. Relative Abundance of Principal Facies Criteria (Beardall, 1983)	16
11. Modes of Origin and Alteration of Dolomite Facies of Hunton (Harvey, 1969)	18
12. Stratigraphic Section of Productive Formations in Cheyenne Valley	22
13. Dolomite Textures (Tucker, 1982)	27
14. Dunham's Carbonate Classification (Tucker, 1982)	28
15. Photomicrograph of Bioturbated Rock versus Non-Bioturbated Rock	30
16. Photomicrograph of Cemented Pellets	31
17. Photomicrograph of Dolomitized Pellets	31
18. Photomicrograph of Silica Grains	32
19. Photomicrograph of Calcite Cement	33

Figure	Page
20. Photomicrograph of Calcite Cement	33
21. Photomicrograph of Precipitated Chert	34
22. Photomicrograph of Illitic Clay	34
23. Photomicrograph of Fine Grained Micrite and Organic Clays	35
24. Photomicrograph of Siliceous Carbonate Clay	35
25. Photomicrograph of Sphalerite	36
26. Paragenetic Sequence	37
27. Photomicrograph of Chalcedony	39
28. Photomicrograph of Chalcedony	39
29. Photomicrograph of Silica Replacement	40
30. Photomicrograph of Silica Replacement	40
31. Porosity Types in Carbonate Rocks (Choquette and Pray, 1970)	41
32. Photomicrograph of Moldic Porosity	42
33. Photomicrograph of Moldic Porosity and Dissolution of Fossils	42
34. Photomicrograph of Baroque Dolomite within Molds	43
35. Photomicrograph of Intercrystalline Porosity Filled with Oil	45
36. Photomicrograph of Intercrystalline Porosity	45
37. Photomicrograph of Enlarged Intercrystalline and Moldic Porosity	46
38. Photomicrograph of Fracture Porosity	47
39. Photomicrograph of Fracture Porosity, Siliceous Carbonate Cements, and Calcite Cement	47
40. Hypersaline Brine Dolomitization Model (Manni, 1984)	48
41. Fresh Water Mixing Dolomitization Model (Manni, 1984)	49
42. Photomicrograph of Cloudy and Clear Rim Dolomite Rhombohedra	51

Figure	Page
40. Hypersaline Brine Dolomitization Model (Manni, 1984).....	48
41. Fresh Water Mixing Dolomitization Model (Manni, 1984).....	49
42. Photomicrograph of Cloudy and Clear Rim Dolomite Rhombohedra.....	51
43. Photomicrograph of Baroque Dolomite.....	52
44. Photomicrograph of Baroque Dolomite Filling Molds.....	52
45. Photomicrograph of Baroque Dolomite Inside an Enlarged Mold.....	53
46. Photomicrograph of Calcite Cement.....	54
47. Photomicrograph of Dedolomitized Rhombohedra.....	54
48. Calibration of Log Signature to Facies, Henryhouse Formation (Al-Shaieb and Fritz, 1984).....	59
49. Pickett Plot of Resistivity versus Neutron Porosity.....	61
50. Map of Inferred Faults.....	64
51. Map of Locations of Cross Sections.....	66
52. Depositional Facies.....	70
53. Porosity Enhancement.....	72
54. Hutton Erosional Patterns Along the PreWoodford Unconformity Showing Karstic Topography.....	73

LIST OF PLATES

Plate

1. Structural Contour Map - Base of Woodford Shale In Pocket
2. Structural Contour Map - Top of Sylvan Shale In Pocket
3. Isopach Map - Woodford Shale In Pocket
4. Subcrop Map In Pocket
5. Isopach Map - Total Hunton Interval In Pocket
6. Hunton Production Map In Pocket
7. Facies Map - Zone B-3 In Pocket
8. Facies Map - Zone B-4 In Pocket
9. Isopach Map - Zone B-3 In Pocket
10. Isopach Map - Zone B-4 In Pocket
11. Porosity Map - Zone B-3 In Pocket
12. Porosity Map - Zone B-4 In Pocket
13. Cross Sections A-A' and B-B' In Pocket
14. Cross Sections C-C', D-D', E-E' and F-F' In Pocket

CHAPTER I

INTRODUCTION

Purpose of Investigation

The focus of this study is the Hunton Group in the Cheyenne Valley Field. Cheyenne Valley Field is located in Townships 21N and 22N, Ranges 13W and 14W in Major County, Oklahoma (see Figure 1) lies structurally along the Northern Shelf of the Anadarko Basin (see Figure 2). The Hunton stratigraphic units in the Cheyenne Valley Field are the Chimneyhill Subgroup and the Henryhouse Formation. The unit varies in thickness from 150 feet to an excess of 300 feet, and is found at a depth of approximately 8600 feet. The regional low homoclinal dip is to the southwest, dipping toward the basin.

The Henryhouse lithology is a combination of dolomites and limestones. The Hunton unit is divided into a variety of zones according to depositional characteristics (see Figure 3). The zones shall be discussed in an effort to identify the facies and the shallowing upward sequences between the minor disconformities.

The goal of this thesis is to identify, explain and predict the location of the productive facies within Cheyenne Valley through intricate subsurface interpretation by using a variety of maps, correlations and cross sections suitable for exploration. A secondary goal is to develop a model which may be used for hydrocarbon exploration within the Hunton in other parts of the Anadarko Basin.

Methods of Investigation

The primary method of correlation and zonation was the analysis of greater than 200 electric logs and respective scout tickets. Production information was accumulated from the Petroleum Information December 1984 production reports. Gamma ray logs and resistivity logs were the most frequently used logs in zone identification and the density porosity log was the preferred tool in identification of porosity. The gamma ray was helpful because of the sensitivity of the tool.

The regressive sequence is an argillaceous carbonate mudstone of the subtidal facies,

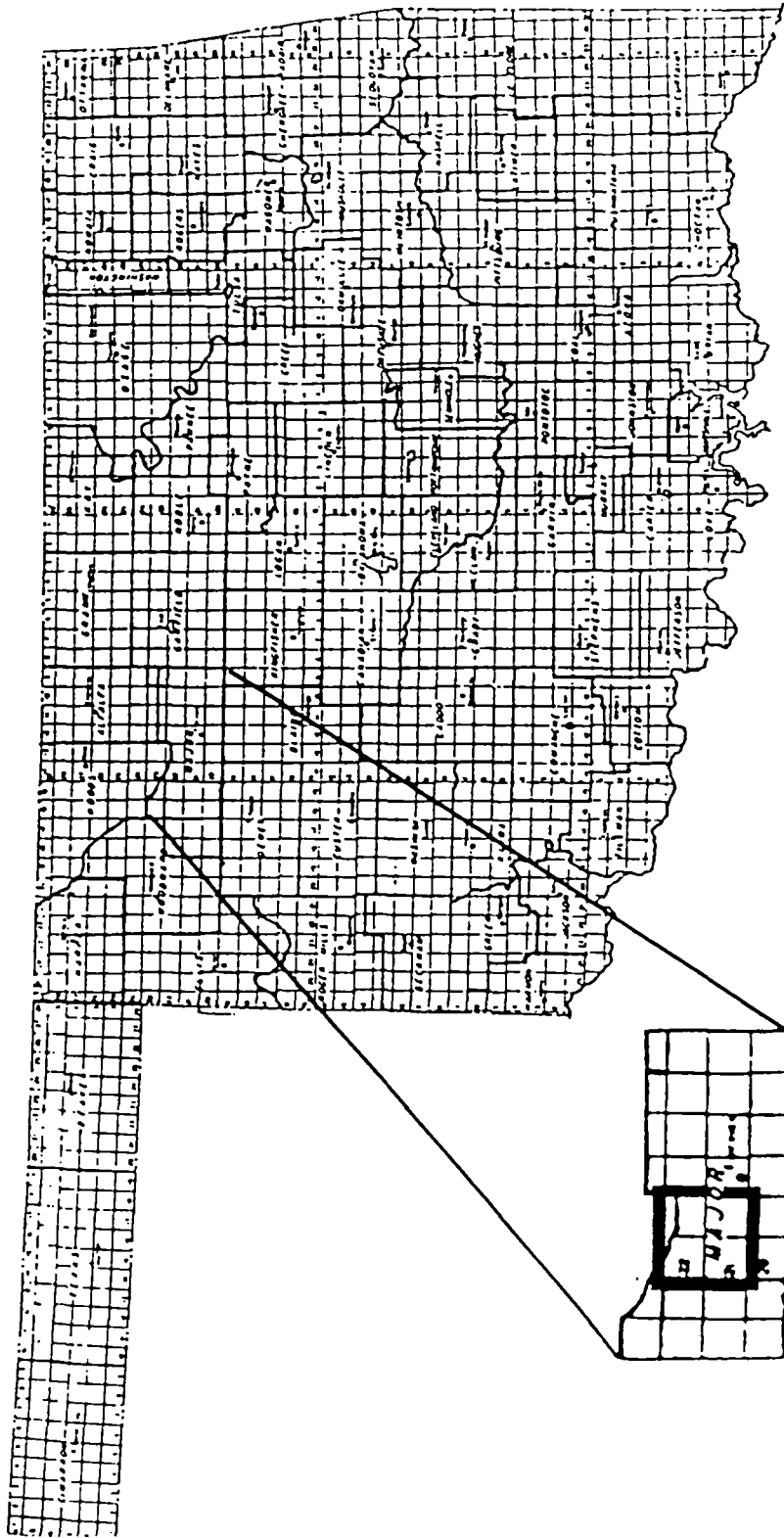


Figure 1. Location of Study Area

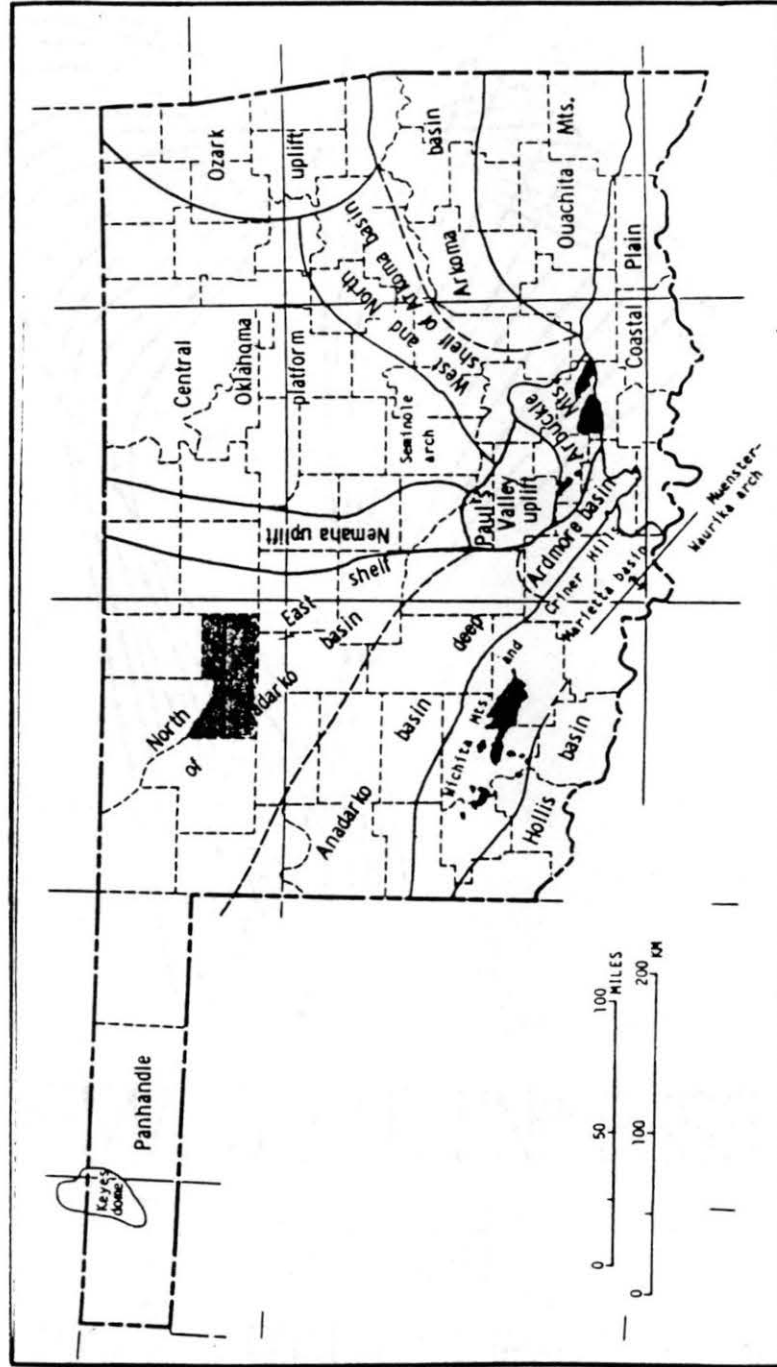


Figure 2. Structural Geology of Study Area

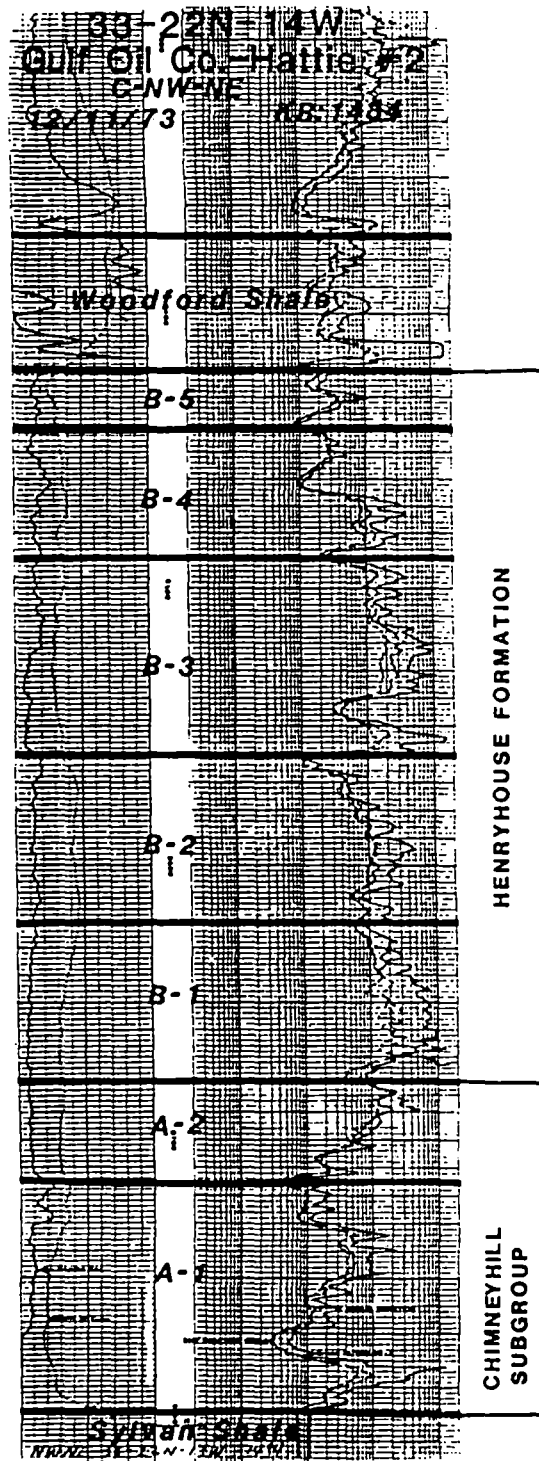


Figure 3. Type Log and Correlations

characterized by comparatively high gamma ray response. The overlying wackestone of the shallow subtidal or intertidal facies shows reduced gamma ray response. Small breaks within the curve identified an increase in terrigenous input, i.e. silica and shale; increased silicates (mostly clay minerals) are correlated positively with an increase in gamma ray count. The higher API reading of the gamma ray is indirectly related to disconformable breaks because of the residual, concentrated siliceous sediment which accumulates. In conjunction with correlation, cross sections were prepared across the field in the direction of strike, dip, north-south, and east-west. The strike-dip direction cross sections were most useful. The strike direction cross section best identified the change in facies. The Cheyenne Valley cross sections were tied into and correlated with cross sections previously prepared by the author thus completing a grid across Northwestern Oklahoma.

Three cores were examined (see Figure 4 for list of the cores examined and the locations) and a petrologic analysis was made of each core so that the facies could be delineated from lithology, sedimentary structures, and other features. The cores were calibrated to the logs. Sixty thin sections were prepared from the cores. Alyzerin Red stain was applied to parts of the slides for an accurate identification and distribution of the different carbonate minerals. Petrographic slides were studied and the cements, mineral content, porosity types, and fossils were identified. X-Ray diffractions were run from 250 to 340 for identification of dolomite or calcite for selected samples. Well cuttings from five wells were examined (see Figure 4 for list of cuttings examined and the locations). Close observation was made of the fragment lithology to identify the facies. Bulk powder X-ray diffraction was run to determine general constituents and degrees of dolomitization.

A variety of maps was constructed from the core-calibrated logs. Isopech maps were prepared for the Woodford Shale and the individual zones. Structural contour maps were made on the base of the Woodford, the top of the Sylvan, and the base of each of the productive zones within the Henryhouse Formation (zones B-3 and B-4). Porosity maps were made of the B-3 and B-4 zones. Finally, facies maps were made on the B-3 and B-4 zones and facies were color coded and schematically drawn in. The combination of these maps delineates the probable depositional environments.

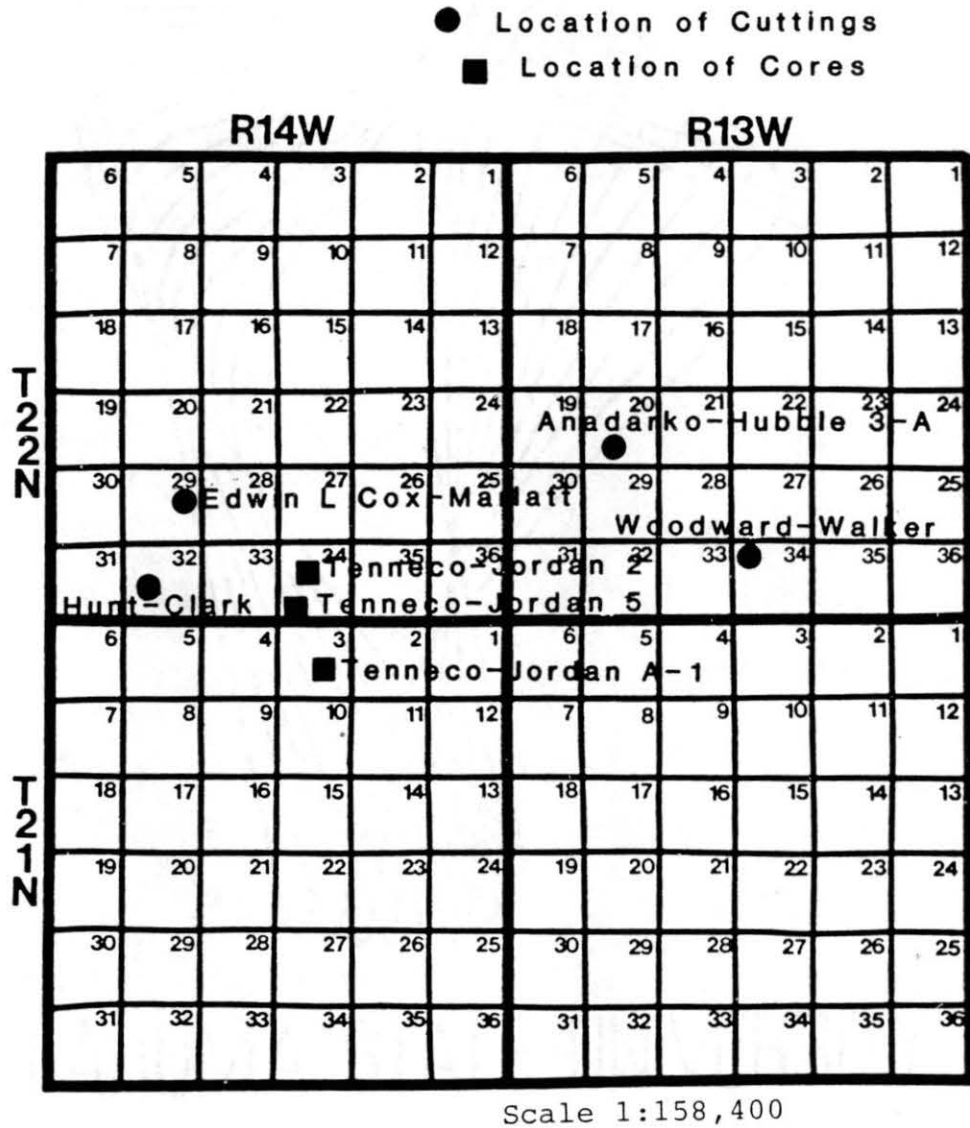


Figure 4. Locations of Cores and Cuttings

CHAPTER II

PREVIOUS WORKS

Stratigraphy

The Hunton Group was first described by C.A. Reeds in 1911. Reeds presented a stratigraphic and paleontological study on the Hunton Group. He proposed a four-fold lithologic and paleontologic arrangement and assigned the units a formal rank of formation. The formation names which were approved by the committee on Geologic Names of the U.S. Geological Survey are from bottom to top: Chimneyhill Limestone, Henryhouse Shale, Haragan Shale, and Bois d'Arc Limestone (see Figure 5). With exception of the lithologic identification, the names remain today.

Further stratigraphic work accomplished by Amsden (1957) and Shannon (1962) closely examines the fauna. Shannon stated that the Hunton Group was "an essentially conformable succession of strata that represents a sequence, or body of rock bounded by time-transgressive interregional unconformities." Subsurface investigations made by Shannon indicate that physical relationships of formations within the Hunton Group illustrate continuous sedimentation within the unit from Middle Silurian through Early Devonian. Shannon's subsurface work strengthened Reeds' four-unit stratigraphic divisions and provided easy recognition of the units on an electric log.

The Hunton Group conformably overlies the Sylvan Shale. The contact can be readily identified in outcrop as well as by distinctive wireline log characteristics. The Chimneyhill Subgroup is a medium to coarse-crystalline white to buff limestone which may be further subdivided into three members: 1.) the Keel Formation, 2.) Cochrane Formation, and 3.) Clarita Formation. Amsden believes the individual members are unconformable because not all the Chimneyhill members are present regionally. Facies relationships are believed to be related to thickening and thinning, or total absence of the members. The Henryhouse Formation lies unconformably on top of the Chimneyhill, and is separated from the Haragan Formation according to distinct lithology changes. At the surface, the Henryhouse and Haragan Formations are recognized as a light yellow gray to medium gray argillaceous, slightly cherty

SYSTEM	FORMATION	
<u>Devonian</u>	Woodford Shale	
	Hunton Group	Erisco Formation
		Fittstown Member
		Cravatt Member
		Haragan Formation
	<u>Silurian</u>	Henryhouse Formation
Chimneyhill Subgroup	Clarita Formation	
	Cochrane Formation	
<u>Ordovician</u>	Sylvan Shale	

Figure 5. Stratigraphic Section

and locally dolomitized limestone. The Henryhouse is commonly differentiated from the Haragan on the basis of faunal characteristics. The Henryhouse fauna is dominated by the brachiopods, some mollusks, and trilobites; whereas the Haragan fauna is dominated by the brachiopods, trilobites, gastropods, corals, ostracods, and bryozoa (Amsden, 1957). Absence of Haragan is common in the subsurface in southwestern Oklahoma.

The Bois d'Arc Formation lies conformably on the Haragan and is previously included as the uppermost member of the Haragan. The base is defined by cherty beds. The unit is medium to coarsely crystalline, white, buff, or yellow-brown, and typically cherty limestone.

The Frisco Formation is the final formation in the transgressive sequence and lies conformably on the Bois D'Arc. The fact that the Frisco is present only on top of the Bois d'Arc may indicate that these two units represent part of the same depositional episode. The Frisco is identified in subsurface by a white to buff fine-crystalline limestone with a high content of fossils.

The total Hunton Group is unconformably overlain by the Woodford Shale or locally present Mansville Dolomite. A considerable time gap is present because of the extreme removal of Hunton in parts of Oklahoma.

In this study, Hunton units examined were the Chimneyhill Subgroup and the Henryhouse Formation. No attempt was made to further subdivide the units on paleontological evidence, but units were subdivided into informal zones on the basis of the wireline log characteristics. The zone characteristics were derived at by a series of correlations and cross sections throughout Northwest Oklahoma.

Geologic History

The area of study is located on the Northern Shelf of the Anadarko basin (see Figure 2.)

During the Cambrian the proto Atlantic Ocean formed, which triggered advancements of the epeiric seas onto the intracratonic basin (Landes, 1970). The Tiptecanoe Sea transgressed during Middle Ordovician and achieved maximum extent during Late Ordovician. Several regressions and transgressions occurred during Silurian and Early Devonian (see Figure 6). The most pronounced structural movement of this period occurred during Middle and Late Devonian when the Hunton strata were tilted and successively truncated northward, (Isom, 1974). The Pennsylvanian orogenies were the major tectonic activities. The Wichita Orogenies caused a series of parallel northwest trending faults (which tend to follow basement structural grain) as well as tilting and minor deformation of strata, (Isom, 1974), (Evans, 1979).

The Anadarko basin was part of an aulocagen. The Anadarko basin is asymmetric, with a steep and highly faulted southern margin. The slope into the basin is gentle from the shelf areas to the northeast, north, and west, (Beardall, 1983). During Sylvan Shale deposition, the Anadarko basin was relatively stable and is considered a passive continental margin. A stable basin is indicated by the relative uniform thickness along strike and the very gradual thickening toward the center of the basin, Harvey (1969). The Hunton rocks were also deposited during a time of tectonic stability, with the exception of slight deformation following the Chimneyhill Subgroup deposition, which caused a minor angular unconformity. The Hunton deposition was influenced directly by the underlying topography of the Sylvan Shale. The climate during Hunton deposition was warm and mild uniform temperature, (Moore, 1949). Oklahoma was located at 10° South latitude as determined by paleomagnetic data (see Figure 7), (Mintz, 1972). Following Hunton deposition and prior to deposition of the Woodford, a period of nondeposition resulted in extensive erosion along the shelf of the Anadarko Basin, (Harvey, 1969). A dendritic drainage pattern developed toward the Wichita Mountains, (Harvey, 1969), (Isom, 1974), Amsden (1975). The eroded topography was almost leveled by the preWoodford unconformity. The Woodford Shale was deposited unconformably on top of the Hunton and filled the topographic lows (see Figure 8), (Harvey, 1969).

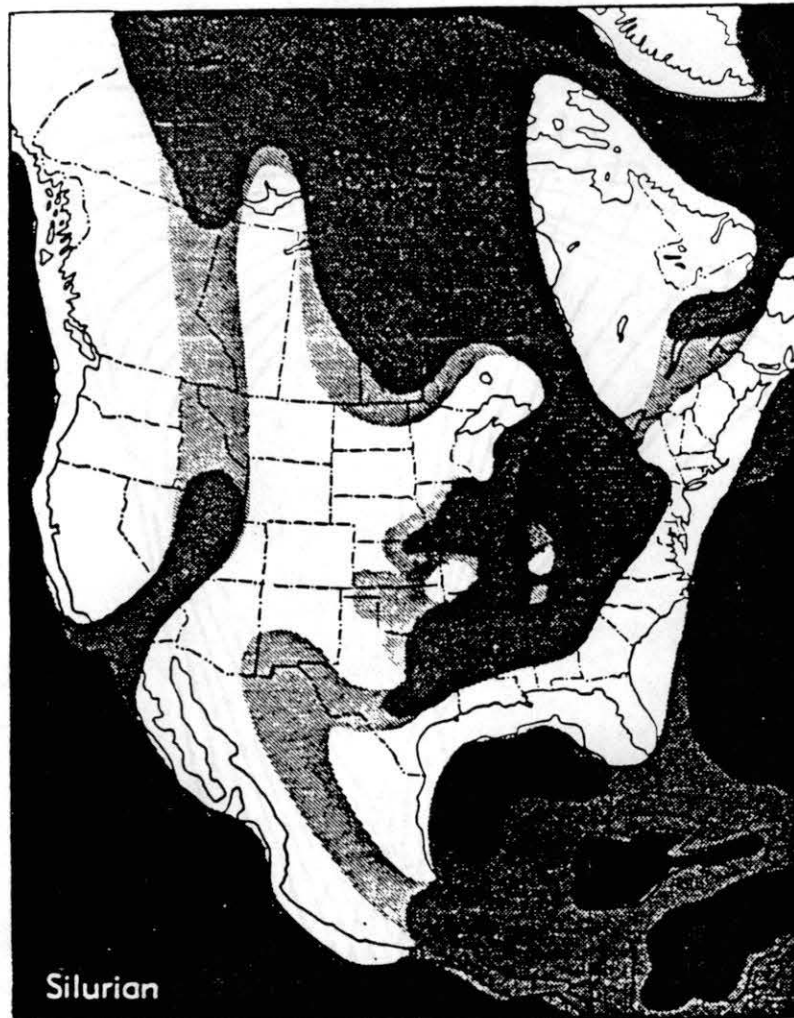


Figure 6. Distribution of Silurian Seas
(Moore, 1949)

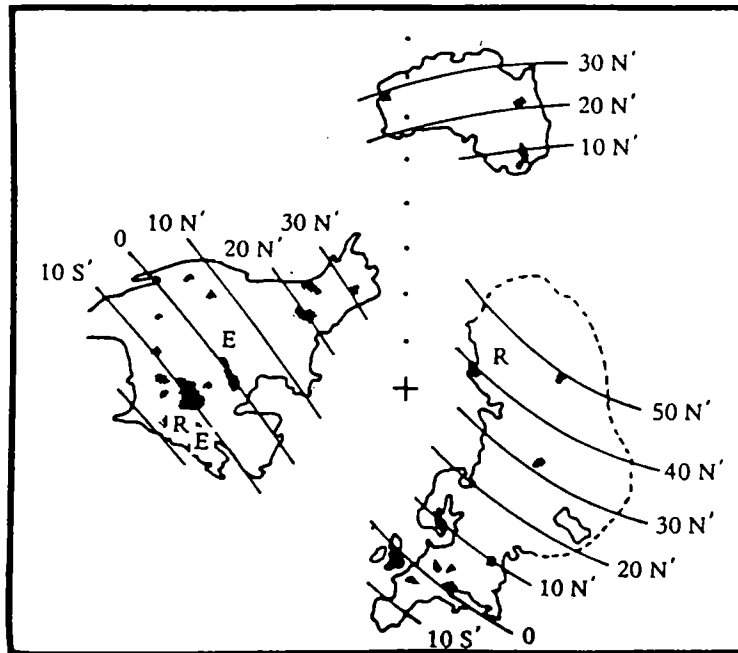


Figure 7. Latitudes for North America, Eurasia, and Australia in Silurian (Mintz, 1972)

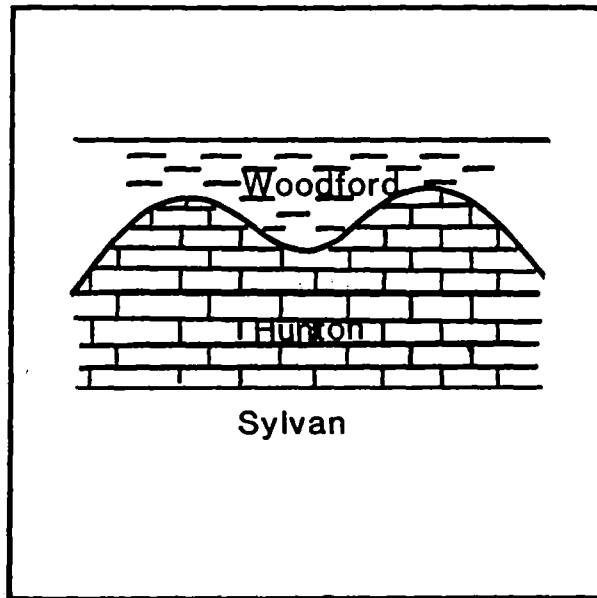


Figure 8. Exaggerated Example of Differential Deposition by the Woodford Shale

Depositional History

(Amsden, 1975) suggested that the Hunton was deposited in a shallow water, low energy transgressive environment. Amsden identified a variety of fauna and specific characteristics which identifies a possible low energy environment. Evidence for the low energy environment is 1.) the mud-supported fabric with the clay or fine silt-size matrix, 2.) the fossils are well preserved, and subjected to minor breakage.

(Beardall, 1983) developed a depositional model for the Henryhouse Formation through a study of various cores. Beardall suggested a broad shallow, low energy epicontinental sea. The deposition is an overall transgressive unit consisting of many regressive sequences. In the cores, the shallower water facies are above the deeper water facies indicating a marine regression or shoreline progradation. The facies Beardall identified are subtidal, intertidal, and supratidal. The facies are derived at by using a variety of criteria through examination of sedimentary structures and fabrics (see Figure 10).

(Morgan, 1985) referred to the Hunton as upward-shoaling cycles. Henryhouse Formation deposition began with a transgression resulting from onlap of deeper water facies, but resulted in a regressive sequence within the transgression evidenced by skeletal buildups within the Clarita Formation, and an oolite shoal within the Henryhouse Formation. The oolite shoal is readily identified on gamma ray logs by its low gamma ray response, which presumably reflects the high-energy nature of this facies and the lack of terrigenous muds. The upward shoaling sequence is first evidenced by deep water, then shallow ramp, and then an oolite shoal facies. (see Figure 9).

Formation of Dolomite and Diagenesis

Various ideas about the formation of the Hunton dolomite were suggested. Amsden (1960) is the first to recognize dolomite in outcrop, and performed extensive geochemical studies to determine the magnesium content of the dolomite. Amsden reported on the various degrees of dolomitization. The question which Amsden asked is when did the magnesium content reach its present position, and is the concentration of magnesium "primary", at the time of deposition, or "secondary", introduced later following withdrawal of the sea? Evidence from a study of the stratigraphic distribution of the beds shows a relatively high concentration of dolomite in localized areas and the transgressive character of the Hunton suggests a secondary dolomite introduced at some time after the end of Hunton deposition.

The essential conditions for the origin of dolomite are a sea rich in magnesium salts, a

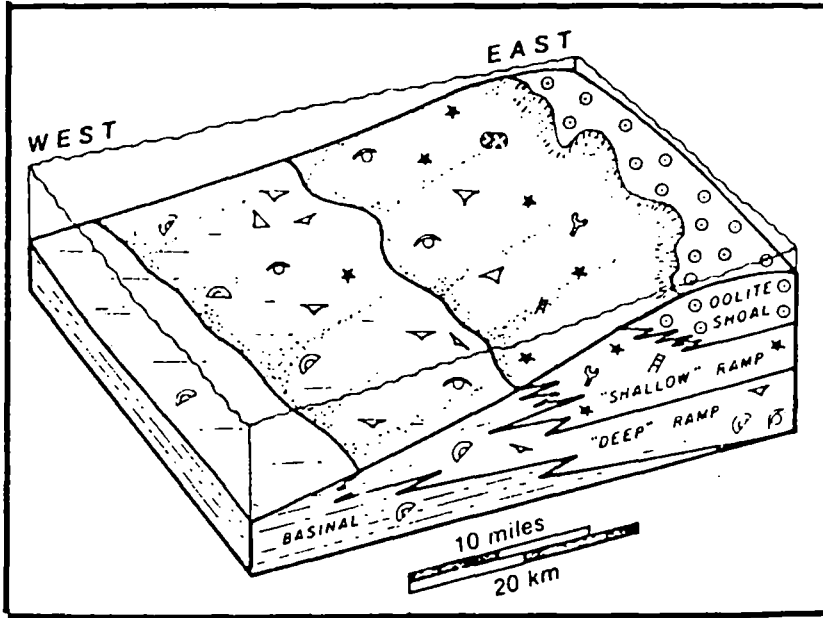


Figure 9. Depositional Model of the Henryhouse Formation During Sedimentation of the Oolite-Shoal Complex (Morgan, 1985)

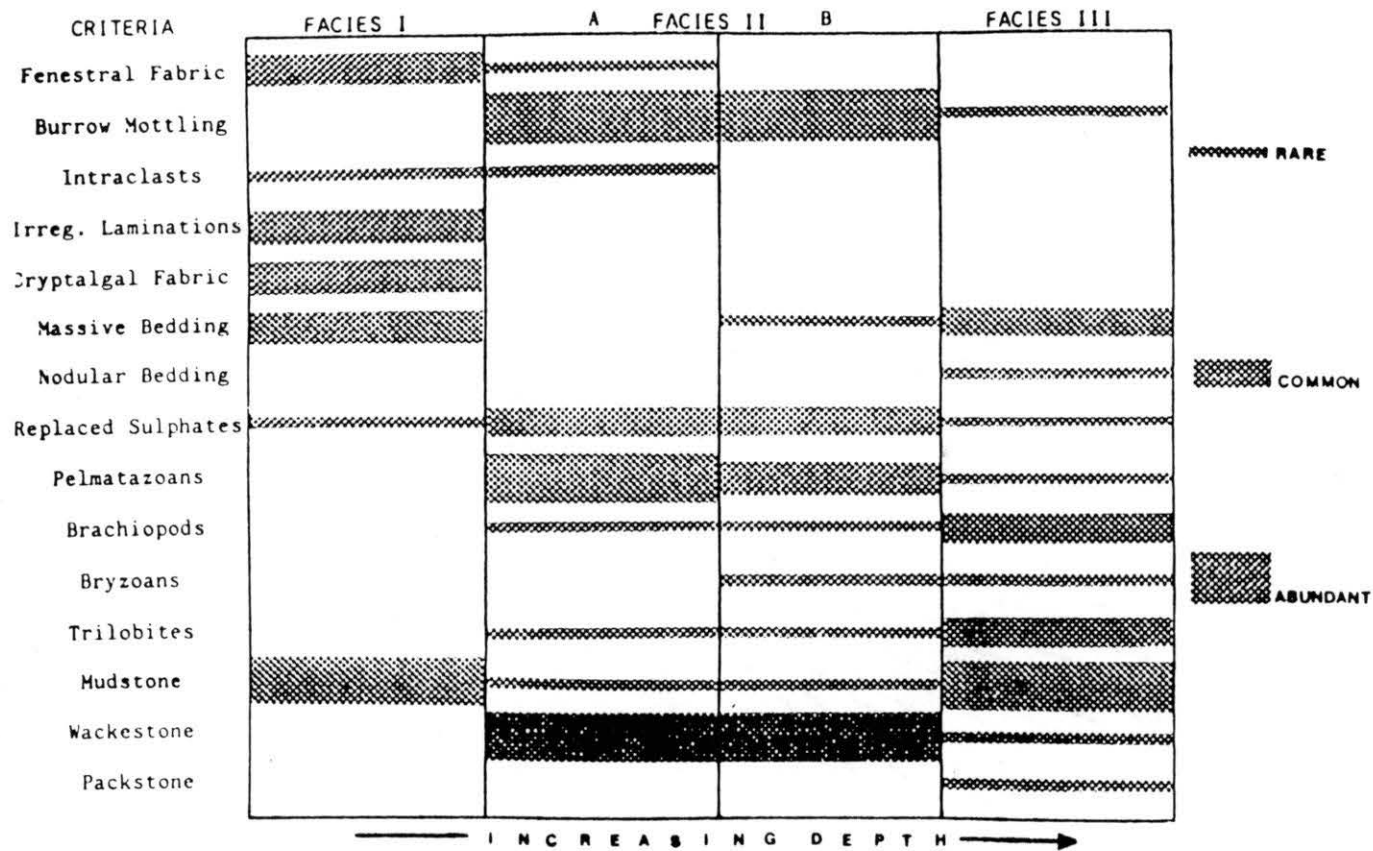


Figure 10. Relative Abundance of Principal Facies Criteria (Beardall, 1983)

fairly warm temperature, a reduced or elevated CO pressure, a high pH, a reducing environment, and the presence of organic matter. These conditions are comparable to a near shore, shallow marine environment (Fairbridge, 1957).

(Harvey, 1969) Harvey believed that formation of dolomite is primary. During deposition, he noted periods of minor oscillations of the sea which create areas of nearshore shallow water deposition of dolomite. Since Harvey observed that the geometric shape of the dolomite is lenticular in shape, various alternative processes for localizing porous dolomite pods were suggested (see Figure 11).

(Withrow, 1971) Withrow believed development of secondary dolomite porosity was related to erosional surfaces.

(Isom, 1974) He suggested two types of dolomitization: 1.) an early replacement type occurring during penecontemporaneous deposition, 2.) a late replacement type. The first type of dolomite is supported by lateral persistence, and has no apparent association with tectonic or erosional features. The second type is complete replacement. Dolomitization results from circulation of high magnesium waters along unconformities and fractures.

Two phases of dolomitization were recognized, eogenetic hypersaline brine, and marine-water mixing with meteoric water. The hypersaline brine dolomite model is evidenced by replacement of anhydrite, isotopes, and cloudy brown centers of the dolomite crystals as seen through petrographic observation. The mixing model is documented by isotope composition, advancing fresh water lense, clean overgrowths of the crystals, and cathodoluminescence (Beardall, 1983).

A third phase of deep water dolomitization, which shall be discussed later by the author, creates a clean baroque pore-filling dolomite which completely diminished moldic porosity.

Friedman suggested a deep burial diagenesis of carbonates in the Anadarko basin. Friedman observed the dolomite had an increased iron content as well as mechanical adjustments such as compaction and fracturing of grains (Friedman, 1984).

Exploratory Efforts

The Hunton was recognized as a significant producer in the Anadarko Basin in early 1950. Logsdon and Brown claimed the Hunton as the "Hottest Play in Oklahoma". At that time most people conducted exploration for hydrocarbons within the Hunton by considering the rock as a thick sequence of limestone, and sought for unconformity

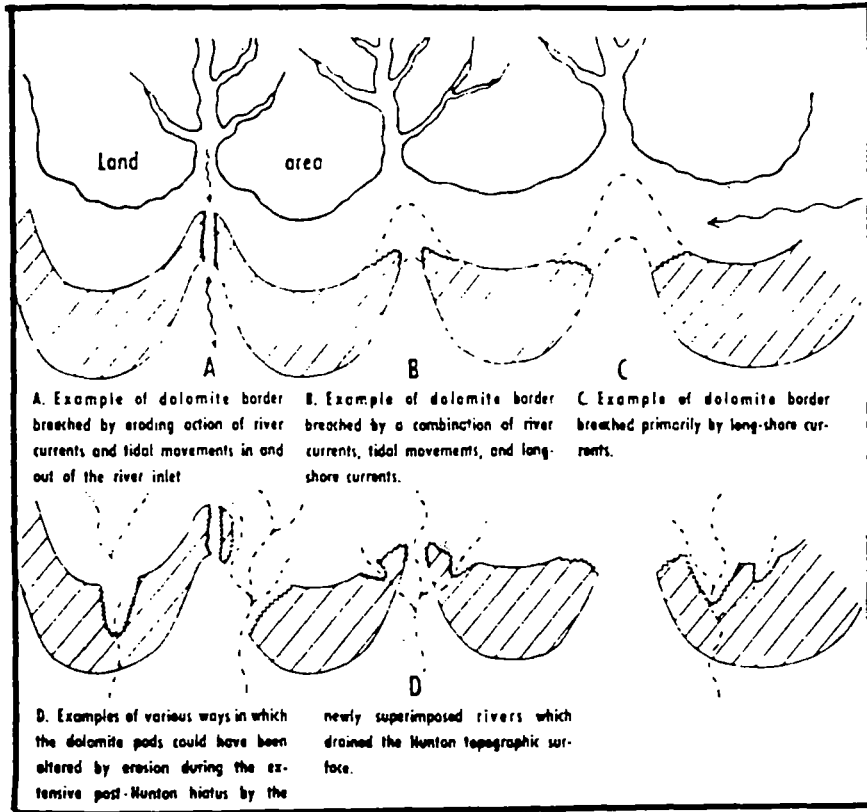


Figure 11. Modes of Origin and Alteration of Dolomite Facies of the Hunton (Harvey, 1969)

traps. The following methods of exploring within the Hunton were suggested: 1.) Map an area large enough to allow conclusions to be based on occasional or subtle geologic happenings, include a Hunton isopach, a Woodford-Kinderhook isopach and facies study. 2.) Recognize the lateral facies changes and environments of deposition. 3.) Pay close attention to Kinderhook-Woodford thickness changes related to Hunton topography. 4.) Review areas of dolomitic facies and good porosity development have a water drive mechanism. 5.) Recognize that stratigraphic factors are probably the original trapping mechanism with subsequent tilting, faulting and fracturing. 6.) Locate the wedge edge of the Hunton by preparing a Sylvan-Hunton isopach map. 7.) Understand that development of Hunton production indicates that the traps are basically a function of porosity development and regional dip (Logsdon and Brown, 1967). Exploration for these primary stratigraphic accumulations depends upon geological skill and stratigraphic interpretation rather than on geophysical delineation of structure alone. Logsdon and Brown's exploratory methods should be considered by a geologist when evaluating the region. Since the time of Logsdon and Brown's paper, more attention was given to the dolomite facies.

(Harvey, 1969, p.568) Harvey explained the West Edmond field development: "The company was searching for thick Hunton dolomite in a structural trap. The thick dolomite was present, but only after development drilling did it become apparent that the accumulation of hydrocarbons was stratigraphic rather than structural." (Harvey, 1969, p.568) Harvey stated: "Because the Hunton hydrocarbons are trapped almost entirely within the dolomite facies, it is essential in exploration for further traps of this type, to relate the origin of the dolomite members to the history of deposition, diagenesis, and oscillations of sea level in developed field such as West Campbell." Although Harvey was aware of the importance of deposition and diagenesis, subsequent exploration efforts toward this goal have been limited and confusing when considering this method. (Withrow, 1971), upon examination of the West Edmond Field determined that larger petroleum reserves are found in secondary dolomite below the pre-Woodford unconformity, and dolomitic zones form large prolific traps throughout the Hunton over the entire northern shelf of the basin. This method of exploration is based on extensive correlations of electric logs and the stratigraphy. Until (Withrow, 1971), little stratigraphic work had been published on the Hunton in Northwestern Oklahoma.

CHAPTER III

HISTORY OF THE CHEYENNE VALLEY FIELD

Cheyenne Valley Field was discovered in 1958. J. M. Huber made an oil discovery in the Chester Sand following a successful completion of the Phillips #1 in the C-SW-SW of 33-22N-14W, Major County, Oklahoma. Gulf Oil, which became active in Cheyenne Valley after the Huber discovery, drilled the dry hole Kaufman #1. The Kaufman #1, completed in April, 1958, was located in the SE-SW of section 33, T22N, R14W. In May 1958, Gulf completed as a Cherokee sand producer, the Sodowsky #1 located in the SE-SE of section 32, T22N, R14W. This well had an initial production flow of 120 barrels of oil and 340,000 cubic feet of gas in six hours. Numerous offsets were made to these wells by Gulf, J. M. Huber, Cities, Pan American, and others. In October 1958, Pan American successfully completed the Hutchinson Unit 'B' #1 in NE-SW of 32-22N-15W as a discovery gas well in the Cherokee and Chester sands. The Hutchinson Unit 'B' had an initial production of 186,000 cubic feet of gas per day from the Cherokee and 1,020,000 cubic feet of gas per day from the Chester. Pan American remained active in the area following the Hutchinson Unit 'B' discovery.

Red Fork Sandstone production, which began in 1962 in T21N, R14W was extended to T22N, R14W in 1970.

In 1963 companies began to look for deeper producing formations. In July 1963, Zimmet Brothers made an oil discovery in the Oswego with the completion of the Phillips #1 in NW of 19-22N-14W. By 1966, other wells producing from the Oswego formation were drilled by Jennings Petroleum, Pan American and others.

The Mississippi Lime is another productive formation in Cheyenne Valley. In January 1969, Midwest Oil drilled the Phillips #1 in SE of 19-22N-14W which resulted in a zone discovery in the Mississippi. In February, 1968, the first economic Hunton well was completed by Edwin L. Cox in SW-NE of 29-22N-14W. The Marlett #1 had an initial pumping production of 65 barrels of oil and 120 barrels of salt water per day. The well was completed in the upper part of the Hunton along the subcrop.

In March, 1968, Tenneco successfully completed a Hunton producer from the lower zone

in the Henryhouse. Tenneco's well, the Jay Jordan Unit #1 in NW-SW-SE of section 34, T22N, R14W, had an initial flowing production of 165 barrels of oil and no water in twenty-four hours. Tenneco continued the development of the field in 1968 and 1969 by drilling wells in section 34. Two zones were found to produce, and are referred to as the upper and the lower Hunton interval. Tenneco has further expanded the pool to include section 33, T22N, R14W and section 3, T21N, R14W.

In 1968, the Hunton Group was regarded as a single deposition unit and production occurred solely along belts of truncation. Tenneco's discovery resulted from a stratigraphic interpretation. The Tenneco geologist studied the Hunton as a series of individual units. Six units were correlated with use of the induction logs. Variations of thicknesses, found within each of the units, were used for prospecting purposes. Following the Edwin L. Cox and Tenneco discoveries, the field was more accurately mapped and a zone correlation was established. A core was taken during the drilling of the second discovery well. Through interpretation of cores, the identification of the depositional environment resulted in better zone correlation. Eventually, a total of three wells were cored by Tenneco. The field was remapped and developed. In 1981, the lower Hunton zone in section 34 was unitized and since that time has been waterflooded.

Gulf Oil Company took an interest in the Hunton following the Edwin L. Cox and Tenneco successes. In December, 1969, Gulf completed the O. Williams #2 well as a Hunton producer with an initial production flow of 338 barrels of oil and 31 barrels of water in twenty-four hours. Gulf developed section 28, then expanded south into section 33.

Gulf, Tenneco, Cox, and latercomer Continental Resources continued the development of Cheyenne Valley Field until the majority of the acreage had been developed by the early 1980's.

The Cheyenne Valley Field, first named in 1958, has five producing formations ranging from 6000 feet to 8000 feet in depth (see Figure 12). The Cheyenne Valley field has produced 5,582,336 barrels of oil from 43 wells and 14 BCF of gas from 28 wells from the Hunton. From 1968 to 1984 the average cumulative production per well was 129,822 barrels of oil and 517 MMCF of gas from 1968 to 1984. (See Table I for individual well reports.)

STRATIGRAPHIC SECTION OF PRODUCTIVE FORMATIONS IN CHEYENNE VALLEY			
SYSTEM	FORMATION	APPROXIMATE SUBSURFACE DEPTH	
Pennsylvanian	Oswego**	6350'	
	Cherokee	Pink Lime	6510'
		Red Fork Sand**	6600'
		Inola Lime Bartlesville Sand	6620'
		Thirteen Finger Lime	
	Morrow		
Missippian	Chester**	7000'	
	Meramec		
	Mississippi Lime**	8000'	
	Kinderhook		
	Woodford	8130'	
Devonian	Henryhouse**	8200'	
Silurian	Chimneyhill	8350'	
Ordovician	Sylvan	8400'	

** indicates productive
formation

Figure 12. Stratigraphic Section of Productive
Formations in Cheyenne Valley

TABLE I
 REPORTS ON INDIVIDUAL HUNTON WELLS

<u>Section</u>	<u>Operator/Farm</u>	<u>Dates</u>	<u>Oil (Barrels)</u>	<u>Gas (MCF)</u>
T21N-R14W				
3	Tenneco-Jordan A-1	7/67-7/85	268,857	434,034
3	Tenneco-U.S.A. 1	12/68-7/85	222,726	1,044,827
3	Tenneco-U.S.A.2	4/71-7/85	509,471	-0-
4	Tenneco-U.S.A. 1	6/71-7/85	333,630	78,291
4	Tenneco U.S.A.2	10/71-7/85	20,744	75,255
13	Hunt-State	11/68-7/83	65,903	-0-
25	Hunt-Davidson	7/73-2/82	-0-	367,628
25	Hunt-Burlison	7/82-12/84	-0-	15,586
31	TXO-Razook	3/81-8/83	3,762	85,985
T21N-R15W				
13	Clark-Cheyenne 2	9/84-12/84	1,323	-0-
28	Anchorage-Rogers	12/82-12/84	-0-	295,783
31	Southland-Jellison	1/80-12/80	-0-	91,165
31	Tema-Jellison	5/79-11/80	-0-	202,459
T22N-R13W				
15	Kirkpatrick-Kliwer	7/73-10/84	-0-	19,676
17	Kaiser Francis-Jester	8/69-11/84	43,744	-0-
18	Earlsboro-Gould Bros.	3/84-12/84	6,418	-0-
19	Champlin-Nicholson 2	3/83-12/84	8,951	-0-
20	Anadarko-Hubble A-2	2/83-11/84	18,031	32,112
20	Anadarko-Hubble A-5	6/84-12/84	14,030	-0-
22	Kirkpatrick-Smith	7/73-12/84	-0-	4,218,744
27	French-Park	12/82-12/84	10,480	360,101
27	French-Sutter	11/73-5/83	-0-	3,874,334
28	French-Cheyenne	10/82-12/84	5,648	-0-
28	French-Victor	11/82-12/84	11,426	269,128

Table I Continued

<u>Section</u>	<u>Operator/Farm</u>	<u>Dates</u>	<u>Oil (Barrels)</u>	<u>Gas (MCF)</u>
T22N-R14W				
9	Earlsboro, Nellie	6/82-12/84	-0-	162,180
9	Ward-Kittel	10/84-12/84	1,822	-0-
17	Gulf-Phillips	3/79-2/84	9,103	342,078
18	Whitmer-Marlett	6/82-11/84	14,718	-0-
20	Tenneco-Wolfe	10/84-12/84	-0-	6,242
20	Cont.Res.-Brown	11/81-2/83	3,316	-0-
20	Cont.Res.-Gould	3/81-7/85	95,130	1,469,482
20	Edwin L. Cox-Gould 2	10/72-6/76	-0-	1,026
22	Ward-WilliamsJordan	8/84-12/84	3,307	-0-
25	Ashland-Byfield	5/78-10/83	-0-	22,416
28	Gulf-Williams 2	12/67-2/81	291,792	-0-
28	Gulf-Williams 3	1/79-12/84	36,959	-0-
28	Gulf-Williams 1	6/73-2/84	4,103	-0-
28	Gulf-Williams 3-C	6/78-2/81	1,228	-0-
28	Gulf-Williams 5	5/73-12/84	284,186	-0-
28	Gulf-Williams 6	11/73-8/84	52,554	-0-
29	Edwin L. Cox-Marlett	1/68-	3,999	-0-
29	Edwin L. Cox-Williams	6/69-12/84	686,525	-0-
30	Harper, Williams C	9/72-12/84	-0-	129,600
31	Burns-Clark	10/83-11/84	36,702	-0-
31	Burns-Edwards 4	8/84-11/84	15,477	-0-
31	Burns-Edwards 2	3/82-11/84	88,824	-0-
31	Burns-Ellison	4/82-9/84	4,503	-0-
33	Gulf-Hattie	8/72-12/84	141,427	-0-
33	J.M.Huber-Phillips	4/72-12/84	522,808	-0-
33	Tenneco-Phillips	4/71-12/84	116,627	48,176
34	Tenneco-ECYLHU		1,227,553	60,022
34	Tenneco-Lichy 1		18,163	460,841
34	Tenneco-Jordan 2	8/68-8/71	283,090	-0-
34	Tenneco-Jordan 4	10/71-7/85	19,944	12,720
34	Tenneco-Lichy 3	0/69-7/85	10,865	316,863
36	Champion-Byfield A-1	5/81-12/81	12,467	-0-
Totals: 56 Producing Wells			5,582,336	14,496,762
Average per well			129,822	517,742

CHAPTER IV

PETROGRAPHY AND PETROLOGY

Introduction

The sedimentary rocks in the Henryhouse Formation located within the limits of the Cheyenne Valley Field are best described by using Dunham's classification (1961). The rocks range from mudstone to packstone, and exhibit varying degrees of textures.

Petrologic Descriptions

The cores examined are the Tenneco-Jordan A-1, the Tenneco-Jordan 5, and the Tenneco-Jordan 2. The core depth of the Tenneco Jordan A-1 is -8489' to -8612'. The interval consists of dolomudstone to dolowackestone in the upper portion with a lime mudstone at the base. The color ranges from tan to orange, and the productive zone is a dark brown. Stylolites are present within the section. Bioturbation, distinctive of the intertidal zone, exhibits a mottled texture. Calcite fills the vugs and organic matter defines the algal lamination. For a detailed description of the core see Appendix for the petrographic log.

The subtidal zone of the Henryhouse is typically a light brown to gray limestone or slightly dolomitized limestone. The rock classified as a mudstone, and is finely crystalline. Palaeozoans and Brachiopods are observed in hand specimen are broken or fragmented. Lamination is detected by small shale wisps in the section. Pyrite and chert are common constituents. Stylolites increase in abundance in the subtidal facies.

The shallow subtidal zone is a light brown to orange slightly dolomitized limestone. The rock is classified as mudstone to wackestone. The visual characteristics of this rock are similar to the subtidal, but there is greater likelihood of dolomitization. The grain size is finely crystalline. Fractures are common and are filled with oil.

The intertidal zone is orange to brown bioturbated dolomite, and is a wackestone. This facies commonly exhibits a bimodal texture of grain sizes and excellent porosity is observed in hand sample due to the extensive burrowing. The bioturbated zones are mottled, crystalline or sucrosic, and porous. The nonbioturbated micrite is finely crystalline. Chert and tripoli nodules are present.

The core depth of the Tenneco Jordan 2 is -8464' to -8570'. The Hunton section is dolomitized. Dolomite crystals fill the moldic porosity. Although most of the core exhibits the subtidal facies the lower portion of the core represents the intertidal facies. Vertical fractures are present at the top, and horizontal fractures are observed at the base. Large chert nodules, bedded chert, and tripoli are observed within the core. The subtidal facies is fossiliferous. (See Appendix for petrologic log.)

The core depth of the Tenneco-Jordan 5 is -8524' to -8550'. Only the upper portion of the Hunton section is cored. This core exhibits the shallow subtidal and intertidal facies. The rock is a light brown to orange mudstone or dolowackestone. The core's upper portion is partially dolomitized limestone, while the lower portion is dolomite. Chert and tripoli are present throughout. A few stylolites were observed. (See Appendix for photographs and the petrologic log.)

Cuttings from Anadarko-Hubble 3A, Edwin L. Cox-Marlatt, Hunt-Clark, Tenneco-Jordan A-1 and Woodward-Walker were examined. The cuttings exhibit similar characteristics as the cores, both show the facies changes. The intertidal chips are brown and porous. X-ray diffraction indicates the dolomite content is approximately 90%. The shallow subtidal zone is a lighter brown to dark gray. The chips are larger and more cohesive. The subtidal zone cuttings are light gray and very dense. X-ray diffraction data indicate a higher calcium content in the subtidal samples.

Sample cuttings are useful for delineating facies.

Petrographic Descriptions

Introduction

Most of the thin sections examined are completely dolomitized, and located within the shallow subtidal or intertidal facies. The primary dolomite textures and fabrics observed are euhedral idiotopic E or anhedral Xenotopic A (see Figure 13).

The rocks are classified as dolomudstone or dolowackestone (see Figure 14).

The textures observed are dependent upon facies. The euhedral idiotopic dolomite, typical of the bioturbated intertidal facies, consists of well defined euhedral rhombohedral dolomite crystals have an average grain size of 20-100 microns. Excellent intercrystalline porosity is present with an average pore size of 20-30 microns, and the pore throat size is approximately one half the pore size or 10 microns. The intercrystalline porosity, enlarged from dissolution, accounts for the large effective porosity.

The subhedral idiotopic dolomite, characteristic of the nonbioturbated intertidal facies,

Idiotopic Dolomite- Rhombic shaped euhedral to subhedral crystals.

Xenotopic Dolomite- Monorhombic, usually anhedral crystals.

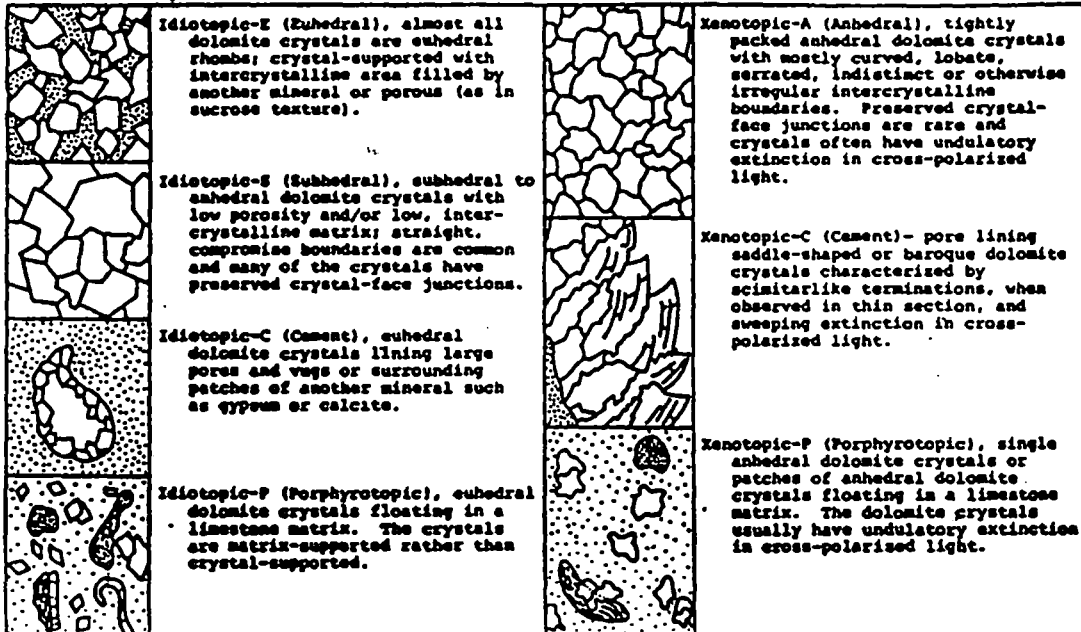


Figure 13. Dolomite Textures (Tucker, 1982)

Original components not organically bound during deposition				Original components organically bound during deposition				
of the allochems, less than 10% > 2 mm diameter			of the allochems more than 10% > 2 mm		boundstone			
contains carbonate mud (particles less than 0.03 mm diameter)		mud absent		matrix supported	grain supported	organisms acted as baffles	organisms encrusting and binding	organisms building a rigid framework
mud-supported		grain supported						
less than 10% grains	more than 10% grains							
mudstone	wackestone	packstone	grainstone	floatstone	rudstone	bafflestone	bindstone	framestone

Figure 14. Dunham's Carbonate Classification (Tucker, 1982)

contains the subhedral dolomite crystals with an average grain size of 30–50 microns. Micritic dolomitic matrix is prevalent and cements easily. There is little or no intercrystalline porosity. Moldic porosity resulted from dissolution of fossils, but fill with late stage baroque dolomite. The intertidal facies bioturbations cause a bimodal texture within the thin section (see Figure 15).

The anhedral Xenotopic A dolomite, located in the near subtidal facies, has an average grain size of 20–30 microns, and contains at least 50% micrite. The rock is completely cemented. The only observed porosity is minor amounts of fracture porosity and moldic porosity resulting from dissolution of fossils.

Constituents

The major constituents are three types of dolomite: 1.) cloudy dolomite, 2.) clear dolomite, and 3.) baroque dolomite. Dolomitized pellets of local importance are present in the rock. The average grain size of the pellets is 20–40 microns (see Figures 16–17). Quartz grains make up one to three percent of the total constituents of the rock (see Figure 18). Calcite, a late localized cement, partially fills the intercrystalline porosity (see Figure 19–20). Dedolomitized calcite, which is observed in some of the rocks, is discussed later. Silica replaces anhydrite in the form of chert, chalcedony or megaquartz. Silica is also reconstituted and precipitated as chert within the pore spaces (see Figure 21). Carbonate silty components and illitic clays are observed in thin sections (see Figure 22–24). The illitic clay is believed to be a result of recrystallization of siliceous carbonate mud. Pyrite is observed in trace quantities. Sphalerite is a trace constituent believed to result from hydrothermal mineralization (see Figure 25).

Paragenesis

Paragenesis is a general term for the order of formation of associated minerals in time succession in the Henryhouse (see Figure 26 for diagram of paragenetic sequence.) In the initial stages of deposition, facies dependent limestone is deposited. In shallow water environments, gypsum is deposited. Silica grains, an influx of clastic material, are deposited among the lime. During deposition, burrowing organisms rework the sediment.

Shortly after deposition, hypersaline brines percolate through the sediment and dolomitize selected rock. At a similar point carbonate siliceous silts are transformed into illite clays.

A second phase of fresh water mixing dolomitization occurs and preferentially creates intercrystalline porosity. At this time, the moldic porosity is formed. Chert and chalcedony

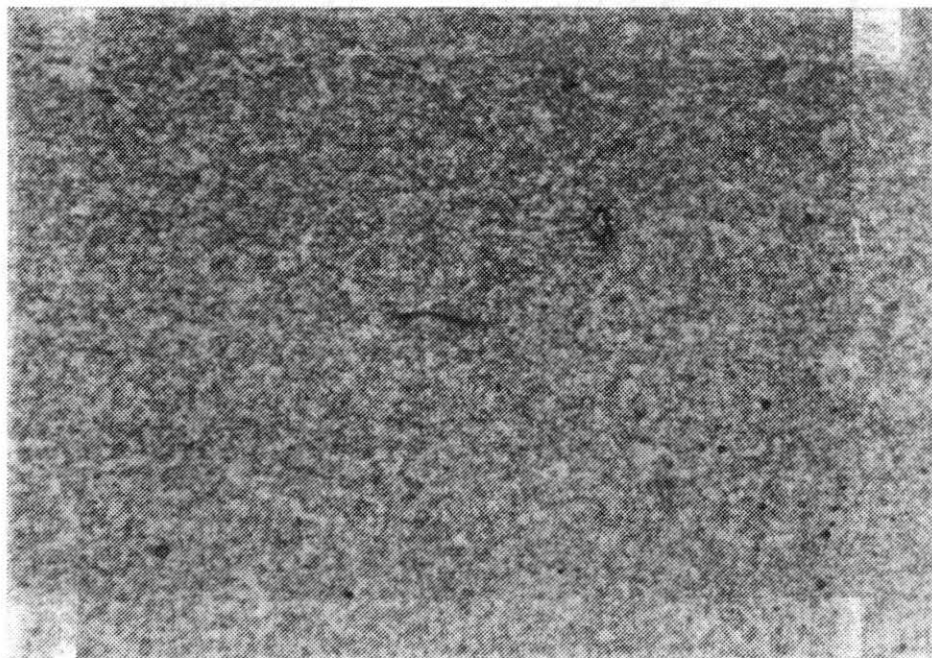


Figure 15. x20 Plane Polarized Light. Intercrystalline
Bioturbated Porosity versus
Non-Bioturbated Rock

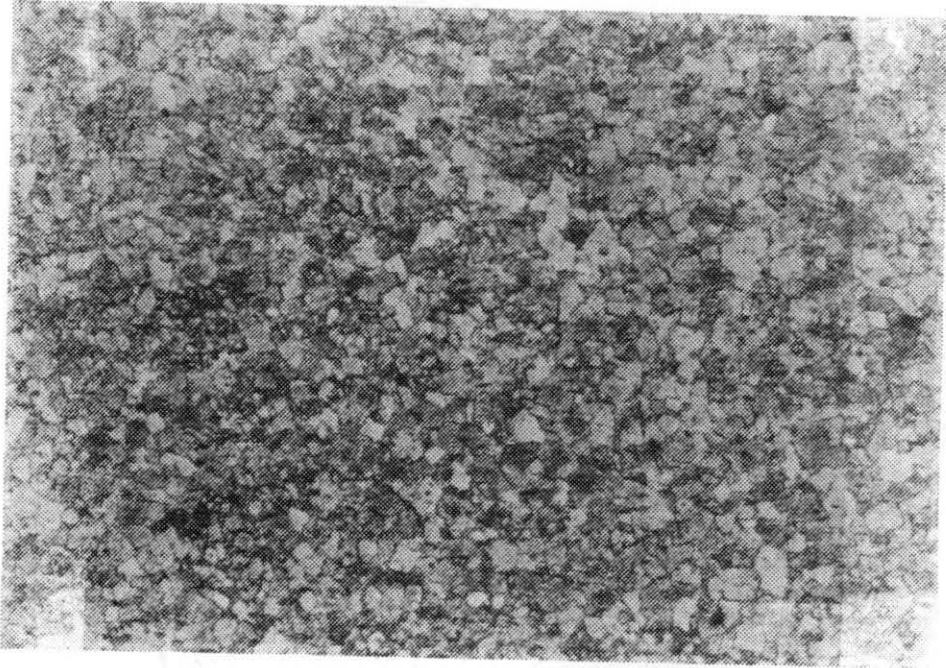


Figure 16. x40 Plane Polarized Light. Completely Cemented Dolomitized Pellet

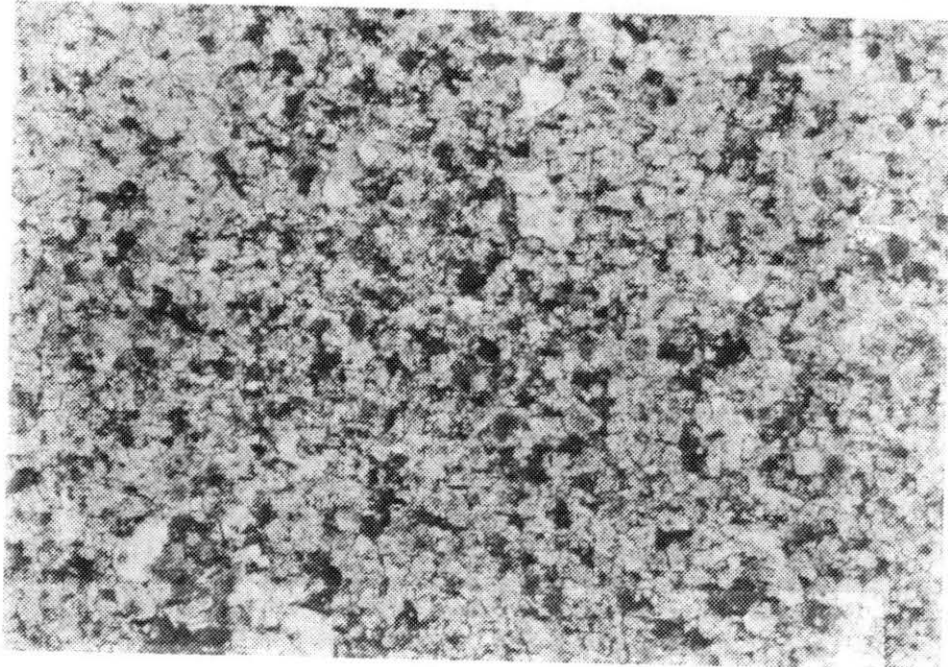


Figure 17. x40 Crossed Nicols. Dolomitized Pellets

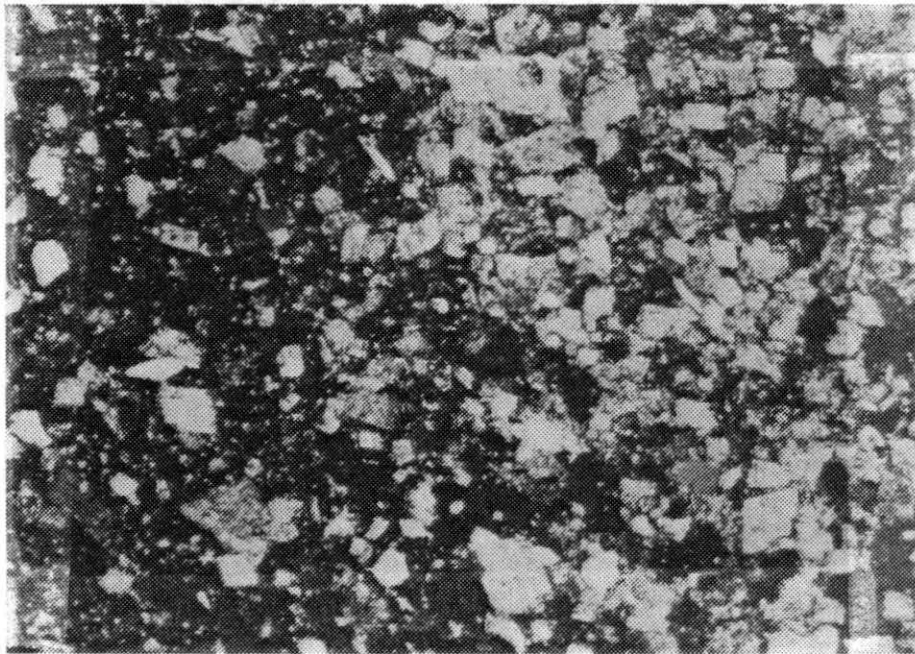


Figure 18. x40 Crossed Nicols. Rounded Silica Grain
(Note slight corrosion around the edges)

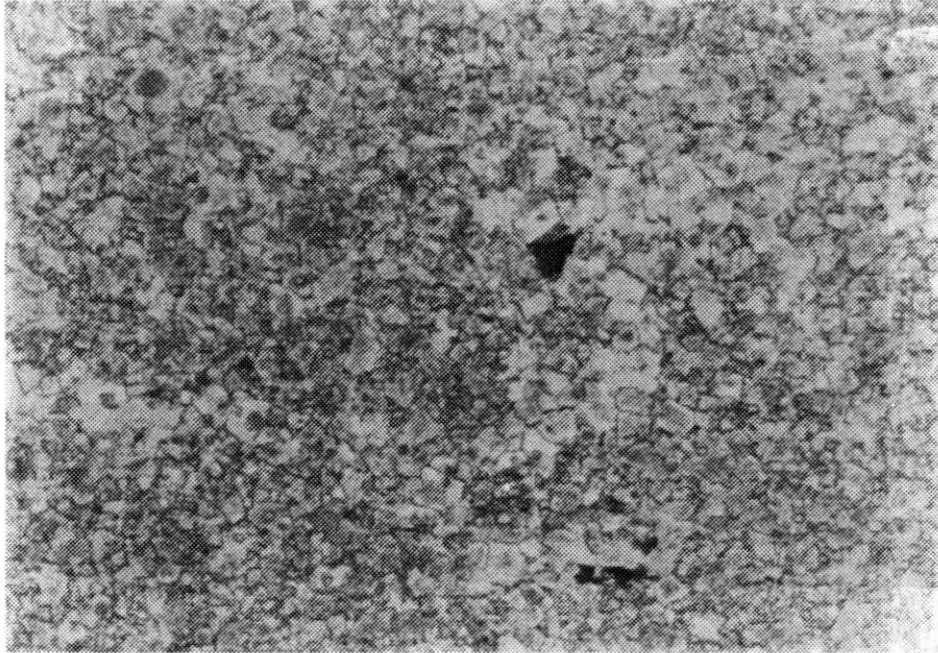


Figure 19. x40 Plane Polarized Light. Calcite Cement Filling Intercrystalline Porosity (Note cloudy centers and clear rims)

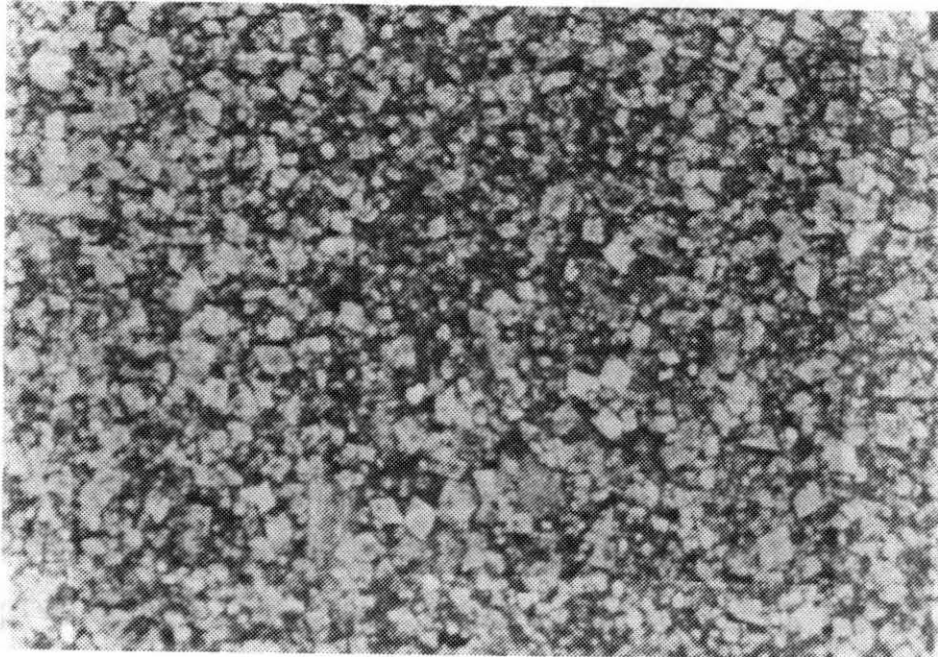


Figure 20. x40 Plane Polarized Light. Dolomite Rhombohedra Cemented with Calcite

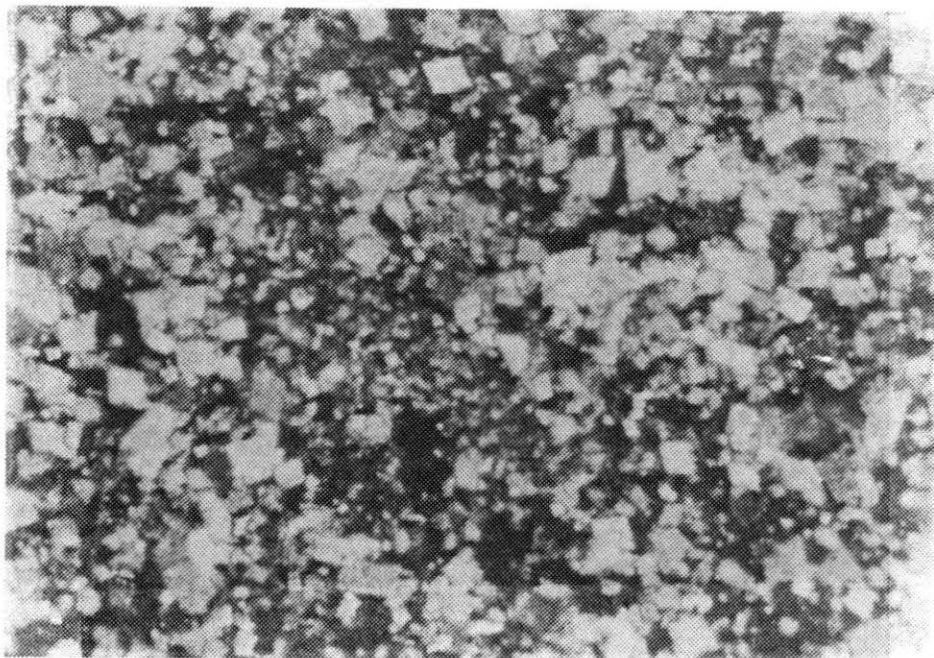


Figure 21. x100 Crossed Nicols. Chert Precipitated within Enlarged Moldic Porosity

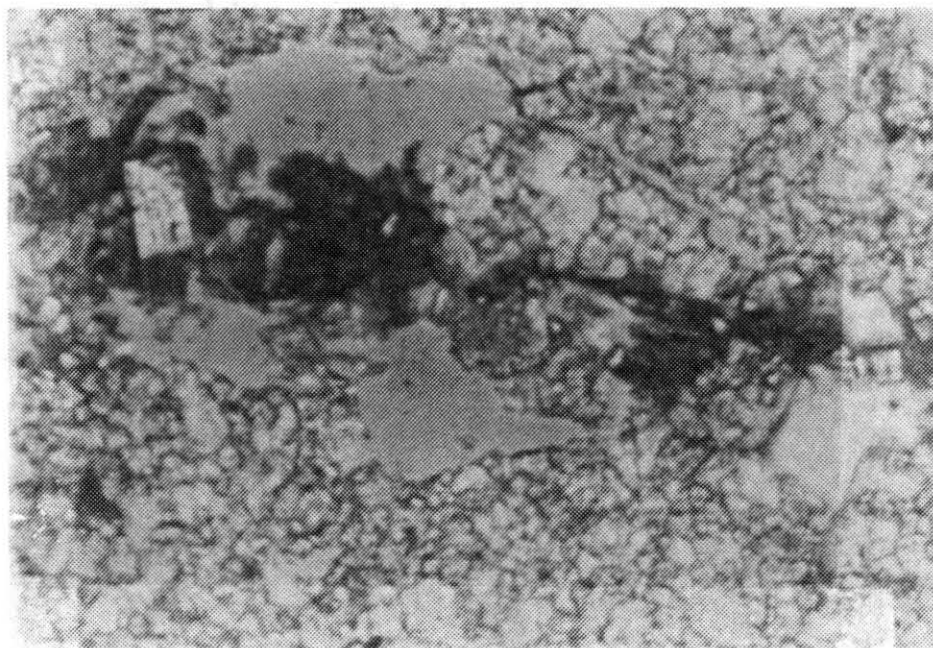


Figure 22. x100 Plane Polarized Light. Illitic Clays Recrystallization of Siliceous Carbonate Mud

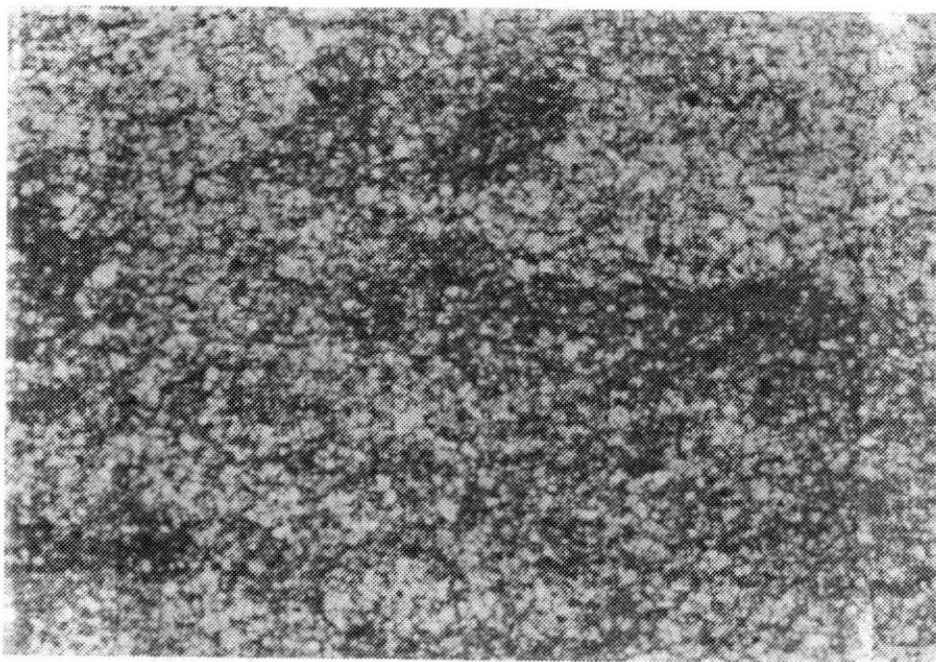


Figure 23. x40 Plane Polarized Light. Fine Grained Micrite with Organic Clays

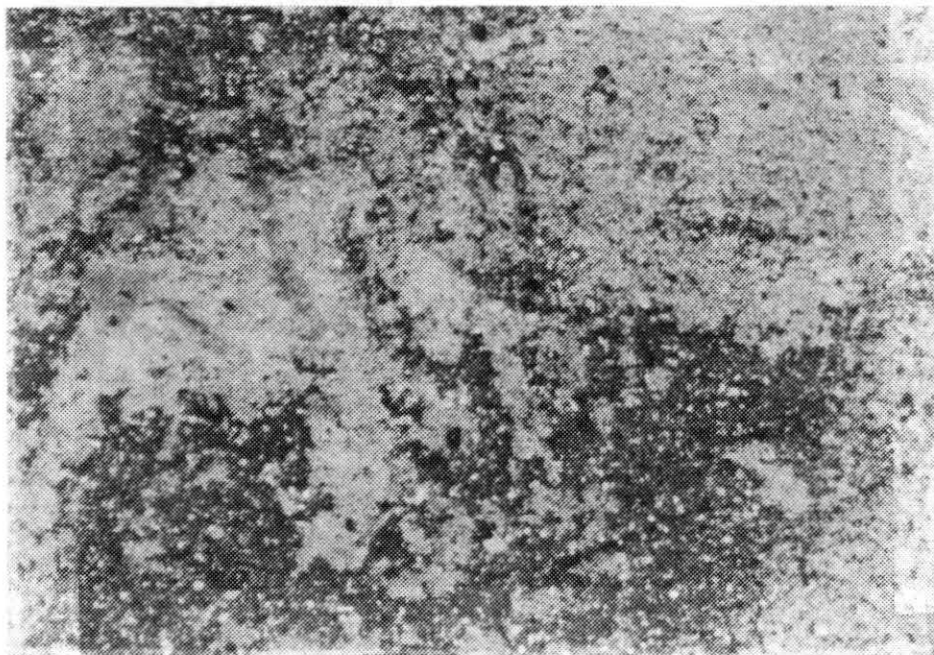


Figure 24. x20 Crossed Nicols. Siliceous Carbonate Clay (Note Anhydrite Laths and Calcite Cement)

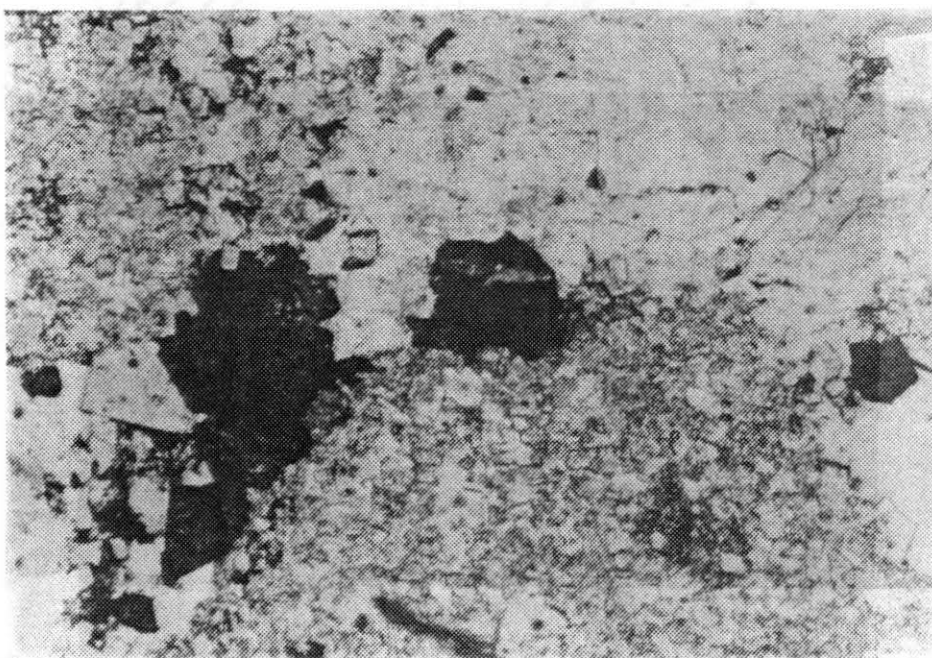


Figure 25. x40 Plane Polarized Light. Sphalerite

Paragenetic Sequence of the Henryhouse Formation

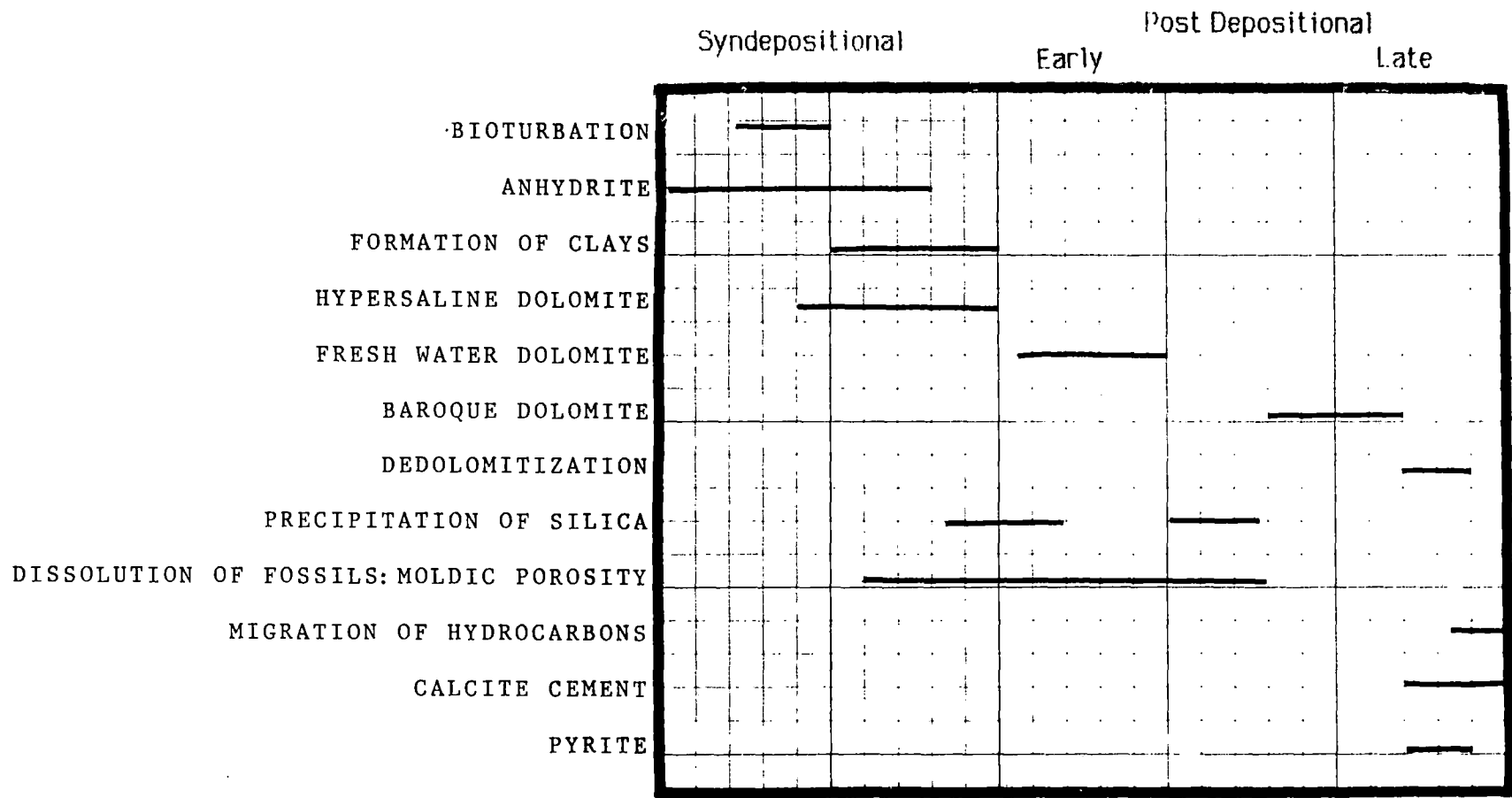


Figure 26. Paragenetic Sequence

precipitate. Chalcedony and megaquartz replace anhydrite (see Figures 27-30).

The rock subsequently becomes buried by overlying sediments. Compaction by the sediments results in fracturing and formation of horizontal stylolites. The environment pH becomes alkaline and calcite precipitation begins with subsequent dedolomitization.

The final stage is deeper burial, and baroque dolomite formation. Pyrite is associated with this stage. Hydrocarbon migration occurs shortly after the precipitation of pyrite and baroque dolomitization.

Porosity

Two general porosity types in carbonate rocks are fabric selective and non-fabric selective (Choquette and Pray, 1970) (see Figure 31). Two fabric selective porosity types are observed in the Henryhouse: moldic and intercrystalline (Beardall, 1983). The non-fabric selective porosity type is fracture porosity.

Moldic porosity is established by dissolution of fossils (see Figure 32). The fossils were completely dissolved, or fossil remnants remain within the mold and become dolomitized (see Figure 33). Baroque dolomite occasionally fill the molds (see Figure 34). Although moldic porosity accounts for a significant percentage of the total porosity, this porosity is often ineffective because the pore spaces are not interconnected.

The preferential development of intercrystalline porosity in the intertidal zone is caused by the loosely packed carbonate in the bioturbated zone which increases the permeability. The permeability increase results in better circulation of the dolomitizing fluids. The intertidal zone is dolomitized because of the rock location in relation to the freshwater mixing lense. Intercrystalline porosity is also caused by dolomitization (see Figure 35-36). When changing limestone to dolomite, there is an increase in porosity due to volume change (Tucker, 1982).

Enlargement of porosity types by dissolution increases effective porosity, thus increasing the reservoir potential. Dissolution commonly causes enlarged moldic or enlarged intergranular porosity (see Figure 37).

Fracture porosity is minor in importance. When present, the amount of fracture porosity is usually only about three percent of the total rock. Fracture porosity does not effectively increase the reservoir porosity, but possibly increases the amount of dolomitizing fluids in contact with the rock. Fractures are believed to enhance the process of dedolomitization (see Figure 38-39) by allowing the calcium rich waters to circulate throughout the rock. In some instances, fractures fill with a late phase of baroque dolomite.

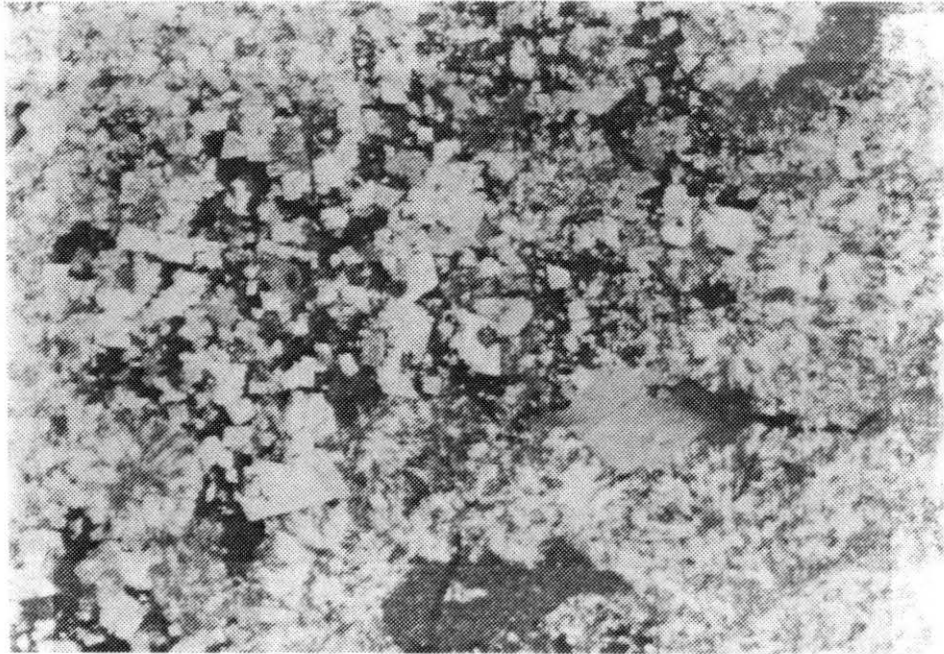


Figure 27. x40 Crossed Nicols. Chalcedony Replacing Anhydrite

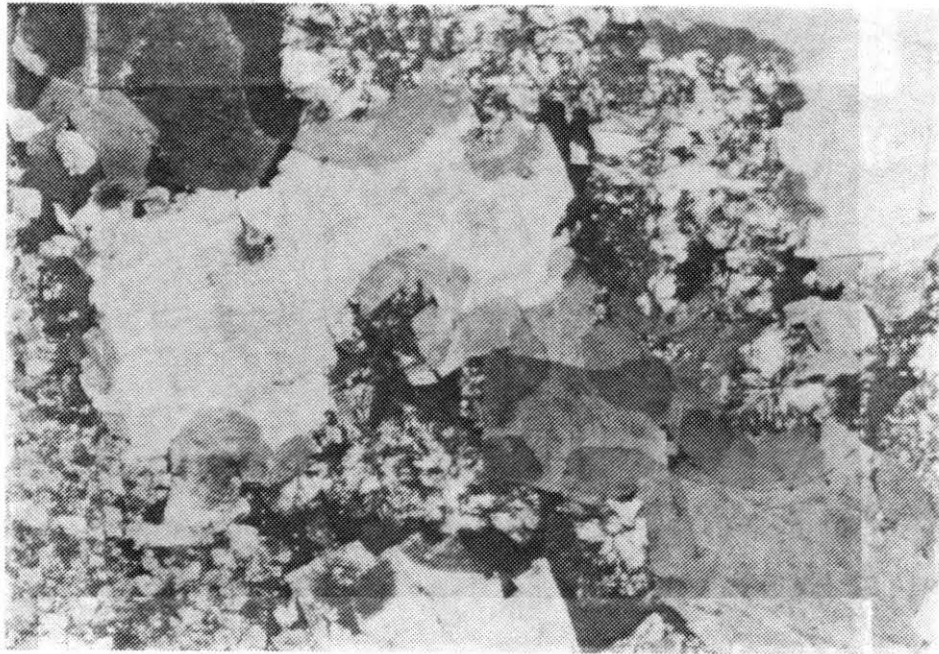


Figure 28. x40 Crossed Nicols. Chalcedony Replacing Anhydrite and Baroque Dolomite

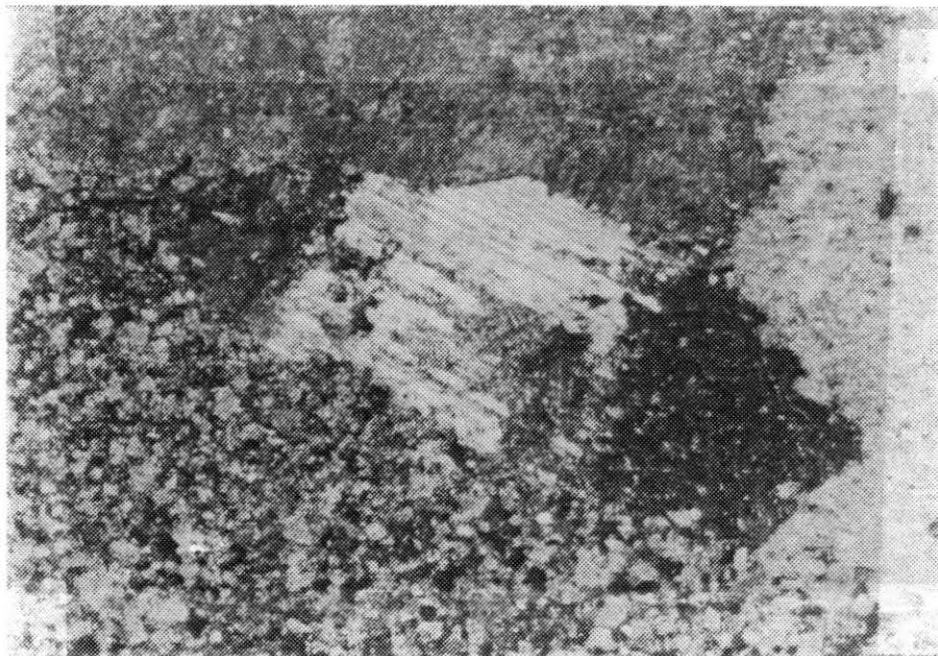


Figure 29. x40 Crossed Nicols. Silica Replacing Anhydrite, Surrounded by Calcite

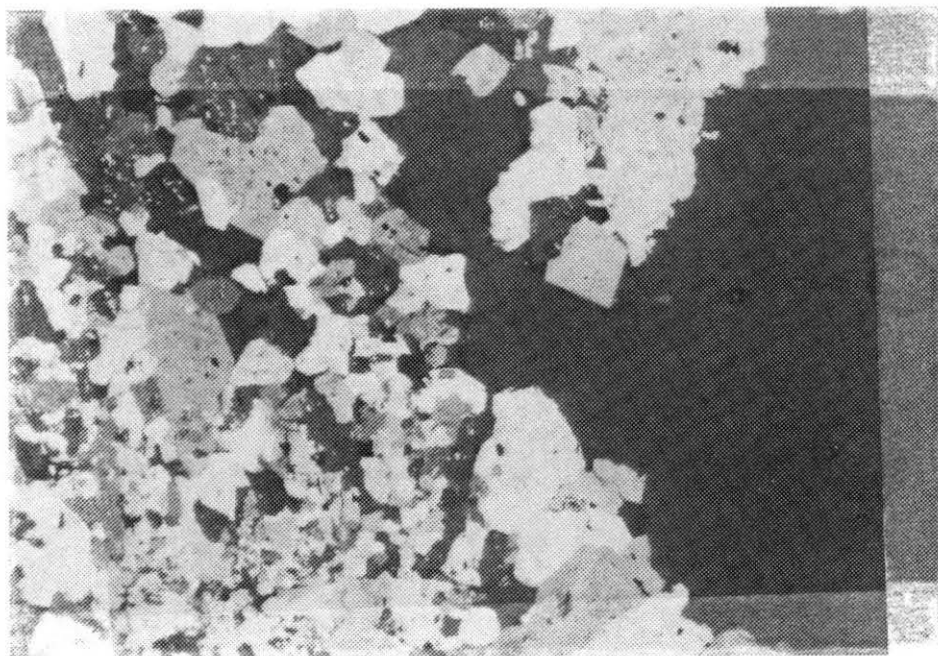


Figure 30. x20 Crossed Nicols. Silica Replacing Anhydrite Nodule (Note oil filled porosity)

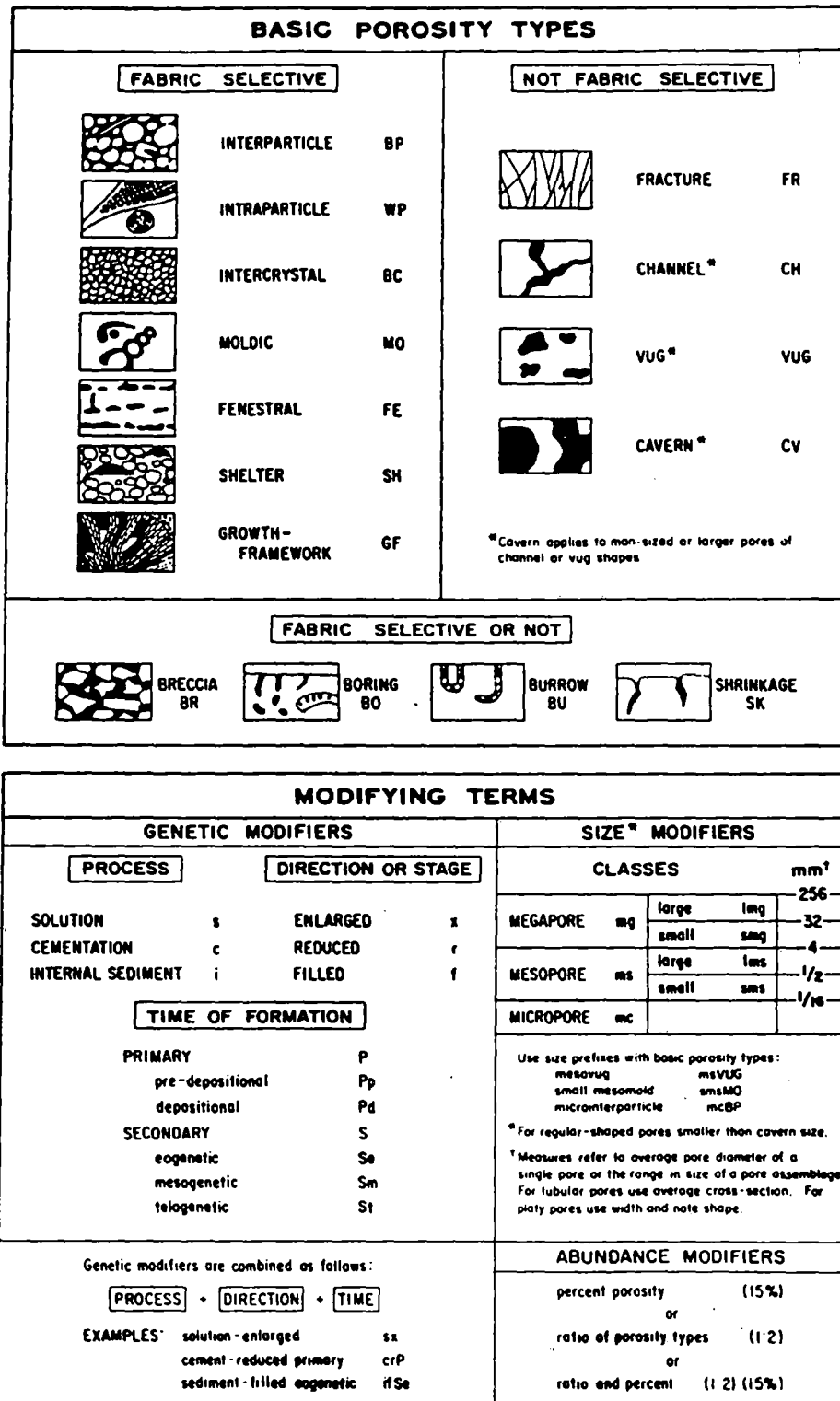


Figure 31. Porosity Types in Carbonate Rocks (Choquette and Pray, 1970)

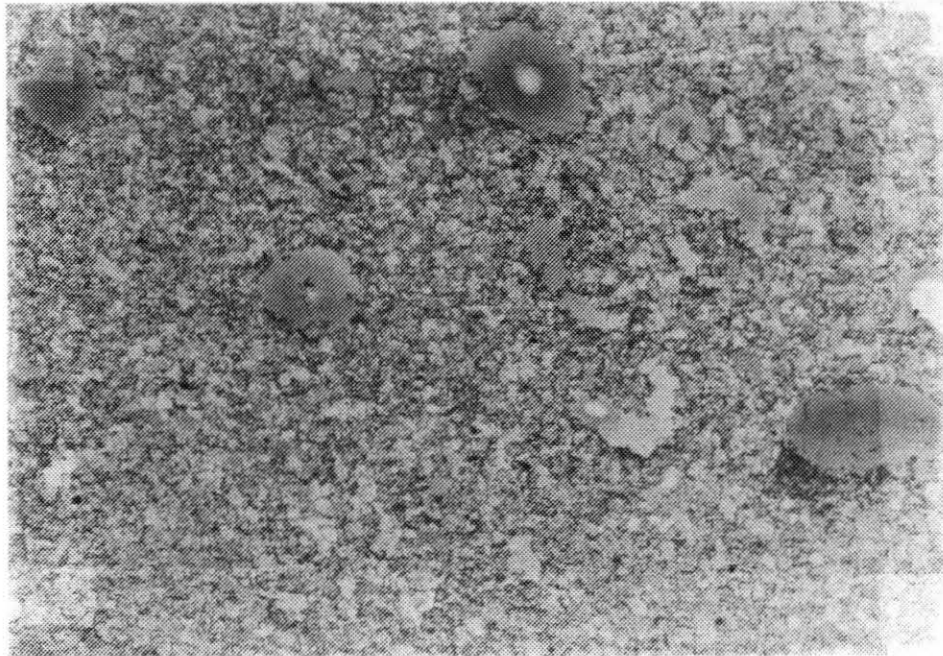


Figure 32. x20 Plane Polarized Light. Moldic Porosity

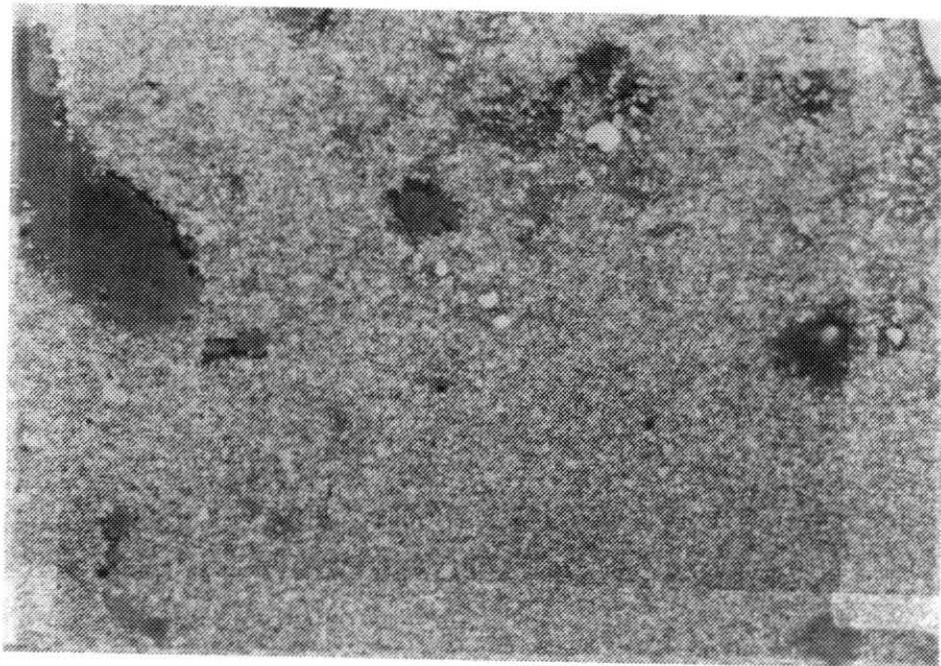


Figure 33. x20 Plane Polarized Light. Moldic Porosity and Dissolution of Fossils

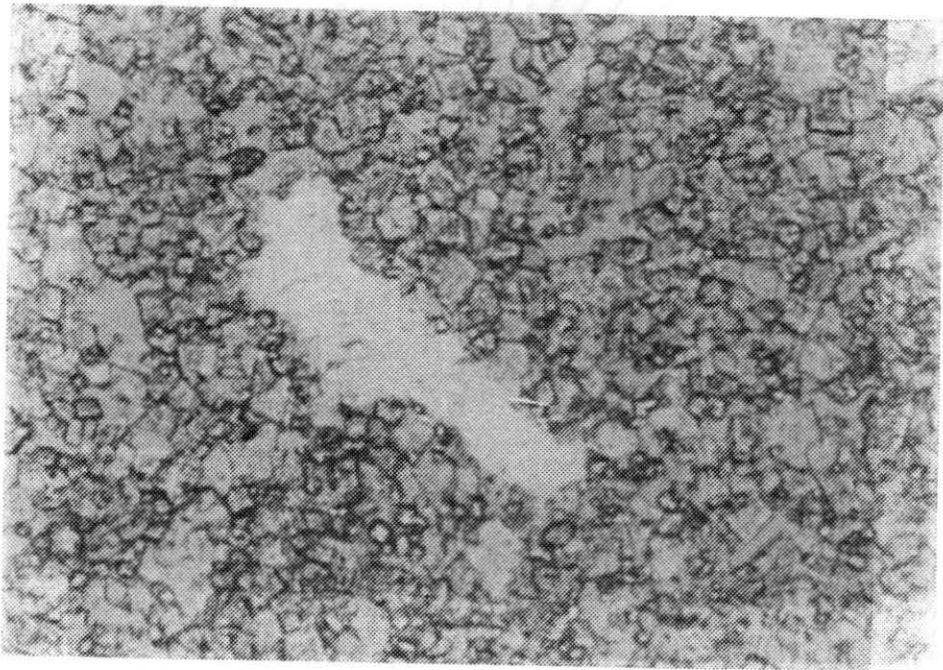


Figure 34. x40 Crossed Nicols. Molds Filled with Baroque Dolomite.

Dolomite

Three types of dolomite are recognized in the Henryhouse: 1.) cloudy dolomite, 2.) clear dolomite, 3.) baroque dolomite.

Cloudy dolomite results from dolomite growing in a void as a pore filling cement, or because of calcite dissolution demanded by growing dolomite. The dolomite grows by replacement of calcite, and is cloudy due to silty inclusions accumulated through growth. The eogenetic hypersaline brine model is the accepted model for the formation of the cloudy dolomite (Beardall, 1983; Manni, 1984) (see Figure 40). During deposition, the Henryhouse was located at 10 degrees south of the equator (see Figure 7).

Due to the continent's geographic location, it is probable that the environment was semi arid to arid, and conducive to hypersalinity in shallow epiceric seas if evaporation exceeded precipitation (Manni, 1984). Evidence seen in thin sections indicative of a hypersaline environment include: 1.) cloudy rhomb centers, 2.) anhydrite laths, and 3.) replaced anhydrite nodules.

Clear dolomite formed by the fresh water mixing model (see figure 41) is white, limpid, translucent euhedral crystals. The euhedral crystals are usually zoned.

Mixed water dolomitization occurs when a zone of fresh water comes into contact with ocean water. The fresh water, likely to come from rainfall, mixes with the ocean water and forms a brackish zone. The mixing of these two waters drastically reduces the salinity, while the Mg/Ca ratio remains high because the amounts of Mg and Ca from the fresh water are very small compared to large amounts found in sea water. This decrease in salinity results in the formation of dolomite (Folk and Land, 1975)." (Manni, 1984 p. 47).

Evidence for the mixing model is clean rhombohedral overgrowths (see Figure 42) and zonation indicated by cathodoluminescence from previous studies by (Beardall, 1983) and (Manni, 1984).

Baroque dolomite is the late stage deep-burial dolomite. This dolomite type is characterized by curved crystal faces and undulose extinction. Baroque dolomite fills the inter-crystalline and moldic pore spaces (see Figure 43-44). The presence of baroque dolomite in fractures indicates a late, relatively deep burial diagenetic mineral. The crystal begins growing on a nucleus (perhaps an inclusion), and begins to fill the mold (see Figure 45). Baroque dolomite is a common form of tectonic dolomite, associated with hydrocarbons and sulfide mineralization. Baroque dolomite, which has been synthesized at temperatures of 60 degrees centigrade and more, is a possible paleotemperature indicator (Tucker, 1982).

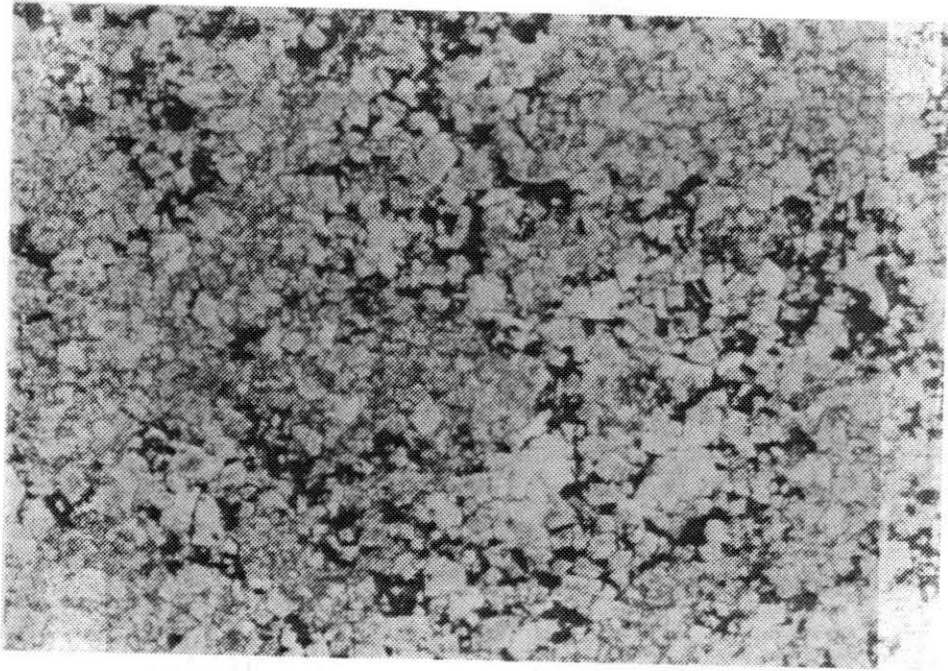


Figure 35. x40 Plane Polarized Light. Intercrystalline Porosity Filled with Oil

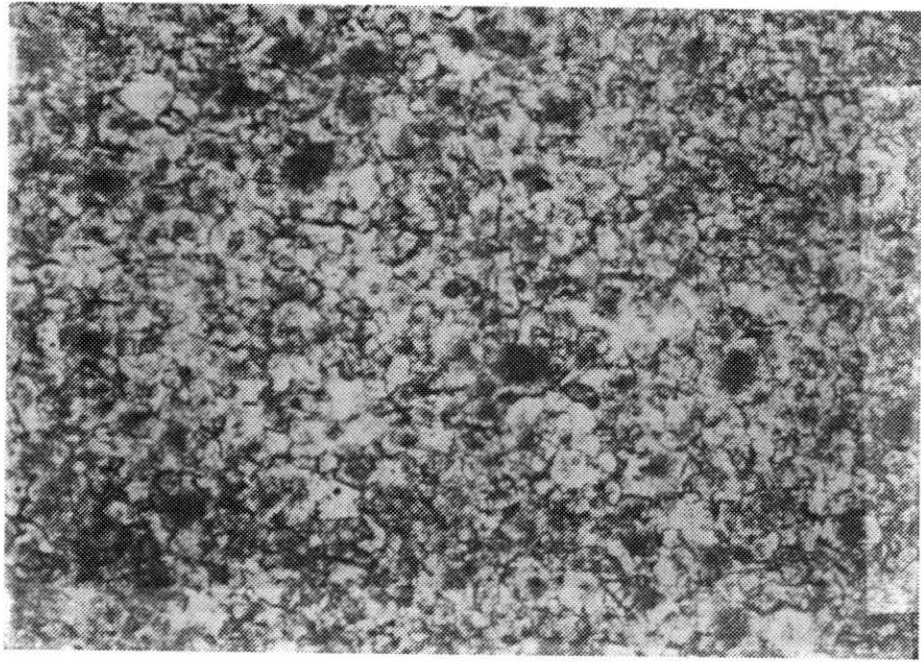


Figure 36. x40 Plane Polarized Light. Intercrystalline Porosity (Note dolomitized pellets)

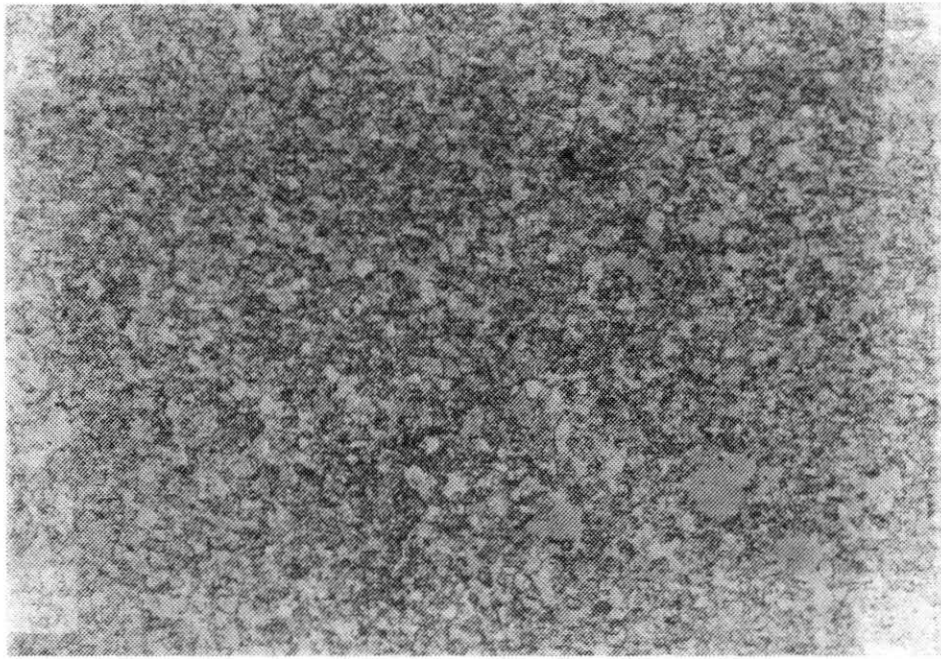


Figure 37. x40 Plane Polarized Light. Enlarged Intercrystalline and Moldic Porosity

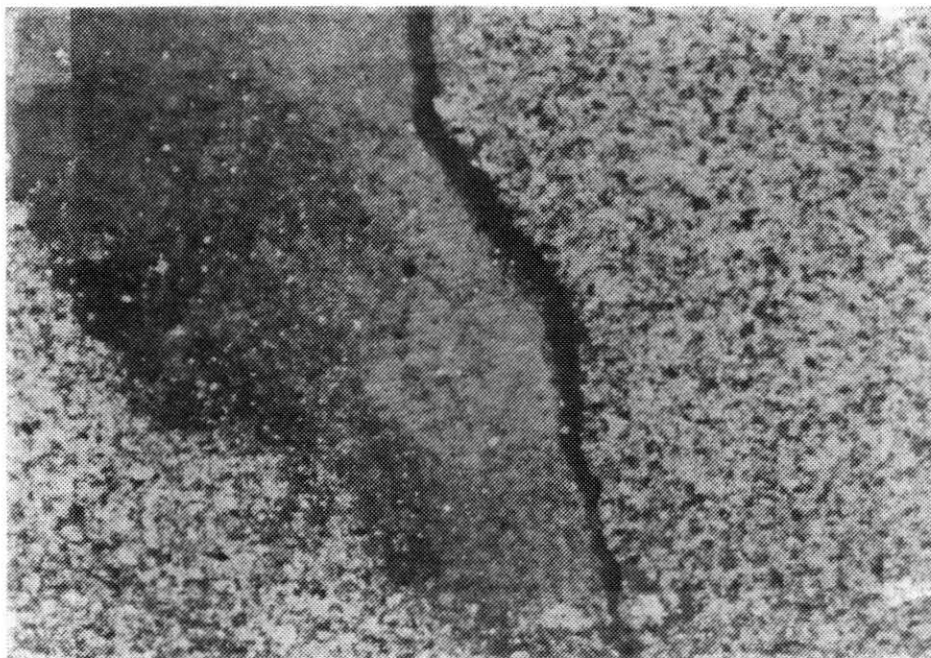


Figure 38. x20 Crossed Nicols. Fracture Porosity
Enhancing Precipitation of Calcite
Cement



Figure 39. x40 Crossed Nicols. Fracture Porosity,
Siliceous Carbonate and Calcite
Cements

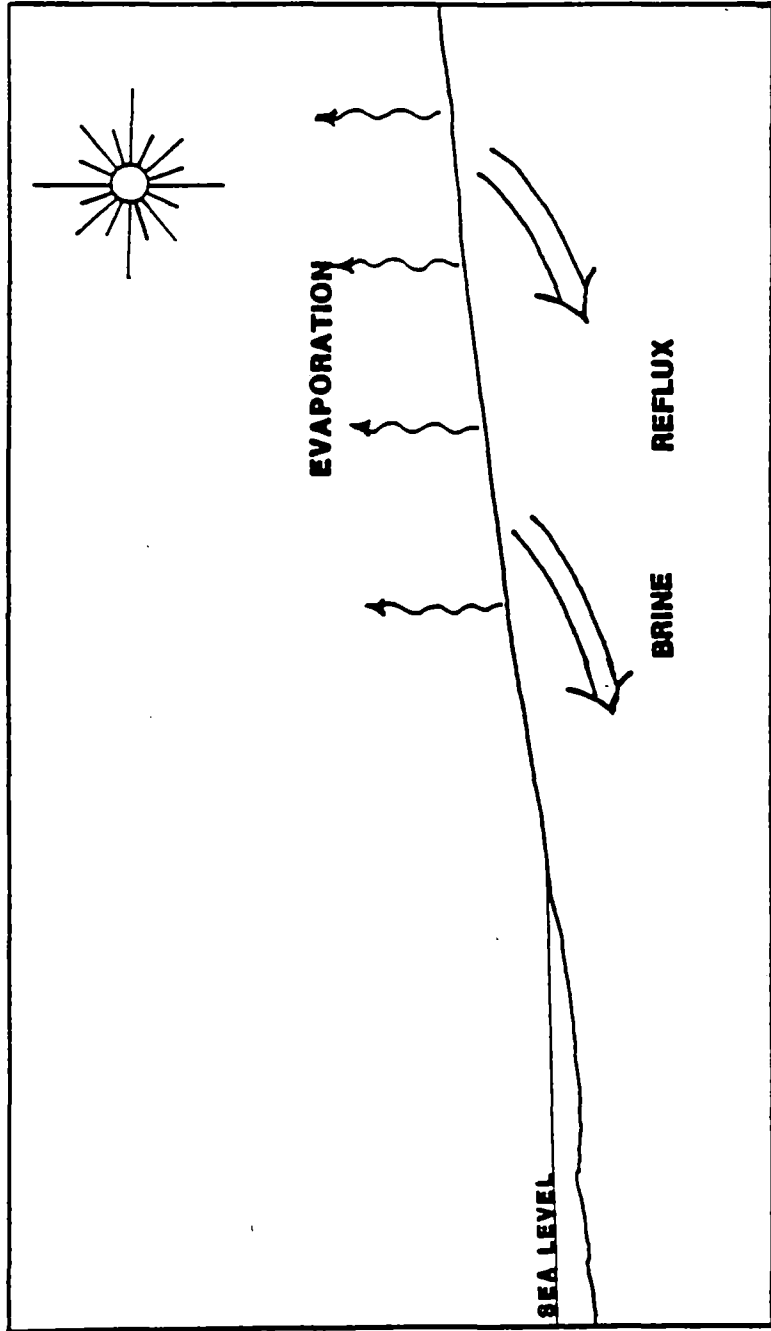


Figure 40. Hypersaline Brine Dolomitization Model
(Manni, 1984)

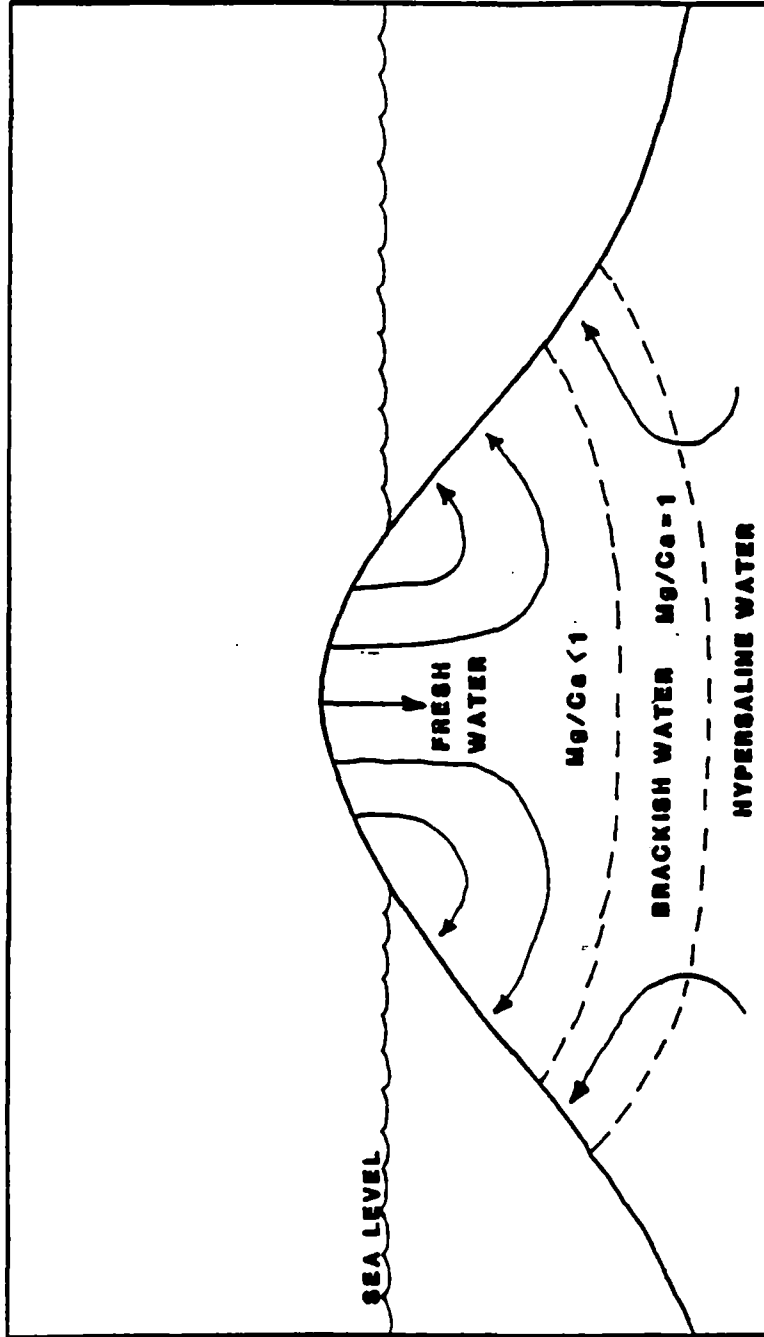


Figure 41. Fresh Water Mixing Dolomitization Model
(Menni, 1984)

Dedolomitization

Dedolomitization is believed to occur in the late phases of diagenesis. The calcite selectively replaces the dolomite. The amount of calcite resulting from dedolomitization does not exceed 15%. This percentage of calcite is derived from X-Ray diffractions from previous studies by Beardall and Manni.

Dedolomitization occurs when carbonate-rich waters with a high Ca/Mg ratio flow through dolomitized rocks. The migration of these fluids results in the dissolution of dolomite and the precipitation of calcite. Where gypsum and/or anhydrite is present, the dissolution of dolomite is enhanced. This occurs because the dissolution of gypsum/anhydrite releases Ca into the system (Manni, 1984).

Dedolomitization evidence is indicated by partial replacement of dolomite with calcite, relict rhombs or corrosion of dolomite by calcite (see Figure 46). Calcite cements the pore spaces, and corrodes the dolomite (see Figure 47). Under new fresh water conditions, dolomite is not stable.

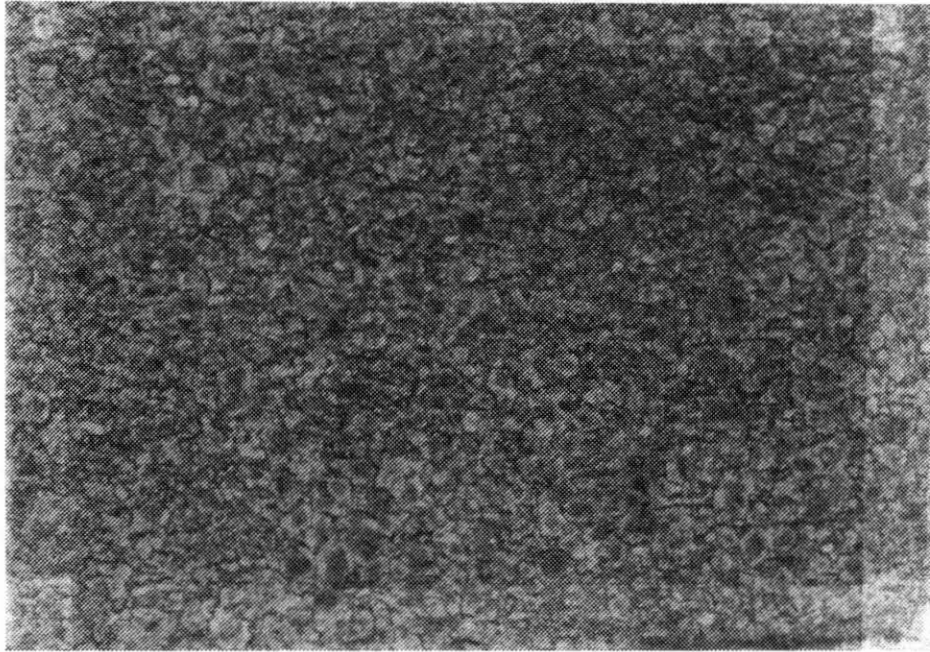


Figure 42. x40 Plane Polarized Light. Cloudy Center
and Clear Rim Dolomite Rhombohedra,
Intercrystalline Porosity

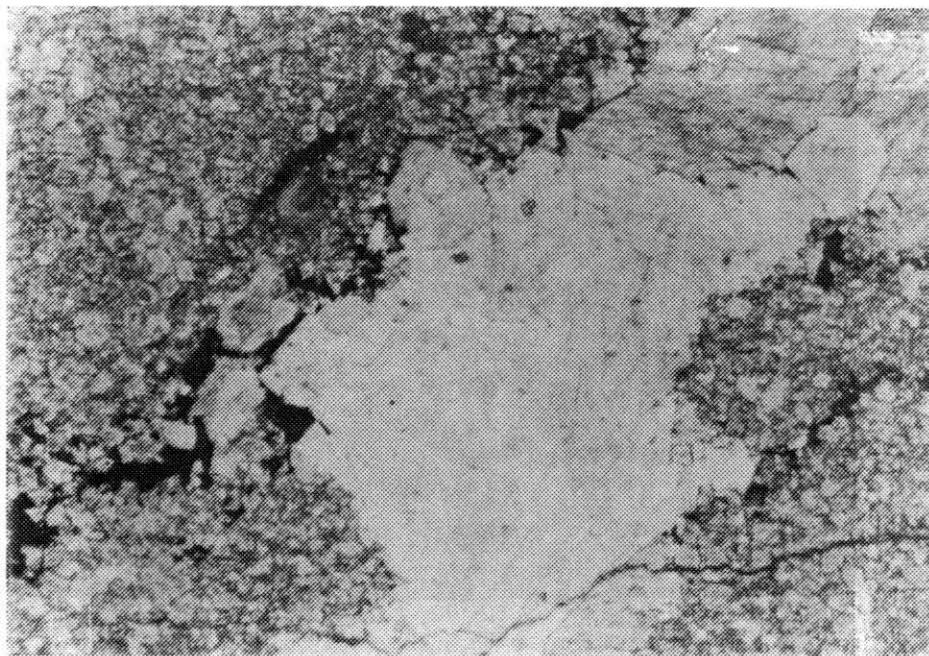


Figure 43. x40 Plane Polarized Light. Baroque Dolomite (Note fracture filled with oil)

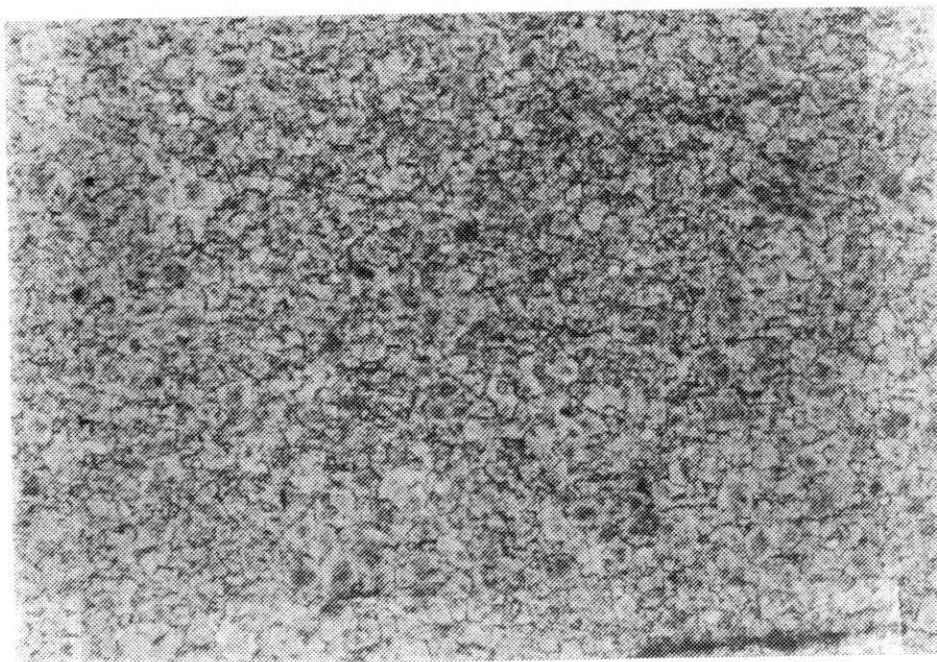


Figure 44. x40 Plane Polarized Light. Baroque Dolomite Filling Molds (Note dolomitized pellets)

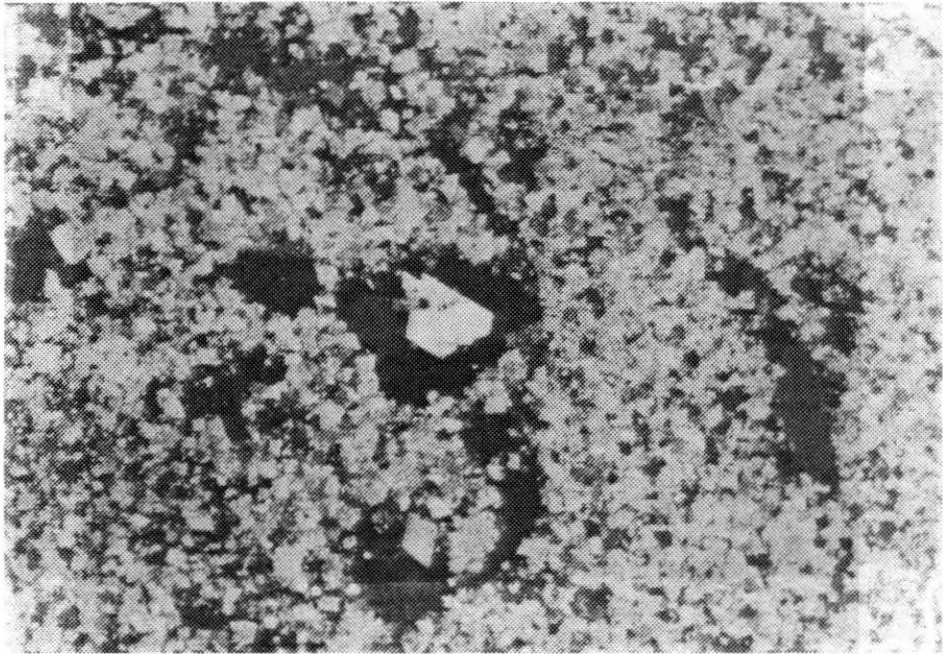


Figure 45. x40 Crossed Nicols. Baroque Dolomite
Inside an Enlarged Mold

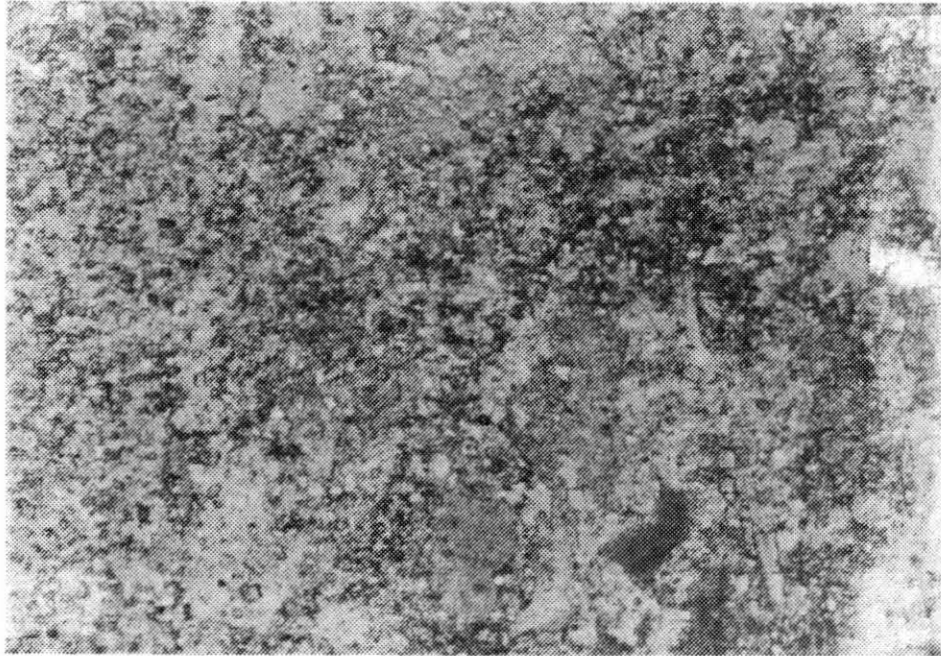


Figure 46. x20 Crossed Nicols. Dedolomitized Rhombohedra

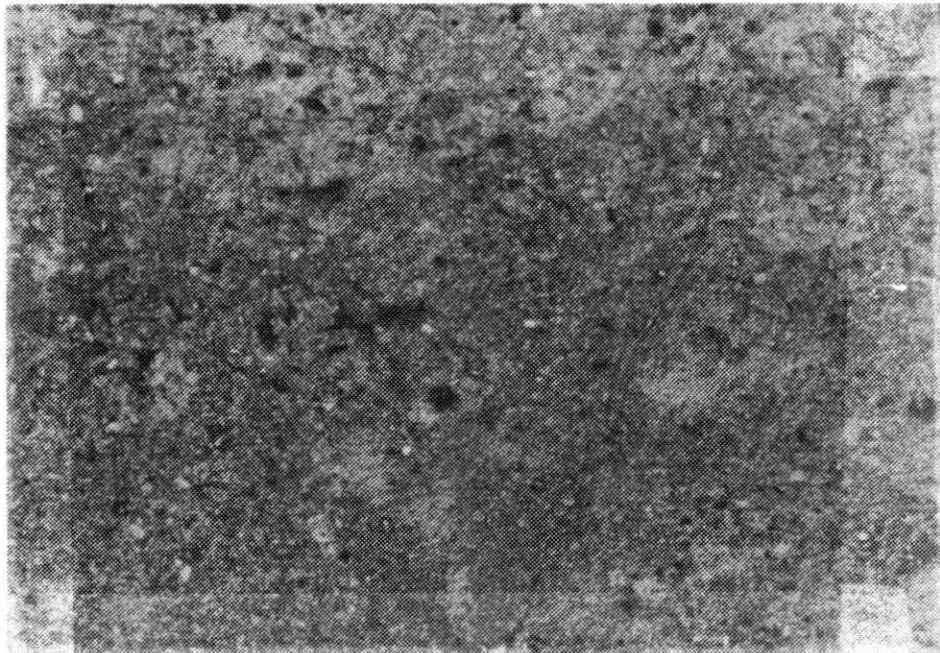


Figure 47. x40 Crossed Nicols. Calcite Cement, indicative of dedolomitization shows Dolomite Rhombohedra and Silica not yet Replaced

CHAPTER V

MAPPING TECHNIQUES

Introduction

A variety of maps were prepared as an attempt to recreate the depositional environment. The types of maps included structural contour maps, isopach maps, facies maps and porosity maps. The thirteen maps are:

1. Structural contour map of the base of the Woodford Shale
2. Structural contour map of the top of the Sylvan Shale
3. Isopach map on the Woodford Shale
4. Subcrop map on the pre-Woodford unconformity
5. Isopach map of the total Hunton interval
6. Hunton Production Map
7. Isopach map of zone B-3 (the lower producing zone)
8. Isopach map of zone B-4 (the upper producing zone)
9. Facies map of zone B-3
10. Facies map of zone B-4
11. Porosity map of zone B-3
12. Porosity map of zone B-4
13. Map of the inferred faults.

This series of maps was prepared to delineate specific characteristics necessary for generation of prospects.

Woodford Structure Map

The structural contour map on the base of the Woodford shale represents an unconformity surface (see Plate 1). The map represents the paleotopography of the erosional surface present during the time of deposition of the Woodford. The regional dip is toward the southwest. Minor troughs are believed to be related to the subsequent Woodford channels. Faults are believed to be present, but are not mapped at this time because of lack of seismic data. Reference is made to the faults later in this text.

Sylvan Structure Map

The structural contour map of the top of the Sylvan indicates the structure of the Hunton

because the Hunton conformably overlies the Woodford (see Plate 2). The homoclinal dip is toward the southwest, and strongly resembles the structural contour map of the base of the Woodford. Antinclinal and synclinal noses illustrated in the map trend north-northeast to south-southwest. Some of the structural highs remain as prominent features on the Woodford isopach map. Although the author believes there is a possibility of faulting in the region, no faults are mapped because of the lack of geophysical data to support the assumption.

Woodford Isopach Map

The Woodford isopach map represents the total thickness from the top of the Hunton to the top of the Woodford Shale (see Plate 3). The Woodford channels directly relate to the zones of dolomitization during the fresh water mixing phase of dolomitization, and therefore serve as an important indicator for location of reservoir rocks. The Woodford, divided into two zones, upper and lower, further delineates the erosional troughs because depositional accumulations are located in the paleotopographic lows. The lower Woodford is absent in the study area; the upper Woodford is the only zone investigated. The lack of lower Woodford indicates the deposition was paleotopographically high in relation to other regions on the shelf hinge. A major northwest-southeast trending channel is present in the middle of the map and the Woodford accumulates a thickness of 70 feet where the channel is observed (see Plate 3). The minor channels trend northeast-southwest, and intersect the major channels at right angles. The dendritic drainage pattern of the Woodford is observed. A relationship exists between the structural contour map on the base of the Woodford and the isopach map of the Woodford. The structural highs receive less sediment because the Woodford is differentially deposited and the lows fill with sediment. There is a relationship between the Woodford thins (less than or equal to 50 feet) and the production. Hunton production generally occurs where the Woodford is thin.

Subcrop Map

Initial correlation of electric logs with the core data developed individual zones representing depositional packages (see Figure 3). The subcrop map is a map view of the paleogeology during Woodford deposition (see Plate 4). The map is prepared for the purpose of assisting the geologist in analyzing the appropriate Hunton thickness, erosional patterns, and possible dolomitization patterns. The subcrop map also defines which zones are available intervals for production as a result of direct contact with the Woodford and subsequent truncation.

The distance of the truncation line from the locations of the wells is directly related to

the average thickness of the zone and the actual thickness on the logs. The isopach map and structural contour map of the Woodford are a primary consideration in the direction of truncation and erosion. Because of the density of control, little interpolation of data is necessary except for the northeast corner of the map for the B-1 zone (see Plate 4). Two points indicating the presence of the zone and the remainder is projected to mirror the truncation pattern of the B-2 zone.

The amount of exposed strata is related to the rocks' resistance to weathering. The B-4 and B-5 zones appear are more resistant than the underlying zones. Once the two upper resistant zones are removed, the zones below will erode more quickly. Evidence of channeling is indicated from the paleogeology. The paleogeology in section 34, T22N, R14W possibly indicates a southeast-trending channel which provides an "inlier" or exposure of older rocks surrounded by younger rocks. Other channel are believed to be located in section 20, T22N, R14W, section 20, T22N, R13W, a large channel in the northern part of the map through sections 2,3,4, T22N, R14W, and section 17, T21N, R13W which is a possible subsequent or tributary channel trending southwest leading into the major southeast system. The channels are important because of their relationship to the fresh water mixing dolomitization model.

Total Hunton Isopach Map

A total Hunton isopach map was prepared for the study area (see Plate 5). The total isopach map shows thinning and thickening related to localized highs and lows, regional trends of the erosional channels, and karstic topography.

The maps show the Hunton regionally thinning toward the northeast, and thickening towards the southwest. The thickest interval is interpolated as 500 feet thick. The most pronounced effect is the erosional channeling which caused removal of Hunton section. The lows appear to be parallel, trending toward the southwest. These lows are tributaries which developed a trellis drainage pattern that lead into a major southeast channel system. Due to the small size of the study area, reconstruction of the complete channel system is not prepared.

Production Map

A production map is prepared with cumulative production, and initial production, and drilling completion data (see Plate 6). All data are collected from scout cards and Petroleum Information biannual reports, December 1984 with the exception of the Tenneco wells. The Tenneco reports are from the Tenneco production department. The map is prepared as accurately as the data permits. Large discrepancies exist between Petroleum Information

reports and company production data.

Individual Zone Maps

Facies Maps

Through extensive core analysis and thin section examination, Al-Shaieb and Beardall identify specific facies within the Henryhouse. The dominant facies are the supratidal, the intertidal, and the subtidal. The supratidal is a fine grain micrite, typical of shallow water deposition and characterized by algae and anhydrite deposits. The supratidal facies is commonly a dense limestone in the subsurface. The intertidal is a bioturbated dolowackestone which is usually completely dolomitized. The bioturbation and subsequent dolomitization results in excellent intercrystalline porosity, and therefore is the reservoir rock. The subtidal is a dense micritic limestone consisting of a variety of fossil fragments. The zone may be partially dolomitized depending on the extent of the fresh water mixing lense. A subtidal shoal facies is also identified, but not discussed in this study because it is not an essential reservoir rock. The shallow subtidal zone is identified from work within this study, and is located on the outer fringes of the intertidal zone. The rock is a wackestone which may or may not be bioturbated. The shallow subtidal zone has some characteristics of the intertidal facies, but is not a reservoir rock. The porosity within the shallow subtidal zone is moldic or intercrystalline. The intercrystalline porosity usually becomes cemented prior to migration of the hydrocarbons.

The facies maps were a fundamental part of the regional subsurface analysis. These maps provide assistance in delineating possible reservoir rock since the reservoir rock is facies dependent. Lithologic logging and core calibrated wireline logs are the essential procedures in evaluating the regions of the facies. From analysis of core data and calibration of wireline logs, typical log signatures are developed to interpret the facies. A type log, which was developed by Al-Shaieb and Fritz, is used for identification of the facies (see Figure 48). The type log was the end product of a large regional study where many cores were analyzed. Another facies interpretation technique is the Pickett plot. Asquith explained the use of the Pickett plot:

Cross plots are used to identify log response-rock type relationships. Pickett's plots can only be used when core or cuttings from selected wells are available. Log responses from the control wells were cross plotted and then areas are outlined where the different rock types cluster. Once the clusters are established, log responses from wells without cores or cutting can cross plotted on the chart and the carbonate rock type and depositional environment determined. Facies maps can be constructed using the Pickett crossplot method. (Asquith, 1979, p. 40).

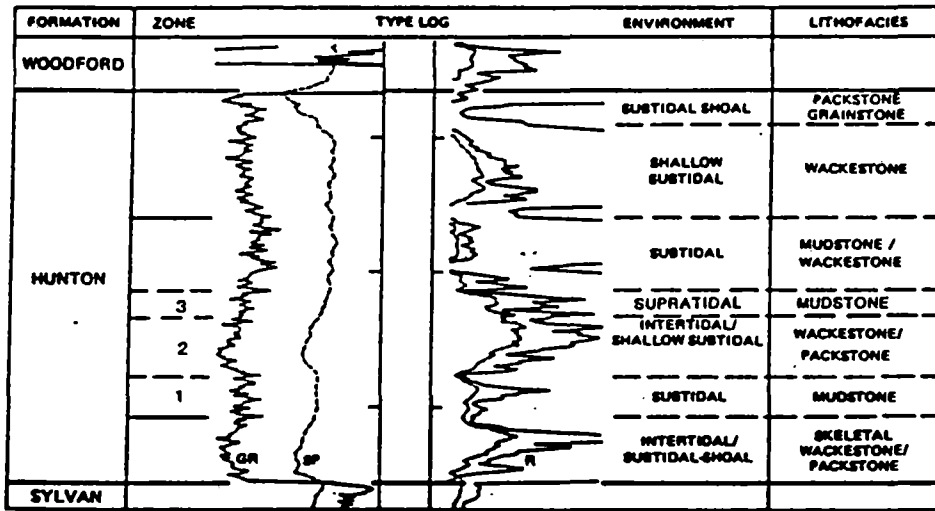


Figure 48. Calibration of Log Signature to Facies,
Henryhouse Formation (Al-Shaieb
1985)

The Pickett crossplot is prepared on triple cycle logarithmic scale graph paper. The percent of neutron porosity versus the resistivity in ohms is plotted. There are three control wells used in this study: 1.) Tenneco-Jordan A-1, 2.) Tenneco-Jordan 5, 3.) Aspen-Federal. The Aspen-Federal well is not in the immediate study area, but the data is chosen because the core has a representative supratidal facies. The data is plotted and clustered (see figure 49). The Pickett Plot is used to predict the environment of other well logs in the study area.

The mapped facies are the intertidal, shallow subtidal and subtidal zone (see Plates 7 and 8). The supratidal is not mapped because the facies is not present within the immediate area. The facies maps are important for locating the reservoir facies.

Interpretation of the facies maps is self-explanatory. The major differences between the two zones is the amount of available reservoir rock. The B-3 zone had more subtidal and less intertidal facies. The intertidal zones and the fringing shallow subtidal zone are less developed in the B-3 zone than in the B-4 zone. The subtidal zone in the B-3 facies map is the primary trapping mechanism. The dense subtidal rocks surround the porous intertidal rocks. The B-4 zone show widespread distribution of the reservoir rock across the study area, along with more intrafacies variation in this zone. An inlet of subtidal zone is seen in the B-4 facies map, and is an updip trapping mechanism. The subtidal zone observed in the southeast corner of the map may be shallow subtidal which is not affected by the freshwater dolomitization, and therefore results in a subtidal log character. Notice the lenticular geometry of the intertidal facies.

Isopach Maps

Isopach maps are prepared for the two productive zones (see Plates 9 and 10). The isopach maps indicate few specific regional trends, but do show minor depositional trends which assist in defining the reservoir rock. The productive intertidal rocks were deposited on the flanks of the thicks. The B-4 isopach shows an excellent example of an productive area not located on a thick or thin, but on the flank of a thick, in section 34, T22N, R14W. The production is bounded by areas of high elevation. The nonproductive limit is defined by the thins. The B-3 map showed an example of the thins defining the productive limit in sections 32 and 33, T22N, R14W. The flanks of the thick structures are stratigraphically important because it is a zone of depositional reworking. The intertidal zones occurred below wave base, but were deep enough to receive the nutrient rich sediment become bioturbated.

The facies which are deposited also determine the amount of fluctuation in thickness. Range 13 west is a relatively constant subtidal facies with minor amounts of change

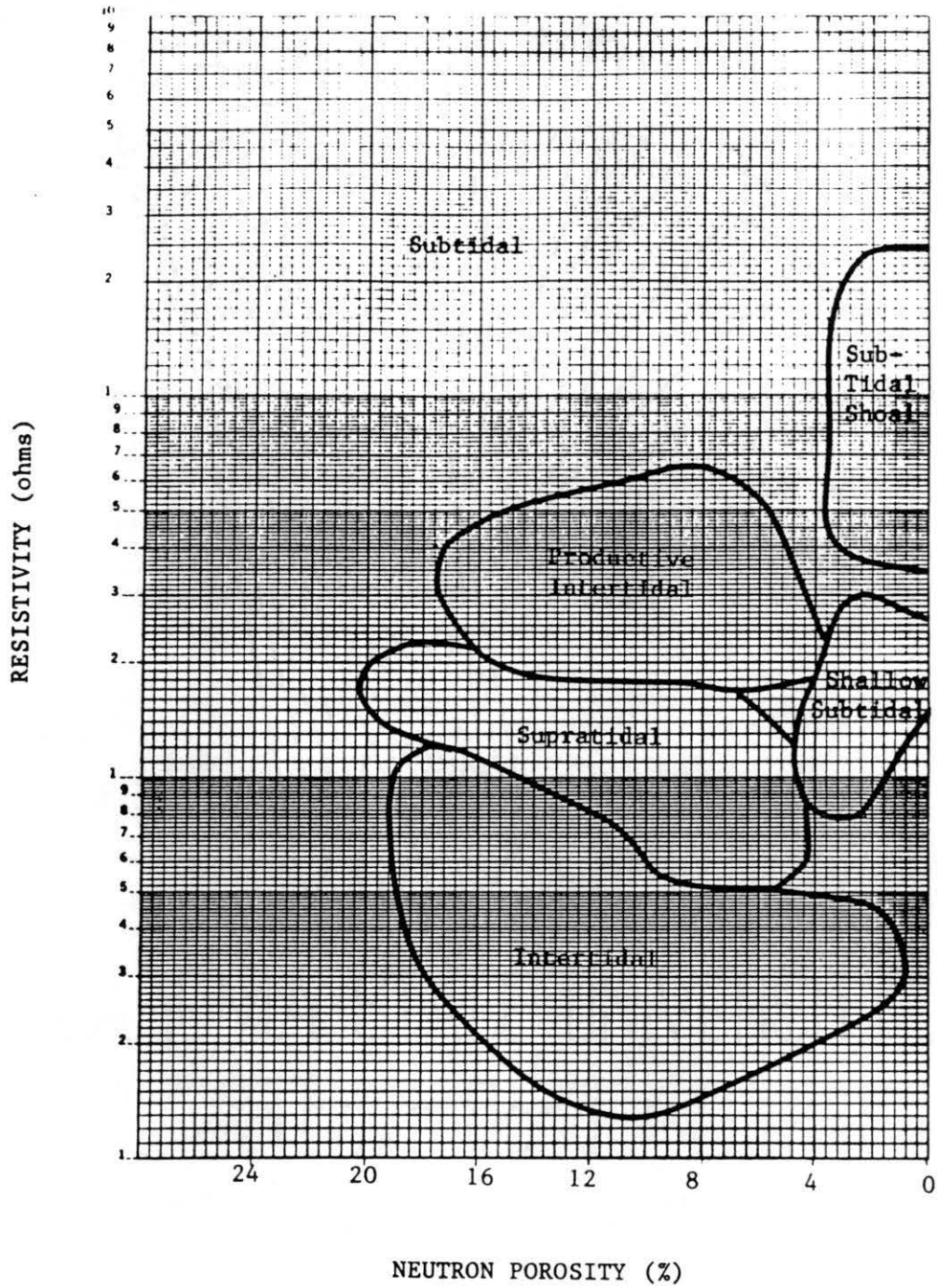


Figure 49. Pickett Plot of Resistivity versus Neutron Porosity

within the zone, whereas range 14 west is the intertidal and shallow subtidal facies which fluctuates frequently. The intertidal facies exhibits rapid and greater variation in thickness.

Although the changes in thicknesses are subtle, the isopach maps provided clues to the depositional environment during the depositional period of the productive zone.

Porosity Map

The porosity maps are prepared for zones B-3 and B-4 (see Plates 11 and 12). The density logs were used for quantitative analysis. Density logs are chosen because they are calibrated to limestone, and the rock is predominantly dolomitized lime. The amount of resultant error is negligible for exploration purposes. Based from core work, the total feet of density porosity greater than six percent is mapped, because 6 percent of porosity is considered to be sufficient to create a commercial reservoir. Hunton rock does not develop any significant porosity outside of the intertidal facies. Commonly, fracture porosity or dissolution porosity occur as 3-5 percent of the rock in the subtidal facies, but does not greatly enhance the productive capabilities of the rock.

The B-3 zone porosity map is a map of the lower porosity zone. The porosity zones are limited locally, small and linear. The porosity occurs in pods parallel to the depositional strike. The porosity pods average one to three miles in length, and any significant amount of porosity does not exceed a mile in width. In sections 23, 33, 34, T22N, R14W the porosity thickens abruptly. The porosity trends do not occur directly on the crests of the thicks, but rather on the flanks. Because the shallow sea was slightly regressive during the B-3 zone period of deposition, and began to develop more shallow water areas where larger areas of bioturbation occurred, the porosity is not as well developed. The organisms were burrowing the sediments on top of localized highs in shallow marine waters.

The B-4 zone is the upper porosity zone. This zone is more porous because the intertidal zone is better developed and localized highs are more established. The environment stabilized during the deposition of the B-4, and began to mound and expand the burrowing habitat. The porosity is not as well developed in the B-3 zone as it was in the B-4 zone. The pods are larger in width than the B-3 zone. The porosity zones continued to develop on the flanks of the thick accumulations. The porosity occur in pods parallel to the strike. The average porosity pod is three to five miles long and two to three miles wide. The seaward side (west) consists of inlet channels of non-porous rock which break up the linear features, but the landward lagoonal side is a smooth shoreline. The sides are commonly steep and abruptly end into non-porous facies. Although the porosity increased in areal extent, the non-porous facies was still widespread and more common.

Fault Map

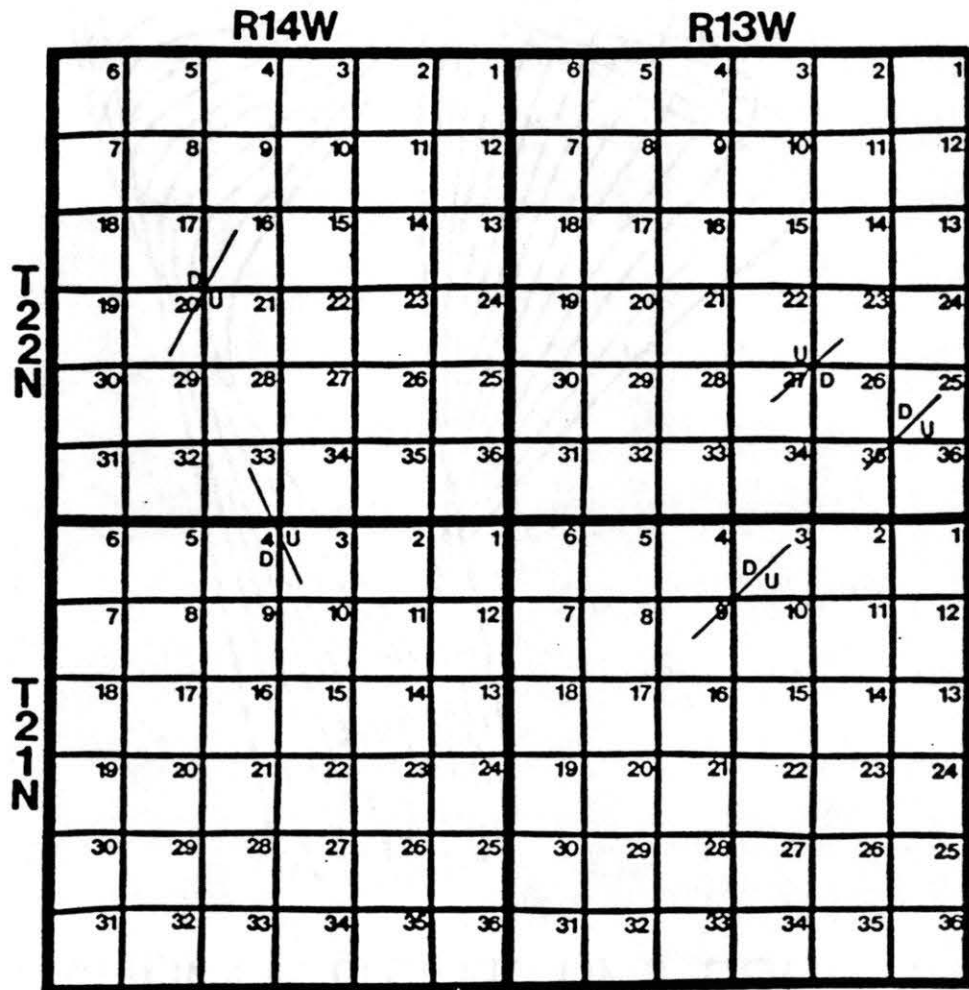
Faults in the study area are believed to be present although proof is not substantial from the well data alone. For definite identification of the discrete fault boundaries, seismic data is needed. Mapping of the oil/water contacts show some relative displacement by faults. The author believes tectonically related faults do exist in the area. An individual map is prepared which indicates possible faults (see Figure 50).

Other possible faults are northeast-southwest trending faults located in section 27, T33N, R13W, section 3, T21N, R13W, section 25, T22N, R13W, and section 21, T22N, R14W. A conjugate fault trend, northwest-southeast, is normal to the principal northeast-southwest trend. The conjugate fault is located in section 33, T22N, R14W.

Faults are identified by anomalies within the structure contour maps. If the identified faults are mapped, the resulting displacement restores the contours to a homoclinal dip.

The faults believed to be located in T22N, R14W were a discrete influence on the field located in sections 20, 21, 33, and 34 because of increased circulation of magnesium rich waters, which resulted in porosity enhancement by dolomitization.

The faults in this region are related to post Hunton tectonics because the Woodford is also effected by faulting. The regional trend is northeast-southwest with conjugate faults normal to the principle faults. Identification of specific fault type, amount of dip, and amount of throw can be made through interpretation of seismic stratigraphy.



Scale 1:158,400

Figure 50. Map of Inferred Faults

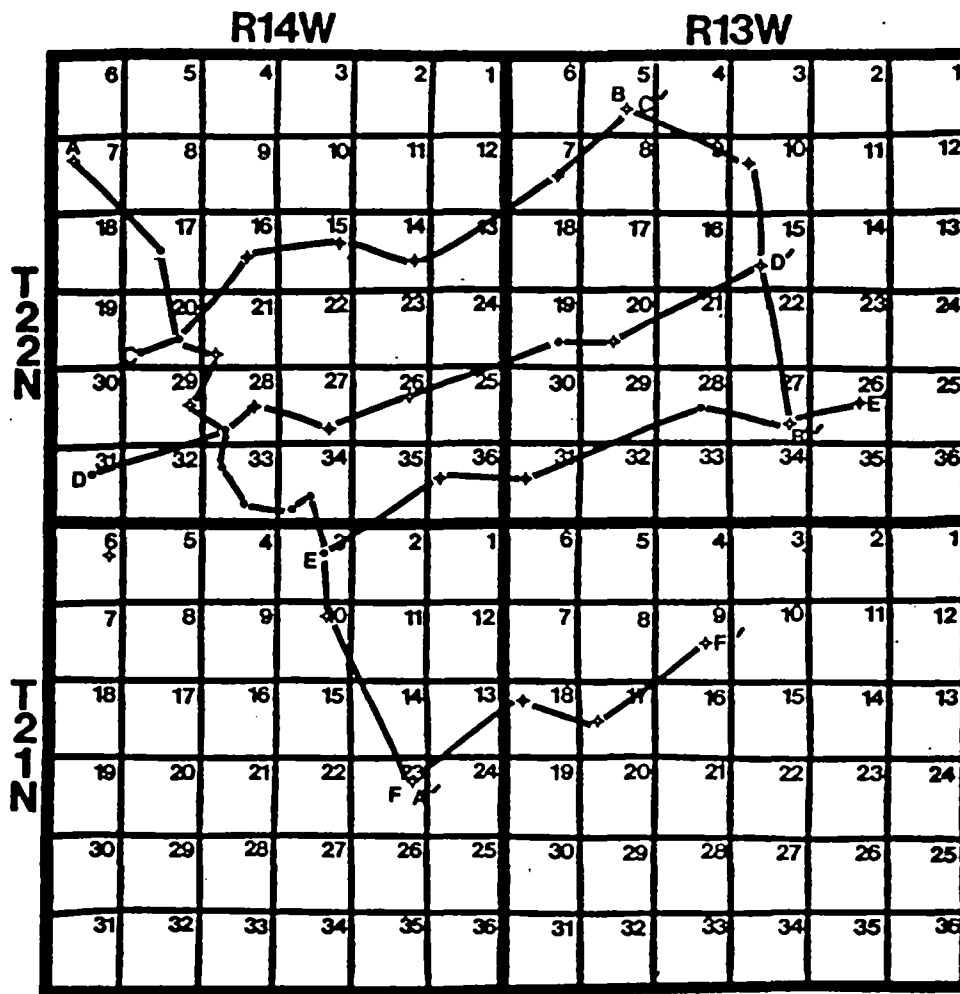
CHAPTER VI
CROSS SECTIONS

Introduction

To illustrate stratigraphic relationships, six strike-dip trending cross sections are prepared (see Figure 51). The cross sections are oriented along strike and dip for maximum identification of deposition facies. The datum of the cross section is on the base of the B-3 zone because this marker is believed to be time correlative. The individual zones represent a single depositional episode, and therefore, relate to each other chronologically instead of lithologically.

The gamma ray, resistivity, and density porosity logs (where available) are the wireline logs analyzed. Although Hunton gamma ray signatures are subtle, changes in the silica content are useful in delineating depositional cycles. The resistivity profile illustrates facies relationships and assists in correlation (see Figure 48). The density porosity provides information for analyzing the porous zones. The porosity logs are not useful in time correlations because the porosity shifts to the respective facies, therefore a common error is when the Henryhouse is correlated by the porosity zones only, instead of dividing into a depositional framework.

Two major unconformities are present within the section: 1.) the first is the angular unconformity at the top of the Chimneyhill, 2.) the second is the Woodford unconformity at the top of the Hunton. The angular unconformity causes thickening and thinning to occur within the A zones and likewise within the B-1 zone (see Figure 3 for zone nomenclature). The change in thickness within zone A is related to 1.) the Sylvan highs and lows, with respective selection of deposition of the Chimneyhill members, and 2.) erosional influences. The unconformity is marked by a resistive marker identified on the resistivity curve. The thickness changes in B-1 are directly related to the paleotopography.



Scale 1:158,400

Figure 51. Map of Locations of Cross Sections

Northwest-Southeast

The two northwest-southeast cross section A-A' and B-B' illustrate the dip toward the basin and trend along the strike (See Plate 13). The Hunton section thickens toward the southwest. Lateral facies changes are observed.

Cross section A-A'. The B-4 zone is completely truncated in well one and partially truncated in well two. In well three, a complete section of B-4 is present and locally productive. The productive zone is a lense of intertidal reservoir rock, and the first in a series of pods within Cheyenne Valley. Wells four and five become the tight shallow subtidal facies and are nonproductive. The wells in sections 28 and 33 begin to develop a second porosity pod in the B-3 zone considered the intertidal facies. The author does not believe these porosity pods are connected because of the log signatures of the wells drilled between the two pods, and the production characteristics of each reservoir. Another porosity zone begins to develop updip in the B-4 zone in sections 33 and 34. Porosity develops in the last two wells on the cross section, but is nonproductive. The erratic nature of the porosity is possibly an indication of nearby reservoir rock. In sections 10 and 28, some of the B-5 zone is truncated, and partially present.

Cross section B-B'. The cross section is located in subtidal facies indicated by tight resistivity profiles and lack of porosity. Section 15 shows some porosity, but is nonproductive. The B-4 zone and part of the B-3 zone are removed by erosion. A recognized feature is the subWoodford or collapse breccia developed by karstification. The collapse breccia is recognized on electric log by the unusually high API gamma ray reading and the absence of section. Karstification is very localized and observed in section 10, T22N, R13W.

Northeast-Southwest

The four northeast-southwest cross sections represent the depositional dip of the Hunton (See Plate 14). The Hunton section thickens westward, and is truncated eastward. The cross section illustrates the widths of the porosity pods. The following are detailed descriptions of the cross sections examined.

Cross section C-C'. A productive zone is observed in well two within the B-3 zone. The width of the porosity zone is approximately one mile. The B-3 zone thickens approximately 25 feet to accommodate the thick interval of porosity this is a typical intertidal feature.

Cross section D-D'. This cross section thickens toward the productive intertidal zone. Well two produces from zone B-3. This zone is shown to be one mile wide. Well one produces from the B-4 zone. Production from well one is related to porosity enhancement from the unconformity.

Cross section E-E'. Karstification is exhibited in section 26, and relates to the same subhorizontal cave system as the well in section 10, T22N, R13W. The Hunton section thins dramatically to the east. The well in section 28, which is enhanced by the unconformity, is only a minor producer from zone B-4 in the shallow subtidal facies.

Cross section F-F'. This cross section contains a complete section of zone B-4 because the cross section is located far enough south so it is not effected by erosion. Zone B-3 remains a fairly constant thickness, and is characteristic of the subtidal facies because of the high resistivity and lack of significant porosity. The B-4 zone is within the nonproductive shallow subtidal facies.

CHAPTER VII

DEPOSITIONAL AND DIAGENETIC HISTORY

The Hunton was deposited in a shallow marine environment. The seas were regionally transgressing and locally regressing which results in sequences of progradation and aggradation. The carbonate sedimentation occurs along the gently dipping shelf margin analogous to the ramp model. Different sedimentary environments, oriented approximately parallel to shoreline, reflect equilibrium conditions between the hydrographic conditions and the associated carbonate sediments. When the seas transgress or regress, the environmental belts migrate accordingly, and form a cyclic stratigraphy (Laport, 1969).

Five different depositional facies were observed in the Henryhouse: 1.) subtidal, 2.) shallow subtidal, 3.) subtidal shoal, 4.) intertidal, 5.) supratidal (see Figure 52). The first environment is the subtidal facies. The sea bottom lies below the zone of wave base and current action. The layers of sediment are micritic and laminated, and contain a variety of fauna. The shallow subtidal is below the zone of wave base. Insignificant amounts of burrowing activity occur within the sediment. The rock is classified as a mudstone to wackestone. The subtidal shoal is located in a zone where sediment is influenced by wave and current agitation during low tide. The rock is composed of oolites, which are indicative of a higher energy environment, and is classified as a packstone. The intertidal facies is influenced by wave and current agitation during high tide and exposed to the surface during low tide. The lithology of the rock is wackestone, and the texture is mottled. The supratidal zone is above sea level, except during occasional storms and floods. The rock is a mudstone with evaporitic minerals and algal mats. The facies most commonly represented in Cheyenne Valley area are the shallow water facies.

Because of the cyclic nature of the facies, periods of regression cause enhancement of primary porosity as a result of the fresh water mixing dolomitization model. Creation of a cell of fresh water mixing with brine is a function of topography which creates the hydrostatic forces. Topography is related to the paleotopography present at the time of deposition and the differential compaction of the finer grained sediments which are deposited in the subtidal facies (see Figure 53). The subsidence results in greater topographic relief

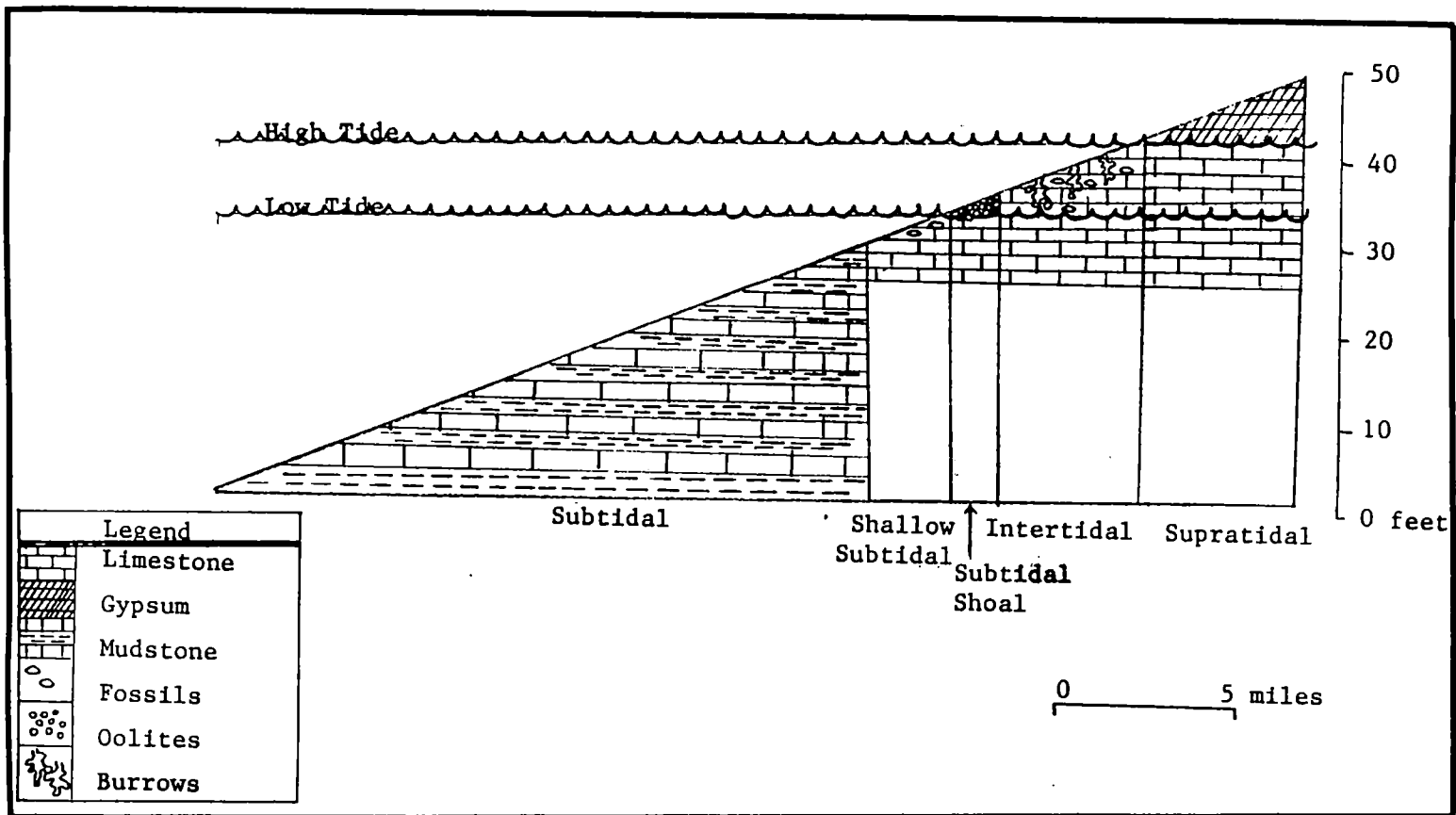


Figure 52. Depositional Facies

and increases circulating fluids.

The preWoodford unconformity resulted in a period of extensive erosion of platform drainage. Internal drainage which resulted in karstification, and external drainage such as streams (see Figure 54) were common.

Karstification is the result of carbonate dissolution by calcium carbonate undersaturated waters. The karstification process occurs through three zones which include infiltration, percolation and lenticular zones. The upper infiltration zone is found in the upper vadose. Surface land forms characteristic of karstification are vertical caves and collapse breccia. The percolation zone occurs next and is found in the lower vadose. Vertical movement of water through pre-existing paths occur here. Because this zone is dominated by vadose water seepage there is little dissolution. Only localized vadose flows show active dissolution. The lowermost zone of karstification is the lenticular zone which is present in the upper phreatic. Subhorizontal caves are the dominant feature, while subvertical caves are minor. Most solution caves occur here and are most abundant just below the water table. Collapse breccias related to the occurrence of caverns are locally abundant. (Manni, 1984, p.87).

The streams resulted in a low gradient meandering stream on the platform shelf which increased to a steep gradient on the platform break. Cheyenne Valley is located within a regional high on the platform shelf which resulted in the lack of definition of stream gradient when contouring the isopach of the Woodford Shale. The streams differentially erode the facies. The subtidal facies is more resistive than the intertidal facies. See Figure 54 for the effects of erosion versus lithology.

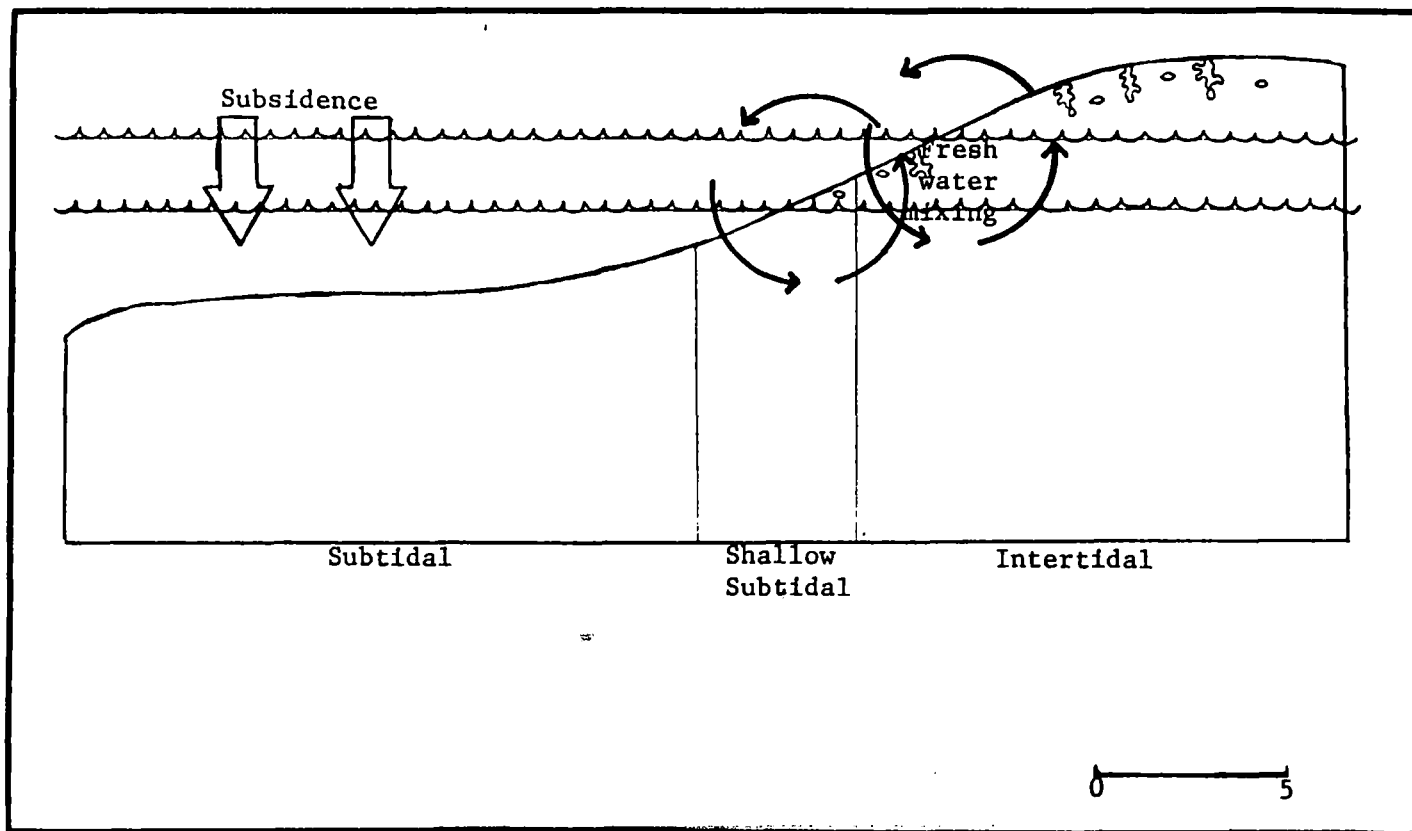


Figure 53. Porosity Enhancement

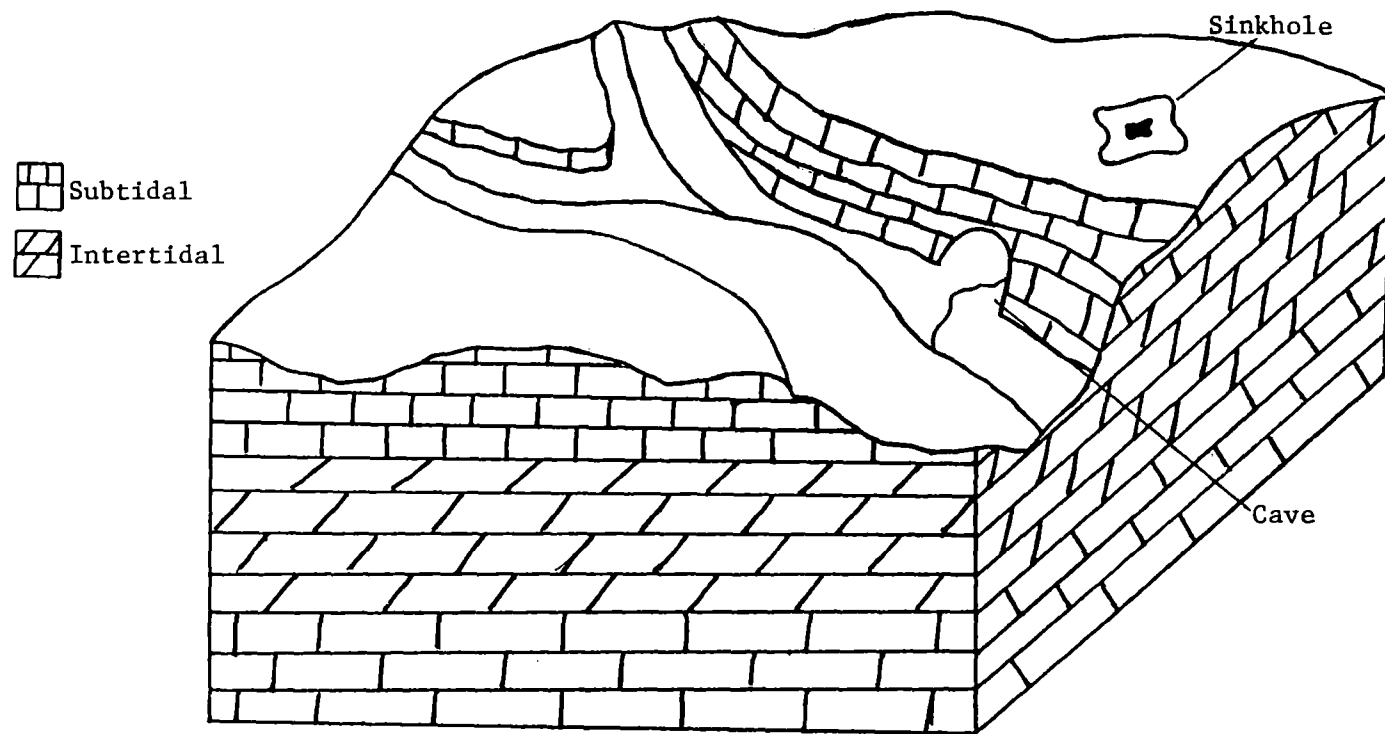


Figure 54. Hunton Erosional Patterns Along the PreWoodford Unconformity Showing Karstic Topography

CHAPTER VIII

CONCLUSIONS

The Henryhouse Formation located in the Cheyenne Valley Field is a prolific producer of hydrocarbons. The field has produced an excess of 5.5 million barrels of oil and 14 BCF of gas since 1968. There are two productive zones within the Henryhouse, the B-3 zone and the B-4 zone. The zones are separated by lithologic characteristics identified from a suite of log signatures, correlation of porosity zones only is misleading. The B-3 zone has produced the greater amount of hydrocarbons.

The Henryhouse is divided into several facies which are observed in core or cutting analysis, and core calibrated logs. The subtidal, shallow subtidal, and intertidal facies are identified in Cheyenne Valley. A Hunton reservoir must be located within a particular facies. The reservoir rock is the intertidal facies. The intertidal facies is a bioturbated wackestone consisting of intercrystalline porosity and bimodal distribution of anhedral xenotopic dolomite to euhedral idiotopic dolomite.

Hunton reservoirs in Cheyenne Valley are stratigraphic in nature, and the structure enhances the reservoir possibilities. Cheyenne Valley consists a sediments with a low, homoclinal dip. Faults are recognized within the field, but are not a controlling factor in hydrocarbon production. Locating a structural high or drilling updip into a anticlinal nose can enhance the well's productivity.

Three models are believed to explain the dolomitization: 1.) the hypersaline brine model, 2.) the fresh water mixing model, and 3.) the late stage, deep burial model. Dolomitization must alter the rock to permit maximum effective porosity. Fresh water mixing with ocean brines creates euhedral crystals form the intercrystalline porosity and result in significant porosity enhancement. Subareal exposure prior to deposition of the Woodford enhances dolomitization by permitting fresh water circulating fluids to be in direct contact with the rock.

Fracture enhancement also creates greater porosity, and a better conduit for oil

migration. Enlarged moldic porosity is beneficial to the reservoir. The dissolution of fossils creates large vugs and enlarged intergranular porosity for oil to accumulate in great quantities.

A variety of phases of diagenesis and of cementation occur within the Hunton during the evolution of the Hunton reservoir. To remain an effective reservoir cementation by calcite or baroque dolomite must not occur.

Most important, hydrocarbons must be present. With the prolific hydrocarbon potential of the Woodford directly above the reservoir, migration of hydrocarbons is favorable through the reservoir rock.

Upon mapping the facies, it was discovered that the intertidal facies occurs as small pods parallel to depositional strike and is located on paleohighs. The Woodford channel is related to the fresh water mixing model of dolomitization which may enhance or destroy the reservoir capabilities of the rock. Specific Woodford channel erosional patterns are mapped. Production occurs on the Woodford thins. A thin corresponds to a Woodford thickness of less than 50 feet. The Woodford thins directly relate to paleohighs at the time of Woodford deposition. Paleohighs are more susceptible to the fresh water mixing dolomitization.

The trapping mechanisms in the Cheyenne Valley Field are facies related. The trapping mechanism is caused by the intertidal facies having an updip lateral contact with the nonpermeable subtidal facies. The subtidal facies rock is the seal.

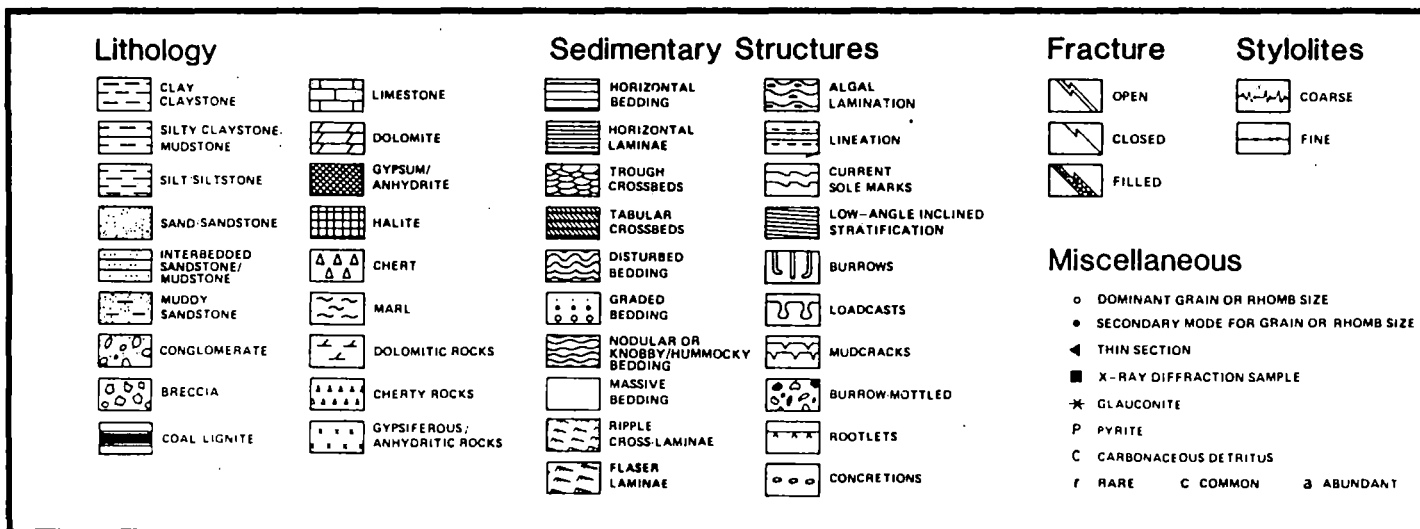
BIBLIOGRAPHY

- Adam, John E. and Rhodes, Mary L. "Dolomitization by Seepage Refluxion." American Association of Petroleum Geologists Bulletin, Vol. 44 (1960) pp. 1912-1920.
- Adler, F. J. "Future Petroleum Provinces of the Mid Continent, in Future Petroleum Provinces of the United States, Their Geology and Potentials" American Association of Petroleum Geologists. (1971), Memoir No. 15, pp. 985-1120.
- Al-Shaieb, Zuhair. "Depositional Facies, Dolomitization and Porosity of the Henryhouse Formation (Silurian), Anadarko Basin." Michigan Basin Geological Society Special Paper No.4, (1985).
- Amsden, T. W. Hunton Stratigraphy: Oklahoma Survey Bulletin 84. (1960), 298pp.
- Amsden, T.W. and Rowland, T. "Silurian and Devonian (Hunton) Oil and Gas Producing Formations." American Association of Petroleum Geologist Bulletin, Vol. 55:1 (1971) pp. 104-110.
- Amsden, T.W. Hunton Group (Late Ordovician, Silurian, and Early Devonian) in the Anadarko Basin of Oklahoma: Oklahoma Geological Survey Bulletin. 121. (1975), 214pp.
- Amsden, T.W., Caplan, W.M., Hilpman, P.L., McOlasson, E.H., Rowland, T.L., Wise, O.A. Jr. "Devonian of the Southern Midcontinent Area, United States." In International Symposium on the Devonian System. Vol.1. 1957, pp. 913-932.
- Asquith, George B. Subsurface Carbonate Depositional Models: A Concise Review. Tulsa, Oklahoma: Pennwell Publishers, 1979, 121pp.
- Back, W., B. B. Henshaw, L. N. Plunmer, P. H. Rahn, C. T. Rightmire, and M. Rubin, 1983, Process and rate of dedolomitization: mass transfer and ¹⁴C dating in a regional carbonate aquifer: GSA Bull., Vol. 94, pp. 1415-1429.
- Bart, Warren. Personal Interview. Telephone Conversation, Oklahoma City, Oklahoma, September 19, 1985.
- Beardall, Geoffrey. "Depositional Environment, Diagenesis and Dolomitization of the Henryhouse Formation, in Western Anadarko Basin and Northern Shelf, Oklahoma." (Unpub. M.S. thesis, Oklahoma State University, 1983.)
- Choquette, P. W. and R. Steinen, 1980, Mississippian non-supratidal dolomitization, Ste. Genevieve Limestone, Illinois Basin: evidence for mixed water dolomitization: SEPM Special Publication, 28, pp. 163-196.
- Davis, R.A. Depositional Systems. A Genetic Approach To Sedimentary Geology. New Jersey: Prentice Hall, 1983.

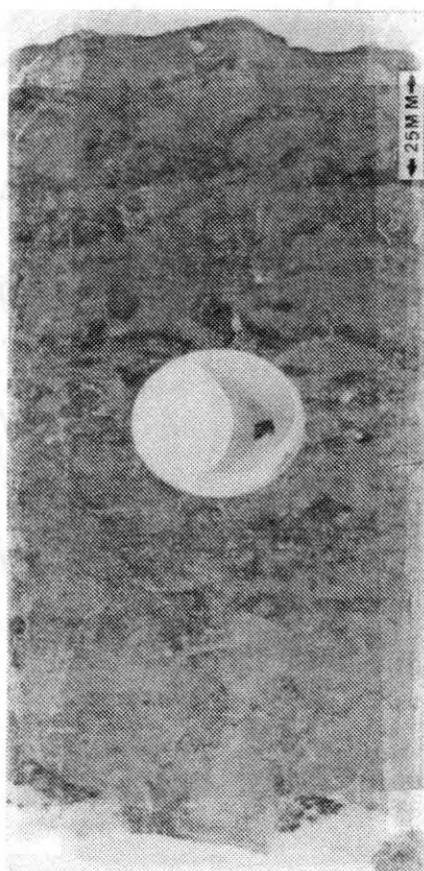
- Downey, Marian. Evaluating Seals for Hydrocarbon Accumulations: American Association of Petroleum Geologists Bulletin, Vol 68:11 (1984). pp. 1752-1763.
- Evans, J.L. "Major Structural and Stratigraphic Features of the Anadarko Basin." In Pennsylvanian Sandstones of the Mid-Continent: Tulsa Geological Society Special Publication, No. 1, 1979, pp. 97-113.
- Fairbridge, R.W. "The Dolomite Question: Regional Aspects of Carbonate Deposition." In Society of Economic Paleontologists and Mineralogists Special Publication 5, (1957), pp. 164-170.
- Frank, J. R., 1981, Dedolomitization in the Taum Sauk Limestone (Upper Cambrian), southeast Missouri: Journal of Sedimentary Petrology, Vol. 51, No. 1, pp. 7-18.
- Folk, Robert and L. Land. "Mg/Ca Ratio and Salinity: Two Controls over Crystallization of Dolomite." American Association of Petroleum Geologists Bulletin, Vol. 59 (1975), pp. 60-68.
- Friedman, G. M. "Deep Burial Diagenesis of Hunton (Late Ordovician to Early Devonian) Carbonates in Anadarko Basin." In Limestones of the Midcontinent, Tulsa Geological Society Special Publication 2. 1984, pp. 183-200.
- Ham, W.E., Dennison, R.E., and Merritt, C.A., 1964, Basement Rocks and Structural Evolution of Southern Oklahoma: Oklahoma Geological Survey Bulletin, Vol. 95.
- Hanshaw, Beck, and Deike. "A Geochemical Hypothesis for Dolomitization by Ground Water." Economic Geology, Vol.66 (1971), pp. 710-724.
- Harvey, R. "West Campbell (N.E. Cedardale) Gas Field, Major County, Oklahoma." Shale Shaker, Vol.18 (1969), pp. 568-578.
- Ingerson, Earl. "Problems of Geochemistry of Sedimentary Carbonate Rocks" Geochemica Et Cosmochimica, Vol.26 (1962), pp. 830-837.
- Isom, J.W. "Subsurface Stratigraphic Analysis, Late Ordovician to Early Mississippian, Oakdale-Campbell Trend, Woods, Major, and Woodward County, Oklahoma." Shale Shaker, Vol.24:1 (1974), pp. 116-132.
- Katz, A., 1971, Zoned dolomite crystals: Journal of Geology, Vol. 79, pp. 38-52.
- Krauskopf, K.B. 1979, Introduction of Geochemistry. 2nd Ed. New York: McGraw-Hill Book Company.
- Laport, Leo F. "Recognition of a Transgressive Carbonate Sequence". In Depositional Environments in Carbonate Rocks, SEPM Special Publication #14, 1979.
- Landes, Kenneth. 1970, Petroleum Geology of the United States. New York: John Wiley and Sons, Inc. pp. 125-127.

- Levenson, A.I. 1967. Geology of Petroleum. San Francisco: W.H. Freeman and Company, 724 pp.
- Logsdon, T. and Brown, A.R. "Hunton, Hottest Play in Oklahoma." Shale Shaker, (December, 1967).
- Longman, Mark W. "Carbonate Diagenetic Textures from Nearsurface Diagenetic Environments." American Association of Petroleum Geologists Bulletin, Vol.64:4 (1980), pp. 461-487.
- Manni, F. M. "Depositional Environment, Diagenesis, and Unconformity Identification of the Chimneyhill Subgroup, in the Western Anadarko Basin and Northern Shelf, Oklahoma." (Unpublished M.S. Thesis, Oklahoma State University), 1984.
- Medlock, P.L. "Depositional Environment and Diagenetic History of the Frisco and Henryhouse Formations in Central Oklahoma." (Unpublished M.S. Thesis, Oklahoma State University, 1984).
- Mintz, L.W. Historical Geology, the Science of a Dynamic Earth. Columbus, Ohio: Charles E. Merrill. 1972, pp. 416-447.
- Moore, R.C. Introduction to Historical Geology. New York: McGraw-Hill Book Company. 1949, pp. 135-176.
- Morgan, Bill. "Silurian Reservoirs in Upward-Shoaling Cycles of Hunton Group, Mt. Everette and Southwest Reeding Fields, Kingfisher County, Oklahoma." Carbonate Petroleum Reservoirs, New York: Springer-Verlag, 1985, pp. 109-120.
- Parks, Gary. Personal Interview. Oklahoma City, Oklahoma, September 11, 1985.
- Reeds, C.A. The Hunton Formation of Oklahoma: American Journal Science. Vol. 182 (1911), pp. 256-268.
- Scholle, P.A. Carbonate Rock Constituents, Textures, Cements, and Porosities. American Association of Petroleum Geologists Memoir 27. (1983).
- Shannon, P. Hunton Group (Silurian-Devonian) and Related Strata in Oklahoma: American Association of Petroleum Geologists Bulletin, Vol 46 (1962), pp. 1-29.
- Tucker, M.E. Sedimentary Petrology, An Introduction. New York: John Wiley and Sons, 1982.
- Withrow, P. "Star-Lacey Field, Blaine and Kingfisher Counties, Oklahoma." Shale Shaker, Vol. 19 (1971), pp. 78-88.
- Wilson, J.L. "Characteristics of Carbonate Platform Margins.": American Association of Petroleum Geologists Bulletin, Vol. 58 (1974), pp. 810-824.
- Wilson, J.L., 1975. Carbonate Facies in Geologic History. New York: Springer Verlag, p.471.

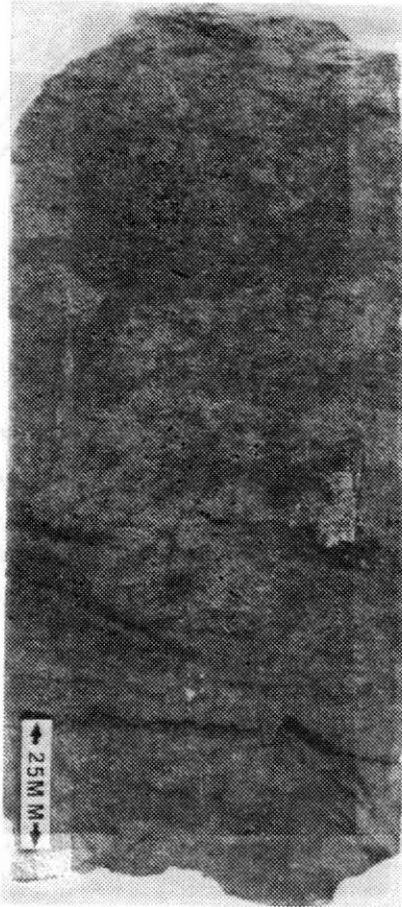
APPENDIX
CORE DESCRIPTIONS AND PHOTOGRAPHS



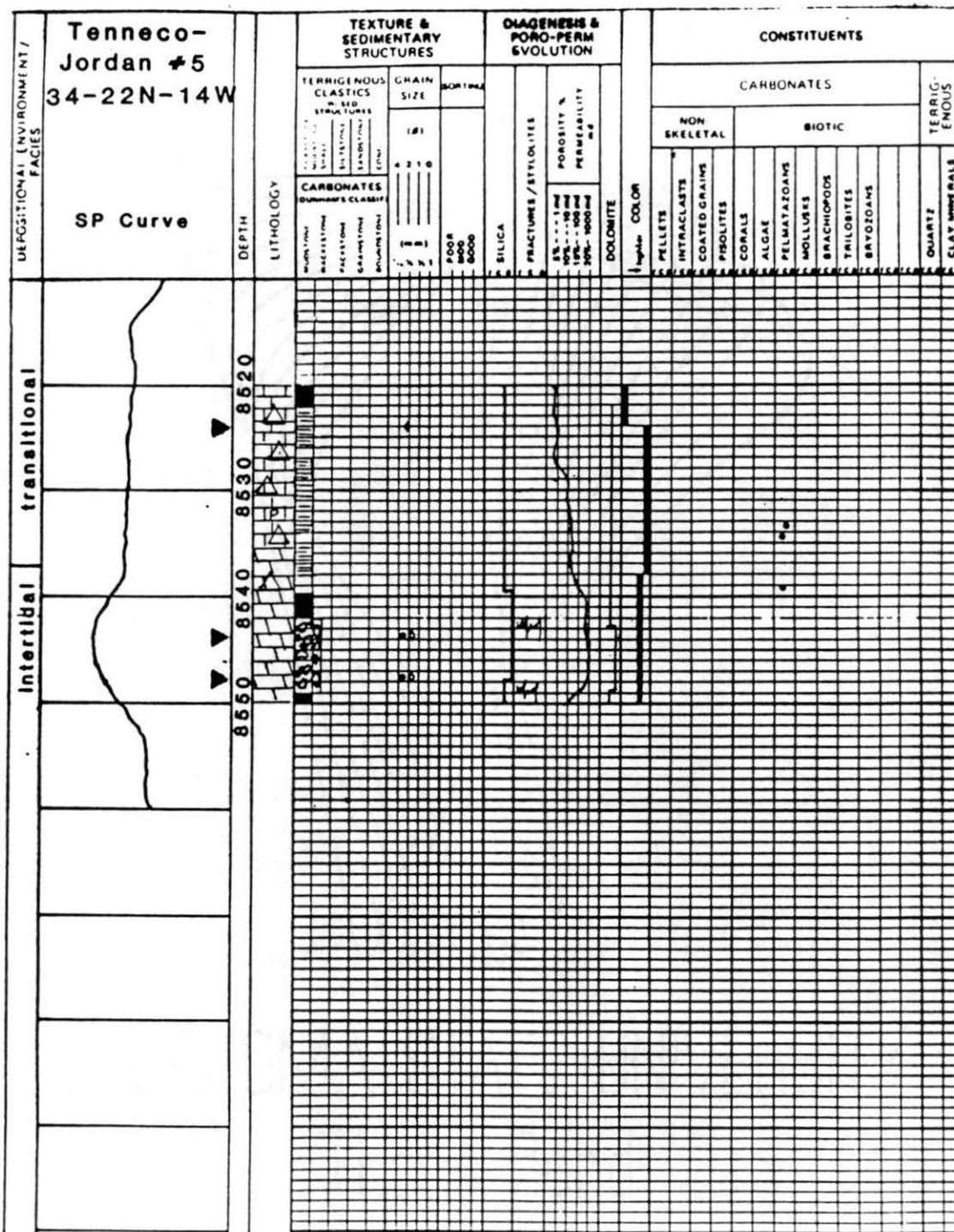
KEY: This key applies to the following core descriptions

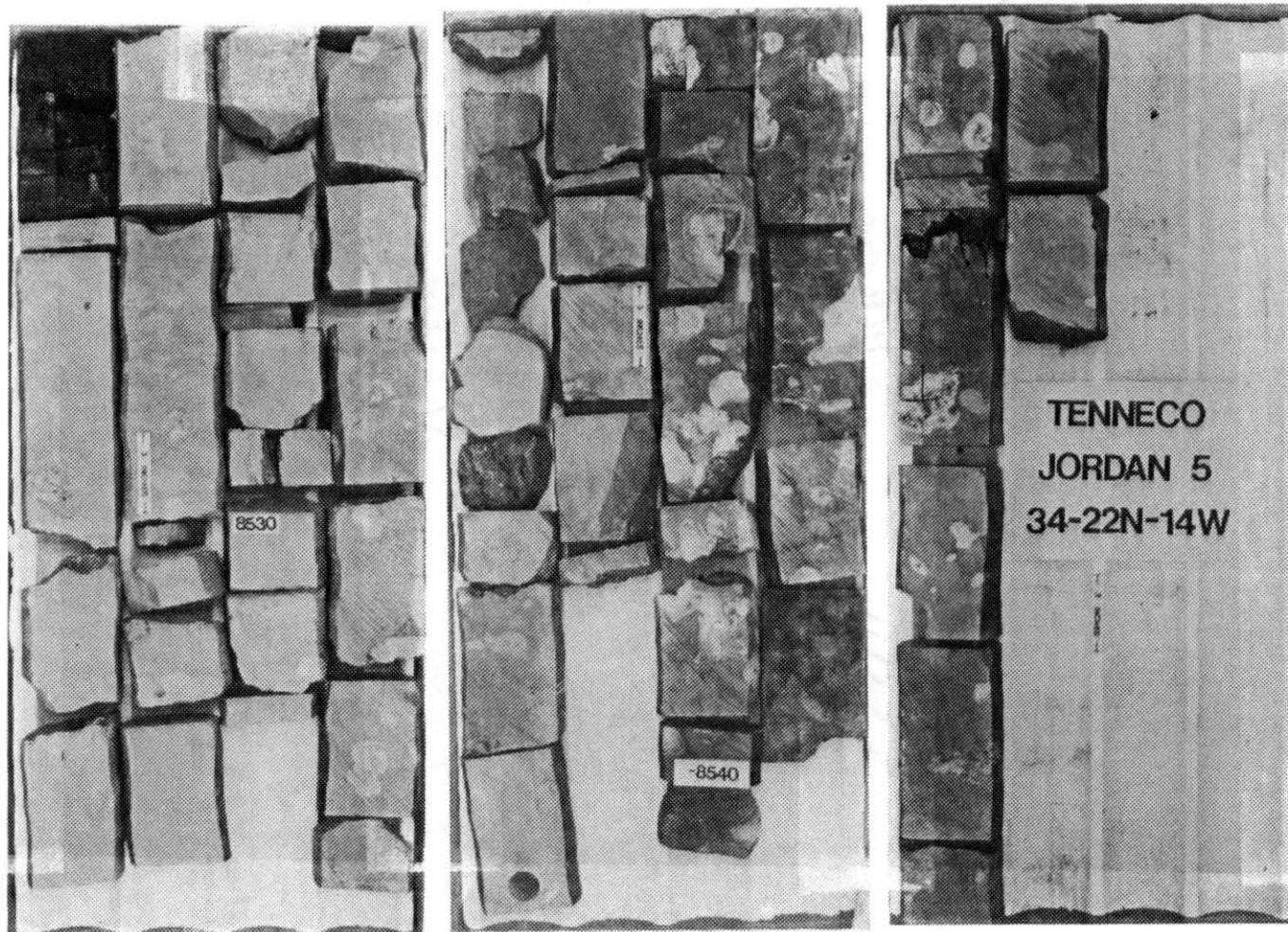


Tenneco - Jordan #2. Photograph of -8538'.
The photograph exhibits horizontal stylolites and
bioturbated sediments. Chert nodules are present at the
bottom of the rock

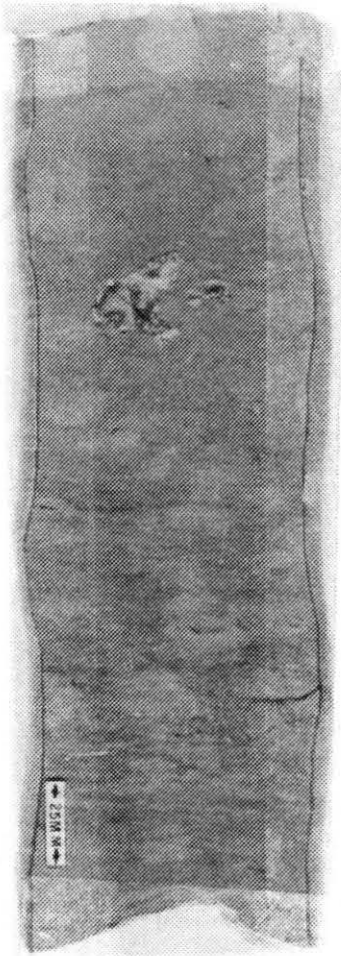


Tenneco - Jordan #2. Photograph of -8544.
Reservoir rock with oil stained bioturbated
intercrystalline and vugular porosity.





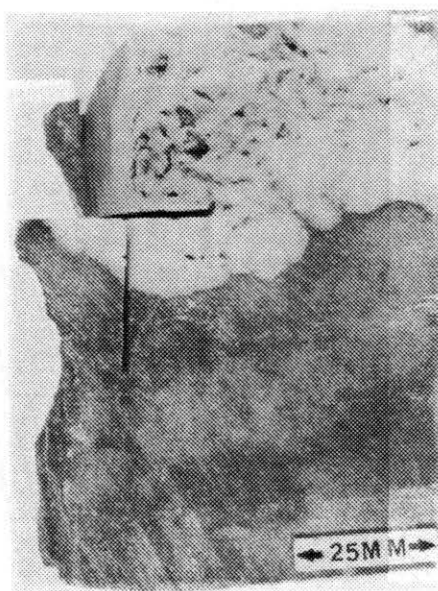
Tenneco - Jordan #5. Photograph of complete core.
The photograph shows the Woodford-Hunton contact, the
transitional facies, and the intertidal facies. Nodules of
chert and tripoli can be observed



Tenneco - Jordan #5. Photograph of -8526'.
The photograph exhibits a tripoli nodule at the top and a
chert nodule towards the center. Minor bioturbation is
evident. Shale wisps vaguely define the lamination.



Tenneco - Jordan #5. Photograph of -8543.
Intertidal rock containing a vug filled with baroque
dolomite.



Tenneco - Jordan#5. Photograph of -8543'.
Highly bioturbated zone with tripoli and chert filling
vugs



Tenneco- Jordan # 1. Photograph of -8454.
The photograph is an example of bedded chert filled with oil. Vertical fractures are also filled with oil.
(Note: This core was not logged because there was no direct way to correlate the log to the core.)

2

VITA

Kathleen Patricia Menke

Candidate for the Degree of

Master of Science

Thesis: SUBSURFACE STUDY OF THE HUNTON GROUP IN THE CHEYENNE VALLEY FIELD;
MAJOR COUNTY, OKLAHOMA

Major Field: Geology

Biographical:

Personal Data: Born in Akron, Ohio, October 17, 1961, the daughter of James F. and Patricia Menke.

Education: Graduated from Putnam City High School, Oklahoma City, Oklahoma in May 1979; received Bachelor of Science Degree in Geology from Oklahoma State University in May, 1984; completed requirements for the Master of Science degree at Oklahoma State University in May 1986.

Professional Experience: Assistant Geologist, Borehole Exploration Corporation, Tulsa, June 1983 to August 1983; Assistant Geologist, Southwestern Energy Production Company, Oklahoma City, May 1984 to present. Member of American Association of Petroleum Geologists, Society of Professional Well Log Analysts, Association of Women Geoscientists, Oklahoma City Geological Society, and Geological Society of America.